NITROGEN LASER EXCITED FLUORESCENCE OF SOME RARE EARTH DOPED ALKALINE EARTH FLUORIDES

C. SUDHA KARTHA

THESIS SUBMITTED
TO THE UNIVERSITY OF COCHIN
IN PARTIAL FULFILMENT OF THE REQUIREMENTS
FOR THE DEGREE OF
DOCTOR OF PHILOSOPHY

LASER DIVISION, DEPT. OF PHYSICS
UNIVERSITY OF COCHIN
1984

DECLARATION

Certified that the work presented in this thesis is based on the original work done by me under the guidance of Dr.K.Sathianandan, Professor, Department of Physics, University of Cochin, and has not been included in any other thesis submitted previously for the award of any degree.

Cochin 682022,
February 2, 1984.

C.SUDHA KARTHA.

CERTIFICATE

Certified that the work presented in the present thesis is based on the bona fide work done by Smt.C.Sudha Kartha, Research Scholar, under my guidance in the Department of Physics, University of Cochin, and has not been included in any other thesis submitted previously for the award of any degree.

Cochin 682022,
February 2, 1984.

Dr.K.SATHIANANDAN
Professor of Physics
(Supervising Teacher).

PREFACE

The spectroscopic studies of doped crystalline substances have revealed the possibility of their use in lasers. In the recent years to come, we may expect a large scale intensive search for laser crystals capable of efficient emission at room temperatures both in the ultraviolet and in the visible regions of the optical spectrum. The possibility of using rare earth ions in crystals as new laser materials has necessitated a complete understanding of the excitation and de-excitation mechanisms of these ions. The advent of lasers initiated the most interesting and highly detailed investigations into the spectroscopic features of laser crystals like $CaF_2:RE^{3+}$.

This thesis aims to present the results of the experimental investigations on the Nitrogen laser excited fluorescence of some rare earth doped alkaline earth fluorides. It also contains the details of a pulsed Nitrogen laser, a fluorescence emission spectrometer and a lifetime spectrometer.

The thesis begins with a brief introduction to the different aspects of the luminescence in crystals. The different factors affecting the luminescence and the

applications of luminescence are described in this chapter. A brief introduction to laser crystals and the spectral characteristics of rare earth ions are also discussed in the second half of the chapter.

It has been observed that a good number of rare earth ions in different crystals absorb the UV radiations of the Nitrogen laser to emit fluorescence in the visible region. Moreover, being a pulsed laser with very high peak power of extremely short duration, lifetime measurements of excited states can be successfully carried out using this laser. A Nitrogen laser was therefore used as the source of excitation in the present investigations and the details of its design considerations are given in the second chapter. Some parametric studies like the power measurements laser spectrum analysis and power variations with additives are also carried out on this laser and the results are presented in the same chapter.

The experimental details on the recording of the fluorescence spectrum and lifetime measurements are given in the successive chapters. Since a knowledge of the behaviour of the pure materials can provide a basis for understanding the behaviour of the doped materials, the fluorescence spectra of pure CaF_2, SrF_2 and BaF_2

were initially investigated with the Nitrogen laser excitation and the results are presented in chapter III.

Fluorescence studies of $CaF_2:Ho^{3+}$ for different concentrations of Ho^{3+} are described in the next chapter. The emission spectra are recorded at both RT and LNT. Temperature dependent concentration quenching of fluorescence was observed for $CaF_2:Ho^{3+}$ and is discussed with the help of the energy level diagram of Ho^{3+}.

Visible fluorescence of Nd^{3+} in CaF_2, SrF_2 and BaF_2 for two different concentrations of Nd^{3+} is also studied with Nitrogen laser excitation and presented in chapter V. Strong blue emission was observed from these crystals. The energy levels and transitions involved in the visible fluorescence of Nd^{3+} are also included in this chapter.

The study of fluorescence of $CaF_2:Er^{3+}$ is given in chapter VI. No visible fluorescence was observed under Nitrogen laser excitation and hence the emission of these crystals was studied with a Xenon arc excitation. The results and conclusions of the investigations are summarised in a separate chapter at the end of the thesis.

The results of the above investigations have been communicated in the form of following research papers.

1. A simple and sensitive PMT preamplifier for low level fluorescence and luminescence studies.
   S.M.Pillai, C.Raghavan, C.Sudha Kartha and C.P.G.Vallabhan, J.Inst.Soc.India, 12, 7 (1982).

2. Fluorescence of $CaF_2:Ho^{3+}$ under N_2 laser excitation.
   Sudha Vijayakumar, V.P.N.Nampoori and K.Sathianandan, Proceedings of DAE Symp. on NP & SSP held at Banaras Hindu University (1982) Paper SEC10.

3. Blue emission of Nd^{3+} in CaF_2 and SrF_2.
   Sudha Vijayakumar, V.P.N.Nampoori and K.Sathianandan, Proceedings of DAE Symp. on NP & SSP held at Banaras Hindu University (1982) Paper SEC11.

4. New vibrational bands in the N_2 laser emission spectra.
   N.Subhash, Sudha C.Kartha and K.Sathianandan, Appl.Optics, 22, 3612 (1983).

5. Temperature dependent concentration quenching of fluorescence of $CaF_2:Ho^{3+}$.
   C.Sudha Kartha, T.Ramachandran, V.P.N.Nampoori and K.Sathianandan, Presented at the 3rd Symp. on Lasers and Applications held at IIT Kanpur (1983) Paper C 2Y-3.

6. Luminescence decay studies of Nd^{3+} in SrF_2.
   C.Sudha Kartha, V.P.N.Nampoori and K.Sathianandan,
   Proceedings of DAE Symp. on NP & SSP held at
   Manasagangothri,University of Mysore (1983),
   SDD5.

ACKNOWLEDGEMENTS

I wish to express my deep sense of gratitude to Professor K.Sathianandan, for introducing me to the field of lasers, suggesting the problem and also for the profound interest and able guidance given throughout the years of my research. He has been an extremely understanding guide whose constant encouragement and suggestions gave me moral support to complete the work.

I am also thankful to all the faculty members of this department, particularly to Dr.V.P.N.Nampoori who extended me all help at every stage of my research work. Let me also take this opportunity to express my gratitude to Mr.K.Sankaran Nair and Dr.V.Unnikrishnan Nair who motivated me for a research career and gave inspiration during the period of research.

I owe a lot to my colleagues of Laser Division, Cochin University, especially to Dr.N.Subhash, Mr.S.M. Pillai and Mr.T.Ramachandran for helping me to solve the various difficulties encountered during the experimentation.

A special note of gratitude goes to Mr.Raghavan and Mr.Madhusoodanan for the instrumentation and laboratory services extended to me.

Thanks are also due to Mr.K.P.Sasidharan for clearly typing the manuscript and Mr.Satheesh Kumar for assisting me in preparing the figures.

I am ever indebted to my parents and in-laws for their love and good wishes and I wish to dedicate this thesis to them. I do not know how to thank my husband, Mr.K.P.Vijayakumar, without whose active assistance and moral boosting I would not have been able to complete this work.

CONTENTS

CHAPTER I

LUMINESCENCE IN CRYSTALS

1.0 Introduction

The phenomenon of luminescence has been known from ancient times. Bio and Chemo luminescence are mentioned in the Indian Vedas and the Chinese Book of Odes. Luminescence is a process which is characterized by the emission of visible and ultra-violet radiation in excess of thermal radiation in a given material. The quality and quantity of luminescent emission are strongly dependent on the nature of the emitting material[1]. The preparation of the first luminescent material was from natural barite powder and after that countless observations of natural and artificial phosphors have been made. The spectroscopic investigations were initiated by Stokes and the laws of luminescence decay were introduced by Becquerel.

Present day research into luminescence began from the middle of 1930 when the two major mechanisms of luminescence, the glow of discrete centres and the glow of crystallophosphors were distinguished. In the former case the absorption and emission processes proceed within the

limits of individual ions and molecules in crystals (spontaneous and induced luminescence) while in the latter the absorption of light is accompanied by internal ionisation and photoconduction (recombinational luminescence).

The band theory of luminescence was also developed at the same time and used in interpreting the glow of crystallophosphors like ZnS, Silicates and Phosphates. However, there were two basic limitations for these investigations. Firstly they remained empirical as the nature of electron capture levels was not considered. Secondly, investigations did not cover crystals with discrete centres whereas the luminescence of discrete centres such as Mn^{2+} and RE^{3+} in silicate, borate and other minerals has much importance. Systematic research into the luminescence of discrete centres began in 1950, when optical spectroscopy of solids received new impetus by the use of the crystal field theory.

1.20 Major developments

The discovery and successful applications of lasers and masers served as a starting point for the most interesting and detailed investigations into the spectroscopic features of laser crystals[2] like $CaF_2:RE^{3+}$,

$CaF_2:RE^{2+}$ and $CaWO_4:RE^{3+}$. Spectroscopic investigations also covered such systems as $CaCO_3:Mn^{2+}$, $ZnS:RE^{3+}$ and $ZnS:Cu^{3}$. The luminescence of rare earth ions in CaF_2 and other alkaline earth fluorides had become the best studied type of luminescence centres. With the development of lasers, various luminescence theories also began to take shape[4,5]. Luminescence of minerals with their spectroscopic characteristics and interpretation uncovered new potentialities for luminescence in mineralogy[6,7]. However, still much has to be done to achieve a sufficiently complete information of luminescence in almost all minerals.

From the traditional materials, luminescence research has been extended recently to inhomogeneously doped crystals[8], amorphous materials[9,10] and structured thin films[11]. There is now a trend to give more attention to research on the applications of luminescence. Extensive investigations on displays—cathode ray screens and electroluminescence displays—are currently on the increase[12,13]. Phosphor particles coated with other phosphors and structured multiple coatings[14] are also being investigated for fluorescent lamps. The luminescent solar collector concept has attracted widespread attention and scientists are in search for suitable materials[15,16].

Research on non-radiative processes and multi-phonon relaxations[17,18], the luminescence and properties of colour centres[19] and the various effects of high excitation phenomena[20,21,22] are also in the forefront of the luminescence studies. Advances in laser technology have made available tunable radiation of extremely high powers opening the possibility of conducting various types of nonlinear spectroscopy on impurity ion systems. They include phenomena such as two or multiple photon absorption by single ions and co-operative transitions by two or more ions.

The application of laser spectroscopic techniques to the study of optical properties of ions in insulators has led to rapid advances in our understanding of various static and dynamic aspects of interactions which affect these optically active systems. Recently Selzer[23] has reviewed the techniques employed in the laser spectroscopy of solids while their application to luminescent ions in crystals is reviewed by Yen and Selzer[24].

General concepts of luminescence

1.30 Absorption spectra

The phenomenon of luminescence can be compared with optical absorption. When a crystal is illuminated with

monochromatic light whose wavelength can be varied, the ions in the unfilled shell pass from the ground state to the excited state and this is attended by the appearance of an absorption band in the optical spectrum.

1.31 Luminescence spectra

Ions in a crystal that are excited to an upper level will return to the ground state either by radiationless transitions or by way of emission transitions. This emission transition will appear in the form of a band in the luminescence spectra. The position of the band in the luminescence spectrum does not depend on the method of excitation, but is determined by the interlevel spacing.

1.32 Excitation spectra

A luminescent crystal absorb photons which excite it, but all these absorbed photons need not excite photoluminescence. The excitation spectra therefore do not necessarily coincide with the corresponding absorption spectra. In the excitation spectra, one can observe a glow as a result of the transition from the emission level. The excitation spectrum shows that for an effective luminescence in the crystal to manifest itself, the emission levels are

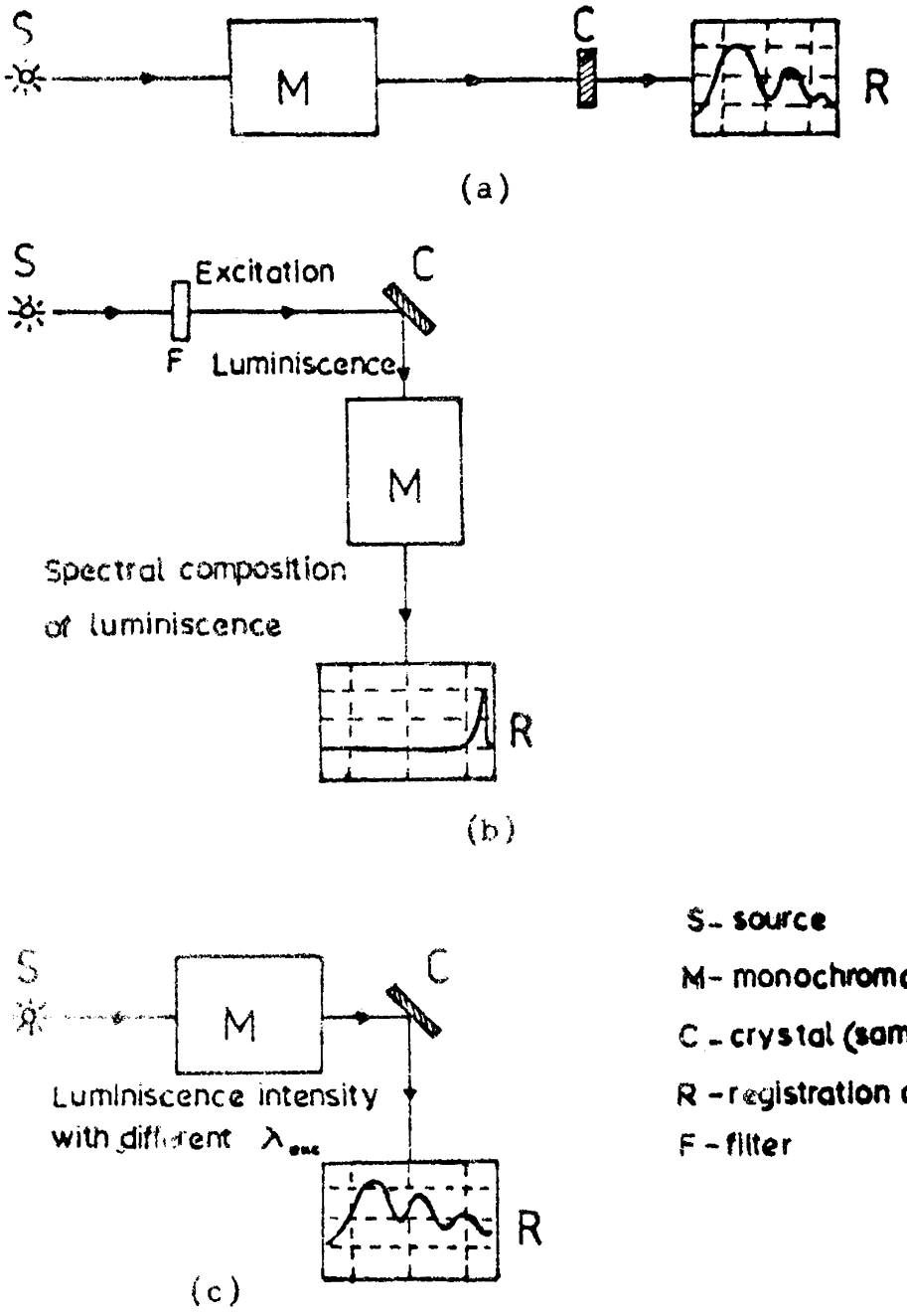

Fig.1.1 Schematic presentation of the experimental set up for recording
(a) - absorption spectrum
(b) - luminescence spectrum
(c) - excitation spectrum

not only necessary, but also must have sufficient absorption. The excitation spectra are made use of for choosing the region of luminescence excitation, and also for determining the pattern of the ion's energy levels, when its concentration is too small to observe the absorption spectra. A schematic presentation of the experimental set up for recording the absorption spectrum, luminescence spectrum and excitation spectrum is shown in Fig.1.1(a,b&c).

1.33 Fluorescence and phosphorescence

The general term luminescence is further classified into fluorescence and phosphorescence. Fig.1.2 shows the processes involved in fluorescence and phosphorescence. If the emitting system is raised by excitation from the ground state f to the excited state e, it will return to the ground state with emission of light. The emission occurs at a time after the excitation, τ being the lifetime of the excited state and is of the order of 10^{-8} sec. for atomic dipole emission. The phenomenon is fluorescence if the emission takes place by one or more spontaneous transitions. But if on the contrary, the emission occurs with the intervention of a metastable state m followed by return to the excited state due to addition of energy it is phosphorescence.

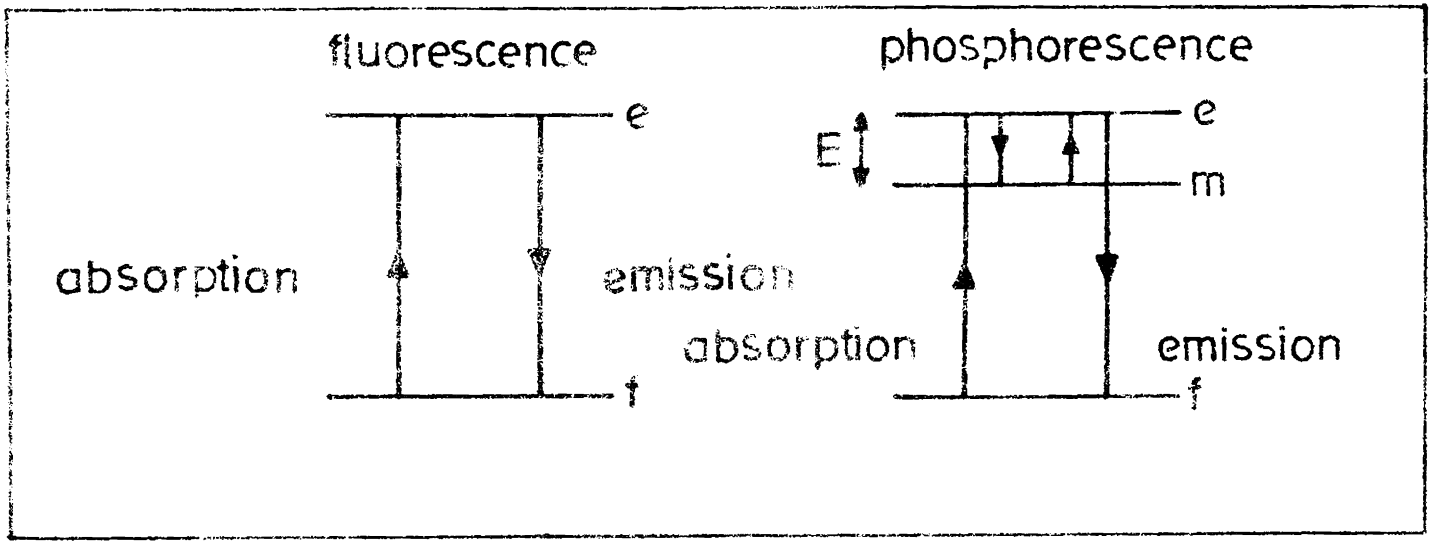

Fig.1.2 Luminescent system.

1.34 Stoke's law

When an electron is excited, the energy levels occupied by the excited electron and its residual positive hole move close together giving up energy as phonons before a radiative transition occurs. Hence resonance radiation cannot be observed in phosphors emitting broad bands. As a consequence, the energy of the emitted photon $h\nu_e$ is usually considerably less than that of the absorbed primary photon $h\nu_a$ ie, $h\nu_a \geq h\nu_e$ and is known as Stoke's law.

1.35 Radiationless transitions

An excited 'free' electron has two means of returning to its ground state. It can make a radiative transition giving out a photon or undergo a phonon assisted transition called radiationless transition. An excited free electron and its residual positive hole usually have appreciable kinetic energies and momenta which differ at least in direction. Their recombination is improbable until energy losses as phonons have reduced their kinetic energies and momenta to sufficiently low values. In other words, a small portion of the available free energy of an excited electron may be sacrificed as phonons to conserve momentum

during a radiative transition. The larger the proportion of excitation energy which is transformed into phonons, the less will be the luminescence efficiency and the greater will be the heating of the phosphor crystal during luminescence. Radiationless loss of energy also takes place by collapse of excitation states by small increments corresponding to phonon energies or by interaction of free electrons with each other as in a gas or interaction with atoms of the crystal.

1.36 Activators

From the earlier studies itself it is clear that most usually the ability to exhibit luminescence is associated with the presence of activators. These activators can be introduced in two ways; they may be impurity atoms occurring in relatively small concentrations in the host crystal or stoichiometric excess of one of the constituents of the host material. The latter is a case of self activation. The presence of a certain type of impurity may also inhibit the luminescence of other centres in which case the former is referred to as a killer.

1.37 Characteristic and noncharacteristic luminescence

In characteristic luminescence the energy levels involved are those of the activator atoms themselves modified

perhaps by the host lattice. Here the incident quantum of energy is absorbed by an activator atom resulting in a transition of one of the electrons from one quantum state to another. When the excited atom returns to the ground state, it looses a part of the energy due to lattice interaction resulting in the emission of a photon of less energy. Thus the emitted radiation will be red shifted (Stoke's shift) compared to absorbed radiation. The non-characteristic luminescence is more complicated. Here a charge transfer through the lattice is an essential part of luminescence process. In addition, the energy levels of the host lattice modified by the presence of activator atoms are involved in the process.

1.3B Effect of crystal field on the spectra of ions

When an atom is located in a crystal it is subjected to various inhomogeneous electric fields produced by the ligands. This results either in the splitting of energy levels, or modification of energy levels which are essentially brought about by perturbation caused by the interaction between ligands and impurity ions. Interaction of the doped ions with host lattice modifies also the lattice energy. Introduction of dopants will change luminescence characteristic of phosphors

due to the change in the distribution of self activated centres and appearance of new centres.

Models of luminescence

1.40 Configuration co-ordinate model

This is a scheme introduced by Von Hippel in 1936 to give qualitative description of optical processes in luminescent centres. Later this scheme was applied to many problems of luminescence. The configuration coordinate model is illustrated in Fig.1.3. The ordinate is the total energy of the system for ground and excited states of the centre including both ionic and electronic terms. The abcissa is a configuration co-ordinate which specifies the configuration of the ions around the centre.

Here the equilibrium position of the ground state occurs at A. When the centre absorbs light it is raised to the excited state at B obeying Franck Condon principle. After the centre has reached the excited state the ions of the system adjust to a new equilibrium C; the energy difference between B and C is given off as lattice vibrations. Having reached the new equilibrium position C the center may return to the ground state at D by emission of a quantum of luminescent light.

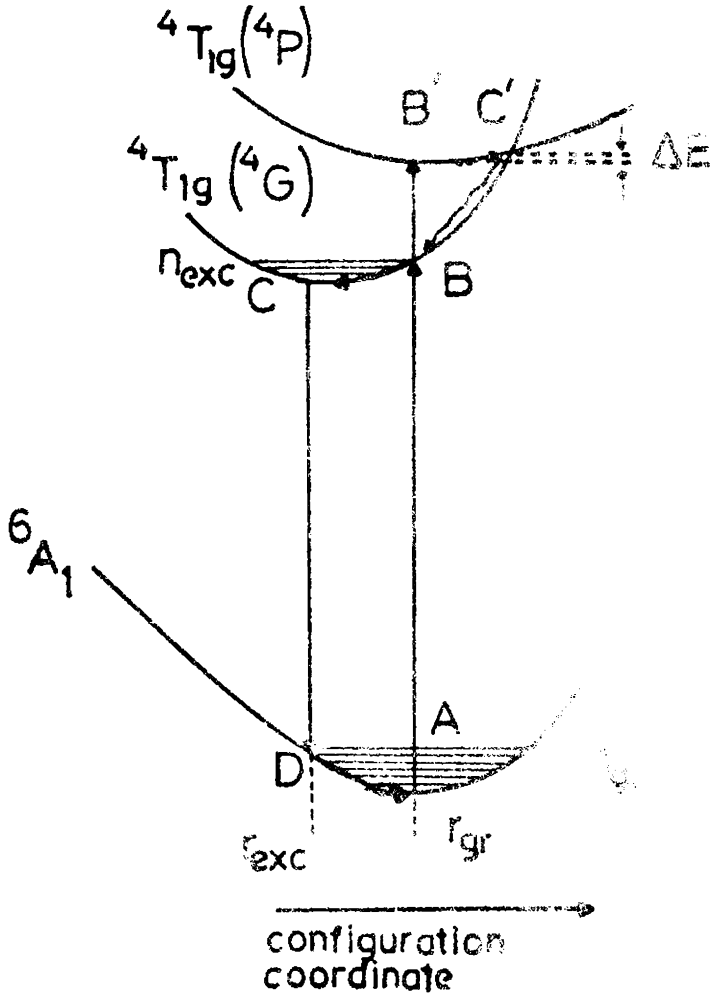

Fig.1.3 Configuration co-ordina
eg: Mn^{2+} ion

Relaxation from D to A is by means of energy dissipation through lattice vibrations. Obviously the energy of the emitted photon is smaller than that of the absorbed photon because some energy is transferred to the lattice. The amount of this shift (Stoke's shift) arising in a given system depends on the interaction of the centre with the neighbouring ions. In addition to the Stoke's shift, these curves account for the sudden decrease in luminescence efficiency at very high temperatures.

1.41 Band theory model

The application of quantum mechanics to the luminescent phenomena resulted in the development of the band theory model for electrons in a periodic potential and the theoretical basis for excitons in crystals. An energy band on the collective electron theory has been developed by many workers to explain the long durational phosphorescence of photoconducting phosphors. When atoms are arranged in an orderly way and in close proximity to each other to form a crystal, the energy states for the electron in atoms are disturbed by mutual interaction. As a result, the discrete electronic states are broadened into bands of allowed energy, separated by forbidden bands. The uppermost completely filled band is called the

valence band and the next allowed band is called the conduction band.

1.50 General remarks on factors that affect luminescence spectra

The emission spectra of phosphors are primarily functions of compositions and structures. The locations and shapes of the emission lines and component emission bands are practically unaffected by the nature or energy of the primary excitant particle at low excitation densities. However, at high excitation densities, the phosphor crystals may become sufficiently heated to produce a relatively small temperature variation of the emission spectra. The spectral distribution of emission of a phosphor is therefore a function of (1) the composition, structure and intrinsic degree of perfection of the phosphor host crystal (2) the kinds and amounts of activators (impurities) in the crystal and (3) the temperature of the phosphor during luminescence.

1.51 Action of host crystal

Phosphor host crystals apparently perform two major functions. (1) The host crystal may have energy levels such that a suitable radiative transition is possible. This becomes more probable when a perturbing intensifier type activator impurity is incorporated in the crystal.

(2) The host crystal may function primarily as a suspension and energy transfer medium which surrounds an originative type activator atom and yet allows radiative transitions to take place chiefly in the field of the activator atom. When either the chief emitting atom or its strongly influential ligands are closely bound to the other atoms of the host crystal, the energy levels of the excited and ground states of valence electrons involved in the radiative transition are usually proliferated into bands.

1.52 Action of activators

Activators may be classified in two major groups according to their influence on the emission spectra. Some activators are found to evoke or intensify a latent emission line or band of the host crystal. These type of activators are known as intensifier activators. There is another class of activators known as originative activators which produce new emission lines or bands at the expense of the original emission bands of the host crystal. Two or more activators in suitable proportions in a given host crystal may sometimes be used to produce different emission bands.

1.53 Action of temperature

In general, the emission bands tend to become narrower and sometimes develop lines as the temperature of

the luminescent material is decreased. But in the case of Sm, Pr and Eu in various host crystals, the locations and widths of the line emission spectra are unaffected by decrease in temperature. This is because for these materials, the emission transition occur between shielded inner energy levels of atoms which have incomplete inner shells. In the case of $Al_2O_3:Cr^{3+}$ at low temperatures, the narrow bands lying on the long wavelength side become more intense in emission whereas those on the short wavelength side become more intense in absorption.

1.54 Quenching

The fluorescence of a substance is generally more affected by the environment than the absorption. For example, the fluorescence can be strongly 'quenched' ie, the quantum yield may be lowered by substances which have little influence on the absorption spectrum. Quenching processes fall into two general types, collisional quenching and quenching by formation of a complex. There are also temperature quenching, oxygen quenching, concentration quenching and impurity quenching. Quenchers of the first type effectively shorten the lifetime of the excited state. Since more collisions are possible with longer excited states, molecules with long excited lifetimes are more sensitive to this type of quenching.

The formulae giving the relation between quencher concentration and fluorescence for collisional quenching is

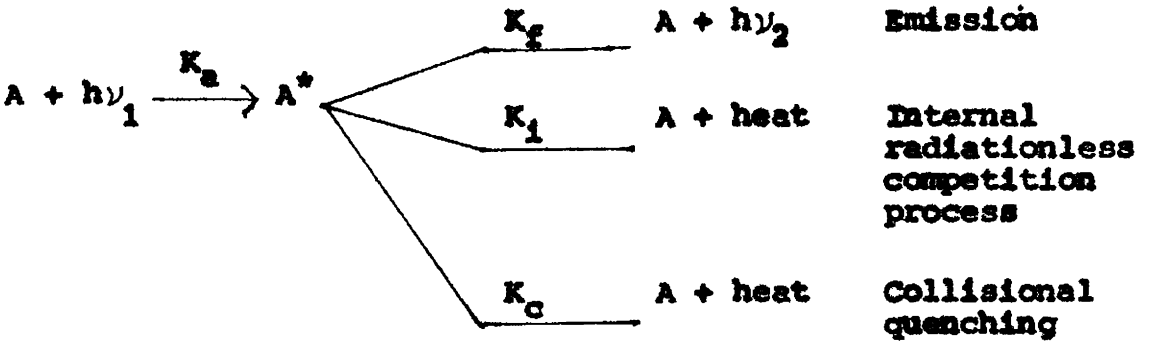

K_a, K_f, K_i and K_c are rate constants for the respective processes. A^* is the number of excited atoms.

(a) Concentration quenching

For most of the activators the luminescence intensity passes through a maximum and then decays with increase in concentration. Change of the luminescence intensity with growing concentration of the activator is different for different activators. Usually for most of the crystals the maximum is observed with the activator content of about 1%. Concentration quenching may also occur due to the interaction between ions of the same kind due to (1) the emission-reabsorption energy transfer between ions of the same kind, (2) nonradiative resonance

multiple energy transfer between ions of the same type and (3) the interaction with the charge transition band.

(b) Quenching in 'pure' crystals

In most inorganic crystals without any substantial amount of impurities, no luminescence is observed (NaCl), whereas some other pure crystals display the presence of luminescence ($CaWO_4$). This is either due to the interaction with the lattice of the excited state and subsequent relaxation or due to energy transfer from one ion to the other.

1.55 Sensitization and energy transfer

When there are two activators in a crystal, though the emission lines do not change due to the presence of the second activator, the following changes are possible. (1) The intensity of the luminescence spectrum of one ion can gain in strength at the expense of the diminishing intensity of the other. (2) An ion not luminescent at a given concentration in a given crystal becomes luminescent in the presence of another ion in a different crystal. (3) Luminescence of an ion can be observed under conditions of an excitation in which it is not luminescent without the

presence of another ion (4) Intensified luminescence can be observed from one ion with complete quenching of the other.

The above changes in luminescence of one ion in the presence of the other are due to transfer of excitation energy from one to the other. Luminescence of ions excited as a result of the energy transfer from other ions excited in the absorption band is termed sensitized luminescence and proceeds as shown below.

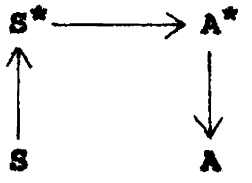

Here S is the sensitizer, A the activator and S* and A* are excited states. Sensitization is employed to raise the effectiveness of laser radiation. The transfer of energy from sensitizer to activator is accomplished by the following types of energy transfer mechanisms (Fig.1.4) (1) emission-reabsorption (2) resonance radiationless and (3) nonresonance radiationless. The energy transfer between different trivalent rare earth ions is one of the most common manifestations of sensitized luminescence.

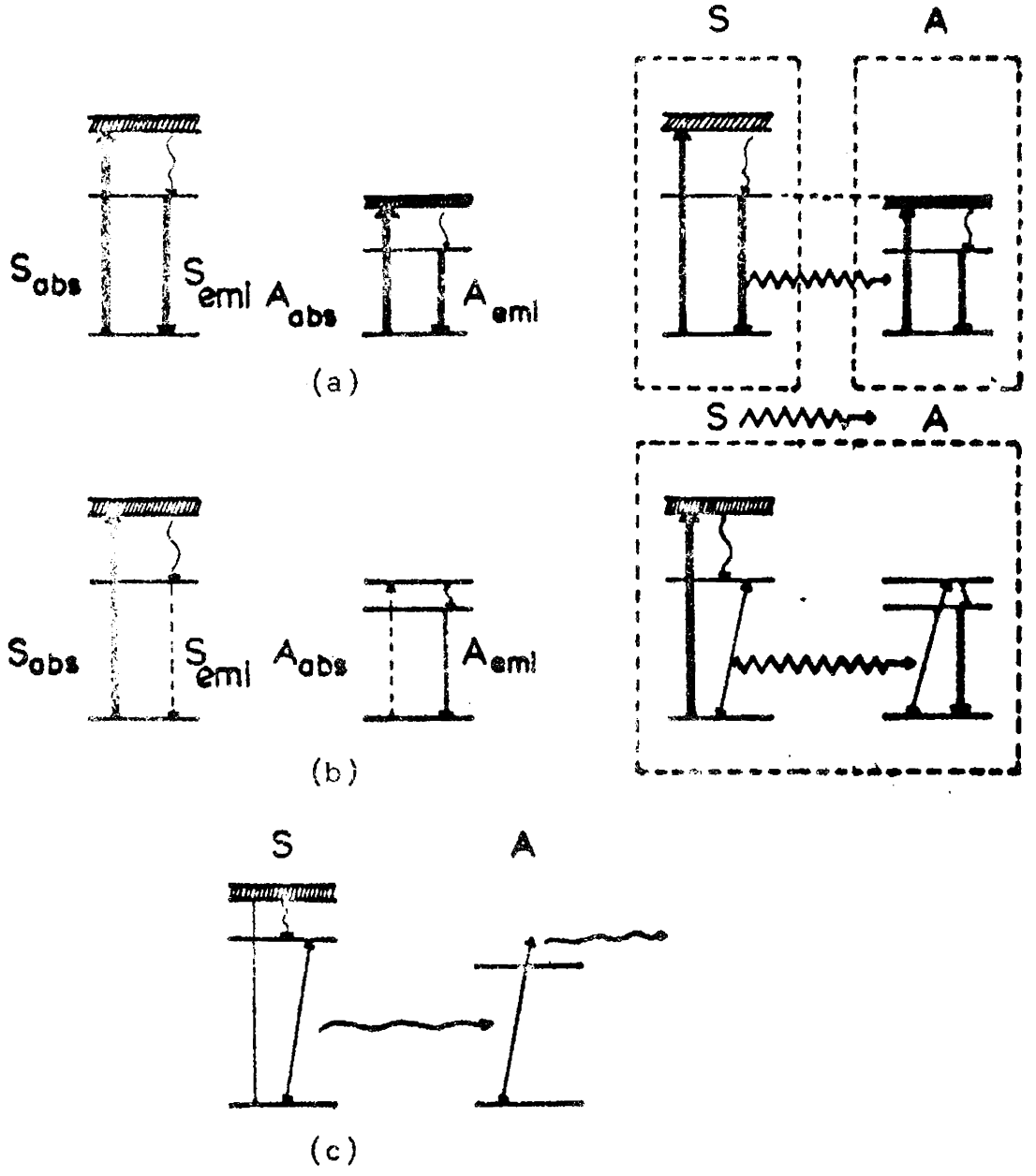

Fig.1.4 Sensitization and energy transfer

(a) - Emission reabsorption mechanism
(b) - Resonance radiationless mechanism
(c) - Non-resonance radiationless mechanism

Decay of luminescence

1.60 Kinetics of luminescence

We usually distinguish two kinds of luminescence processes that with kinetics of the first order (monomolecular mechanism) and that having second order kinetics (bimolecular mechanism).

(a) First order kinetics

The number of excited electrons 'n' decreases according to a constant probability law

$$\frac{dn}{n} = -\alpha dt \qquad (1)$$

which gives $n = n_o e^{-\alpha t}$ and since the luminescence intensity $I = \frac{dn}{dt}$

$$I = I_o e^{-\alpha t} \qquad (2)$$

The major characteristic of excited states is their lifetime, ie, the average stay of ion in a given excited state.

(b) Second order kinetics

The probability for recombination is proportional to the number of available centres

$$\frac{dn}{n} = -\alpha n dt \qquad (3)$$

and so 'n' decreases hyperbolically with time

$$n = \frac{n_o}{(1 + n_o \alpha t)} \qquad (4)$$

the luminescence decay then being given by

$$I = \left|\frac{dn}{dt}\right| = \alpha n^2 \qquad (5)$$

$$\text{thus } I = \frac{I_o}{(1 + at)^2} \qquad (6)$$

where $a = \sqrt{I_o \alpha}$

The decay thus becomes more rapid as the excitation intensity is increased.

1.61 Lifetime of a level

The lifetime of a level τ_m is related to the probability A_{mn} of transition between levels m and n and also to the oscillator strength for the absorption band f_{nm}. Relations among τ, A and f in the case of a free ion and also for an ion in a crystal are shown in Fig.1.5. In a free ion, lifetime τ_m of the excited state 'm' is inversely proportional to the transition probability A_{mn} from this level.

$$\text{ie, } \tau_m = 1/A_{mn} \tag{7}$$

The transition probability A_{mn} is linked with the oscillator strength 'f_{nm}' through the relation

$$A_{mn} = \frac{8\pi^2 e^2 \nu^2}{3m_e c^3} f_{nm} \tag{8}$$

$$\text{ie, } f_{nm} = \frac{3 m_e c^3}{8\pi^2 e^2 \nu^2} A_{mn} \tag{9}$$

Substituting the values of e, m_e and C one can write

$$A_{mn} = 0.22 \frac{\nu^2}{c^2} f_{nm} \tag{10}$$

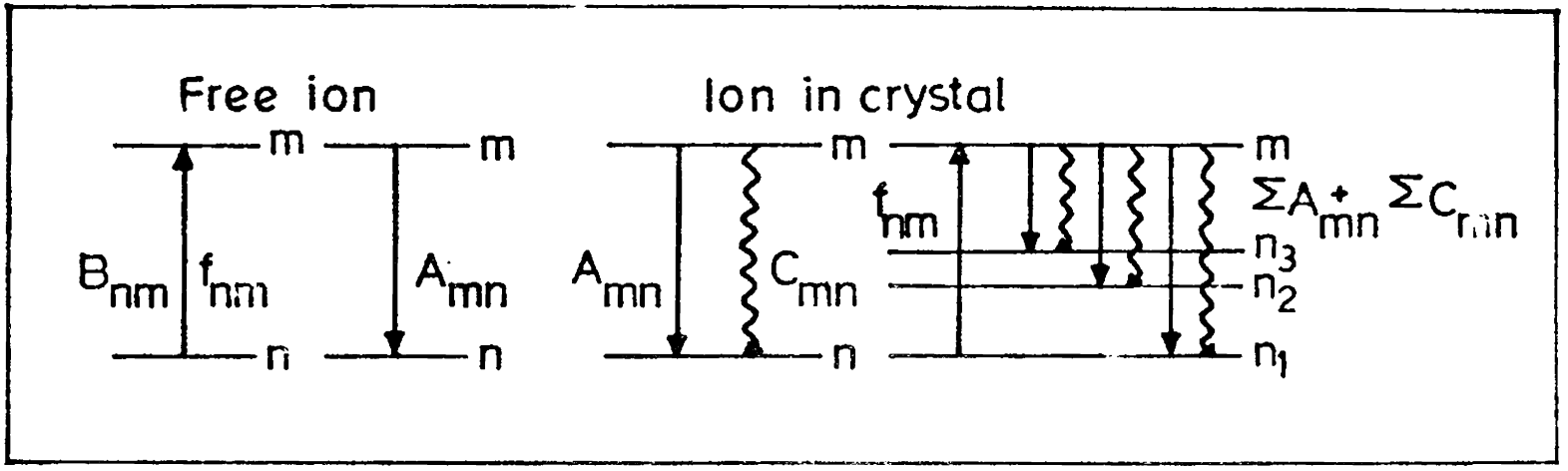

Fig.1.5 Relations among τ, A and f in the case of a free ion and for the ion in crystal

B_{nm} - probability of transition with $n \longrightarrow m$ absorption

f_{nm} - oscillator strength for absorption band $n \longrightarrow$

A_{mn} - probability of emission transition $m \longrightarrow$

ΣA_{mn} - sum total of probabilities for emission transitions $m \longrightarrow n_1$, $m \longrightarrow n_2$, $m \longrightarrow n_3$

C_{mn} - probability of radiationless transition $m \longrightarrow n$.

ΣC_{mn} - sum total of probabilities for radiationless trans $m \longrightarrow n_1$, $m \longrightarrow n_2$, $m \longrightarrow n_3$.

$$\text{or} \quad f_{nm} = 4.5 \frac{c^2}{\nu^2} A_{mn} \tag{11}$$

From the above relation one can obtain the values for the transition probabilities A_{mn} (in s^{-1}) and lifetimes τ_{mn} (in s).

If transition from a given level m occurs over several adjacent levels, the lifetime τ_m is given as

$$\tau_m = \frac{1}{\Sigma A_{mn}} \tag{12}$$

The ion in a crystal interacts with the surrounding ions resulting in radiationless transitions. The probability of radiationless transitions is the probability of luminescence decay. The lifetime of the energy levels of an ion in a crystal is then reduced due to radiationless transitions.

$$\tau_m = \frac{1}{\Sigma A_{mn} + \Sigma C_{mn}} \tag{13}$$

where C_{mn} is the probability of radiationless transition.

This value of τ_m determines the experimentally measured value of the duration of glow.

1.62 Quantum yield

The fraction of emission transitions (ΣA_{mn}) with respect to the sum of emission and radiationless transitions ($\Sigma A_{mn} + \Sigma C_{mn}$) is defined as quantum yield .

$$\eta = \frac{\Sigma A_{mn}}{\Sigma A_{mn} + \Sigma C_{mn}} \qquad (14)$$

The quantum yield may be defined as a ratio of the number of photons emitted from a given level to the number of photons excited to a given or other upper levels. The ratio between the number of photons emitted to the number of photons incident on the crystal is the apparent quantum yield. To get the true yield, the proportion of energy absorbed by a given ion with respect to the whole of the incident energy should also be considered.

$$E_{abs} = (1-R)\frac{K - K_o}{K}(1-e^{-kt}) \qquad (15)$$

where 'R' is the crystal reflection coefficient.

K_o and K are absorption coefficients of the pure crystal and the ion within the crystal. 't' is the thickness of the crystal.

1.63 Decay law

The luminescence decay law determines the diminution of the number of emitted photons with time and is designated as $N_i(t)$

$$N_i(t) = -\frac{dN_i}{dt} = -N_m A_{mn} = -\frac{N_m}{\tau_m} \qquad (16)$$

The decay law can also be rewritten as

$$N_i = N_m e^{-A_{mn}t} \qquad (17)$$

$$\text{ie.,} \quad N_i = N_m e^{-t/\tau} \qquad (17)$$

The decay thus proceeds by following the exponential law.

The radiation power P is associated with the probability of transition A_{mn}.

$$P = h\nu_{mn}A_{mn} \qquad (18)$$

Hence the emission intensity $I_{emission}$ (of free ion) can be written as

$$I_{emission} = N_m h\nu_{mn} A_{mn} \qquad (19)$$

The intensity of emission is thus determined by the probability of transition 'A_{mn}' and the oscillator strength 'f' of a given transition. In the event of transitions with great oscillator strength an interaction with the lattice can lead to a reduced emission intensity due to radiationless transitions.

1.70 Different kinds of luminescence

Luminescence may be regarded as a way of converting various kinds of energy, such as optical, nuclear, electric, mechanical and chemical into light emission. The type of luminescence emission depends on the type of energy employed for the excitation. The following types of luminescence are distinguished by the methods of their excitation.

(a) Photoluminescence - This is produced by absorption of light, usually ultraviolet.

(b) Cathodoluminescence - This luminescence is excited by accelerated particles like electron.

(c) Radioluminescence - Here excitation is by means of high energy particles like protons, α and β particles and fission fragments.

(d) Electroluminescence - Here excitation is produced by the application of an electric field.

(e) Triboluminescence - In this case the radiation is emitted by a substance subject to mechanical forces.

(f) Chemiluminescence - Excitation with liberation of a part of the energy in the form of light energy. ie, in this case emission accompanies a chemical reaction.

(g) Bioluminescence - Excitation is produced due to biological processes.

(h) Roentgenoluminescence - This is excited with the help of ordinary X-rays and its intensity increases with rising voltage.

1.71 Different types of luminescent systems

Luminescent systems in mineralogy is based on the type of the electronic structure of the glow centres. Thus we have the following luminescence systems.

(a) Transition metal ions

Fe^{3+}, Cr^{3+} and Mn^{2+} are the most largely used ions of this group and these are also used in lasers. The energy level diagram of the ions form a starting point for the analysis of their luminescence[25]. Among these levels there are emission and radiationless states and also levels onto which transitions yield broad absorption bands. The emission of the $Al_2O_3:Cr^{3+}$ system has been studied in great detail[7,26,27]. The luminescence of Mn^{2+} has also been studied well[28,29,30]. In this group Fe, Co and Ni ions are strong quenchers of luminescence.

(b) Rare earths

The spectroscopy of rare earths include optical and luminescent spectra, laser emission, formation of additive and radiation centres, EPR and thermoluminescence. By studying the RE^{3+} ion luminescence we can get information about excitation, energy transfer, the charge capture, radiation ionization, compensation of the charge and formation of electron hole centres. In mineralogy this trend has a great potential, since all the trivalent and nearly all divalent ions of rare earths are identified in the luminescence spectra of minerals.

Feofilov[4] and Dicke[31] have summed up the results of investigations on the rare earth luminescence spectra made till 1967. A summary of the lines, energy levels and parameters of the RE^{3+} in $LaCl_3$ is given by Dicke and Passwater[31,32]. The spectra of rare earths in fluorite CaF_2 were also subjected to detailed examination[33-38]. The spectra of rare earths in synthetic fluorites are now the most extensively studied system[39-43]. Fluorites with Sm^{2+}, Dy^{2+}, Tm^{2+}, Nd^{3+}, Er^{3+}, Tm^{3+} and Ho^{3+} find use as materials for lasers.

(c) Actinides

Detailed structural spectroscopic investigations of actinides have helped a lot to obtain characteristics of their electron structure in different crystals, and to interpret optical and luminescent spectra within the framework of the crystal field and molecular orbital theories[44-48]. Optical absorption and luminescence spectra of U^{2+}, U^{3+}, U^{4+} and U^{6+} in synthetic fluorite as well as the EPR spectra[49,50] along with the spectra of U^{4+} in synthetic zircon[51] have been studied in great detail.

(d) Mercury like ions; Pb^{2+}

In the activator group the next important group

of ions is of the Hg^{o} type such as Zn^{o}, Cd^{o}, Ca^{+}, In^{+}, Tl^{+}, Ge^{2+}, Sn^{2+}, Pb^{2+}, and Bi^{3+}. Of all these ions, Pb^{2+} is the only impurity which has been well studied[52-58]. This type of luminescence has become interesting for mineralogical studies after the interpretation of the Pb^{2+} spectra in feldspars and calcites[59].

(e) Electron hole centres

It is only in the case of two types of electron-hole centres that luminescence proves to be an effective method, namely for molecular ions S_2^-, O_2^- and for the F aggregate centres. The luminescence of F centres has been studied in great detail in alkali halides[60] and it has been observed in halite and fluorite[7].

(f) Crystallophosphors of the ZnS type

Natural sphalerite is a model system of considerable importance for the theories of luminescence and is a base material for luminophors[61-68]. The mechanism of its glow was subjected to detailed investigations.

1.80 Applications of luminescence

Fluorescent analysis of solids, solutions and vapours is now attracting a good deal of attention as

fluorescent substances find important industrial applications. Fluorescent impurity estimations provide a very sensitive means of detecting trace impurities in a variety of media including solvents, aromatic hydrocarbons, the atmosphere and water. Besides we can get information about molecular and crystal structure from fluorescence process and also provide insight into excitation processes which can help in defining reaction phenomena. Fluorescent analysis has developed as a special method that finds application particularly in analysing mineral raw materials[69,70]. The construction of electron probe, microanalysers and of a UV microscope made luminescence to serve as one of the methods used conjointly with microscopy.

Technical applications of luminescence include the conversion of (1) invisible light into visible in luminescent lamps (2) electron excitation into visible light, in cathode ray tubes (in radiolocation and television), (3) X-ray emission into visible light in X-ray screens and (4) nuclear radiation into visible light, in scintillators. These are joined by thermoluminescent dosimeters used for registration of nuclear explosions. Investigations into the stimulated emission of quantum generators--lasers and masers--provide a host of information on the fluorescence of rare earth ions, actinides and some transition metal ions.

Stimulated emission has been observed from some of the fluorescent crystals particularly rare earth doped crystals and are known as laser crystals. The study of the rate of luminescence decay and the quantum yield of luminescence is significant in laser physics as they are used to predict whether a given luminescence medium is suitable for lasing or not.

1.90 Laser crystals

Trivalent rare earth ions have taken a dominant position as laser-crystal activators responsible for stimulated emission processes. This is very much due to the fundamental investigations of the spectroscopic behaviour of rare earth ions in various media carried out by several scientists early in the 'prelaser' period. Stimulated emission has been observed so far in more than 280 insulating crystals. A great number of mixed fluoride crystals with RE^{3+} ions are also used in laser systems.

The most extensively used activator ion in laser crystals is trivalent Neodymium. It acts as a laser ion in about one hundred and thirty media. In the second place is Holmium followed by Erbium and Thulium. Voronko et al have extended the range of active media that have good prospects for high power lasers by including the CaF_2-Dy^{2+} crystal[71].

A good deal of impetus to research on the properties of activated crystals, particularly on the concentration quenching of the RE^{3+} ion luminescence was given by Weber et al[72]. They investigated self activated NdP_5O_4 crystals, which are now-a-days used as a model for studying weak concentration quenching of the Nd^{3+} ion luminescence.

Significant advances in the theoretical aspects of laser crystal physics were made by the investigations on the theory of crystal fields[73] and general theoretical problems of RE^{3+} ion spectroscopy. Judd and Ofelt[74] have described the theoretical aspects of RE^{3+} ion spectral intensity while Carnall, Fields and Rajnak report the theoretical analysis of energy levels of RE^{3+} ions[75]. Theory of electronic-vibrational transitions, multiphonon nonradiative transitions and chemical aspects of crystal field theory are also studied by several researchers[76].

1.91 Spectroscopy of rare earths in crystalline matrix

The most impressive feature about the spectra of rare earth (RE) ions in ionic crystals is the sharpness of many lines in their absorption and emission spectra.

The narrow optical lines suggest that the interaction of RE ions with the crystalline environment is relatively weak.

The rare earths in solids are either divalent or trivalent. Their electronic configurations are $4f^n5s^25p^6$ and $4f^{n-1}5s^25p^6$ respectively. The most common valence state of the rare earth ion in solids is the trivalent one. Table 1.1 gives some basic information about the rare earth: atomic number, element, outer electronic shell, free ion ground term and Lande g_j factor for the trivalent state.

The 4f electrons of the rare earths are not the outermost ones. They are shielded from external fields by two electronic shells with larger radial extension ($5s^25p^6$), which explains the atomic nature of their solid state spectra. Due to the shielding, the 4f electrons are only weakly perturbed by the charges of the surrounding ligands.

This is why the rare earth ions are used as probes in solids. The spectroscopic properties can be understood from a consideration of the free ions. The energy levels of the 4f configuration for trivalent free

Table 1.1

The rare earth elements and some of their spectroscopic properties

Atomic Number	Element	Electron configuration RE^{3+}	Ground term RE^{3+}	Lande' factor $g_J RE^{3+}$
57	Lanthanum	$4f^0(5s^25p^6)$	$^1S_0$	0
58	Cerium	$4f^1(5s^25p^6)$	$^2F_{5/2}$	6/7
59	Praseodym	$4f^2(5s^25p^6)$	$^3H_4$	4/5
60	Neodymium	$4f^3(5s^25p^6)$	$^4I_{9/2}$	8/11
61	Promethium	$4f^4(5s^25p^6)$	$^5I_4$	3/5
62	Samarium	$4f^5(5s^25p^6)$	$^6H_{5/2}$	2/7
63	Europium	$4f^6(5s^25p^6)$	$^7F_0$	0
64	Gadolinium	$4f^7(5s^25p^6)$	$^8S_{7/2}$	2
65	Terbium	$4f^8(5s^25p^6)$	$^7F_6$	3/2
66	Dysropium	$4f^9(5s^25p^6)$	$^6H_{15/2}$	4/3
67	Holmium	$4f^{10}(5s^25p^6)$	$^5I_8$	5/4
68	Erbium	$4f^{11}(5s^25p^6)$	$^4I_{15/2}$	6/5
69	Thulium	$4f^{12}(5s^25p^6)$	$^3H_6$	6/7
70	Ytterbium	$4f^{13}(5s^25p^6)$	$^2F_{7/2}$	8/7
71	Lutecium	$4f^{14}(5s^25p^6)$	$^1S_0$	0

rare earth ions have been analysed in the arc spectra for Pr^{3+}[77] Gd^{3+}[78] and Er^{3+}[79].

If the ion is introduced into a crystal, the ion experiences an inhomogeneous electrostatic field—the crystal field, which is produced by the charge distribution within the crystal. It removes the M_J degeneracy of the free ion 4f levels. Experiments have shown that for trivalent rare earth ions, the crystal field interaction is smaller than the energy separation of the various free ion terms.

Fig.1.6 shows energy levels of all RE^{3+} in the CaF_2 lattice.

(a) Absorption spectra of rare earth ions

In the absorption spectra of the rare earth ions in crystals transitions are observable between levels arising within the limits of the $4f^n$ configuration (f-f transition) and the levels of $4f^n \longrightarrow 4f^{n-1}5d$ and other mixed configurations. Transitions within the $4f^n$ configuration lead to the line spectrum consisting of weak narrow absorption bands revealing a fine structure.

Transitions onto the levels of mixed $4f^{n-1}5d$ configuration, and also onto the $4f^{n-1}6s$ and $4f^{n-1}6p$

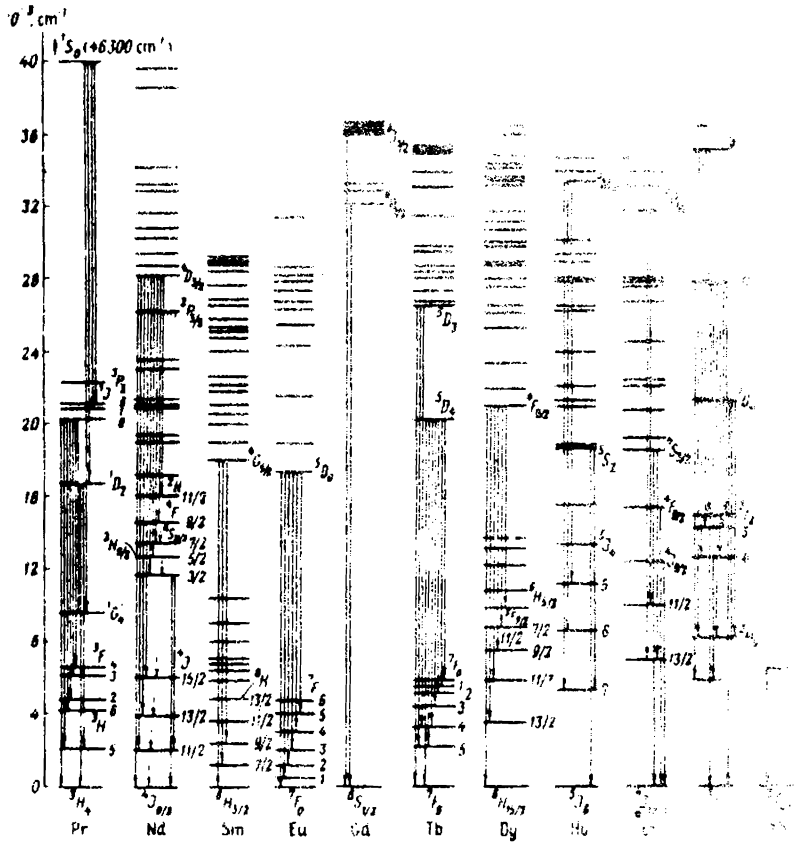

Fig.1.6 Schematic diagram of energy levels and transitions of rare earth ions in CaF_2 lattice.

levels, result in the appearance of broad intensive absorption bands. In these transitions, the oscillator strength is 3-4 orders higher than that for the forbidden f-f transitions. The oscillator strength is found to be of the order of 10^{-2}-10^{-5}. At low temperatures very narrow lines of electron-vibrational transitions appear superposed upon broad bands.

(b) Luminescence spectra of rare earth ions

The RE^{3+} spectra arising from f-f transitions are line spectra and they consist of a large number of narrow and weak lines. The presence of a large number of lines in the RE^{3+} luminescence spectra is due to the splitting up of lower multiplets into terms. The fine structure of the RE^{3+} absorption and luminescence spectra depend on the characteristics of the crystal, the presence of co-activators, local or nonlocal compensation of the charge, the manner of the ion's incorporation in the complex with an F centre and concentration of the activator. The luminescence spectra also depend on the conditions under which the spectra are observed like temperature and method of excitation.

Three individual cases are distinguished in the RE^{2+} luminescence spectra[80], (1) broad bands due to

d-f transitions (Eu^{2+}, Sm^{2+} in CaF_2) (2) line spectra of the f-f transitions (Dy^{2+}, Ho^{2+}, Er^{2+}, Tm^{2+} in CaF_2) and (3) broad bands at room temperature and line spectra on cooling (Sm^{2+} in SrF_2 and BaF_2). In low temperature spectra of some RE^{2+} (Sm^{2+}, Eu^{2+}) narrow lines with electron-vibration replicas are seen superposed on the bread bands. It is also observed that even if the concentration is kept the same the relative intensities of the luminescence of different rare earths are different because of the variation in oscillator strength.

1.92 Fluorites

Investigations into the spectra of rare earths in synthetic fluorites are now the most extensively studied system. The investigations include mainly observation and interpretation of the luminescence spectra with low and high resolution.

Luminescence and absorption spectra of all the RE^{3+} and RE^{2+} in fluorite have been reproduced and interpreted and some of the rare earths are observed to form a complex centre (RE^{3+} + F centre) in fluorites. With high resolution several types of incorporation in the structure, depending upon the mode of the charge compensation can be

distinguished for each RE^{3+} ion. Fluorites are widely used as materials for lasers after doping them with rare earths. For the study of the relations of RE^{3+} in natural fluorites with different compensation, the high resolution luminescence spectra, absorption spectra and the EPR spectra are necessary.

1.93 Colour centres in crystals and their luminescence

In contrast to the wealth of data available on most alkali halide single crystals, we still know very little regarding the nature of the trapping centres and the mechanism of luminescence in activated artificial MeF_2 type crystals where Me = Ca, Sr or Ba. A considerable amount of investigations were done earlier on the thermostimulated luminescence and colouring of natural fluorite[81-86]. Further experiments have shown that the low temperature thermoluminescence may be due to the destruction of the self trapped state of the holes. It is known that when MeF_2-TR^{3+} phosphors are irradiated at a temperature of 77°K or lower, the holes formed in the crystals as a result of the Coulomb interaction approach a neighbouring F^- ion (Fluorine ion) form an F_2^- quasimolecule, and thereby enter into a self trapped state[82,87] which can be detected either by observation of electron paramagnetic resonance, or by

measurement of the additional absorption in the optical region. The presence of electron acceptor impurities in crystals greatly enhances the formation of the self trapped state. According to the data of Hayes and Twidell,[87] this self trapped state in CaF_2 is destroyed at a temperature of about 138°K. An appreciable part of the released holes recombine with trapped electrons, while a certain part may again be trapped, forming centres analogus to the V_F and H centres in LiF and other alkali halide crystals.

The colour centres in alkali halides are usually divided into electron centres F and F aggregate and hole centres, V centres. In the optical absorption spectra of alkali halides one can observe V absorption bands in the UV region in addition to the intense F band and bands due to F aggregate centres occurring in visible region. The models of these centres were originally suggested by Seitz[88] by analogy with the models for F centres. V_1 centre (hole trapped by cation vacancy) is antimorph of the F centre, V_2 centre (two holes trapped by cation vacancies) is antimorph of R_2 centre model etc.

Molecule ions Hal_2^- (Hal-Halogen) occur in three varieties depending on defects with which they are linked.

(i) V_K centre is a molecule ion Hal_2^- taking up the position of two usual ions, when one of them looses its electron[89].

This centre is linked neither with vacancies or interstitials. It is called a self trapped hole. In the fluorite V_K centre F_2^- is oriented along [100] and accordingly has three non-equivalent positions and the V_K centre disappears at 138 K. Similar V_K centres have been observed in SrF_2, BaF_2 and $SrCl_2$.

(ii) H centre is a molecule ion Hal_2^- replacing the position of one Hal^- ion. Chemically, it is equivalent to an interstitial Hal^0 atom, but is better described as Hal_2^- ($Hal^0 + Hal^- = Hal_2^-$). It is an interstitial Hal_2^- centre[90].

(iii) V_F centre is a molecule ion Hal_2^- replacing the position of the cation M^+ vacancy ie, it is a hole centre antimorph to the F centre ie, a hole trapped by the cation vacancy, but divided not among six anions surrounding it, but only between two of them. In natural fluorites after their X-ray irradiation at 77K and heating above 138K one can observe V_K centres representing F_2^- molecule ions taking up the Ca^{2+} vacancy position[91].

All the Hal_2^- ions have the same 11 electron configuration. These eleven electrons are distributed all over the molecular orbitals $(\sigma_g)^2$ $(\pi_u)^4$ $(\pi_g)^4$ $(\sigma_u^*)^1$ The unpaired electron occupies the antibonding orbital. If one looks

at the $HalI_2^-$ centre as a molecule with an axial and not an orthorhombic symmetry then the ground state is to be designated $^2\Sigma_u^+$ and the excited states as $^2\Pi_g$, $^2\Pi_u$, $^2\Sigma_g^+$.

REFERENCES

1. H.W.Leverenz, An introduction to luminescence of solids, John Wiley & Sons Inc, London (1950).

2. A.A.Kaminskii, V.V.Osiko, Neorg laser material with ionic structure, Neorg.Mater, 1, 2049; 3, 417; 6, 629 (1965, 1967, 1970).

3. V.V.Antonov-Romanovsky, Kinetics of photoluminescence of phosphor crystals, Moscow Nauka (1966).

4. Feofilov, The luminescence of rare earths, Proc.Int. Conf.Luminescence, Budapest, 2, 1727 (1968).

5. M.V.Fock, Introduction to kinetics of luminescence of crystallophosphors, Moscow, Nauka (1964).

6. B.S.Gorobels, G.A.Sidorenko, Luminescence of secondary uranium minerals at low temperatures, Atomic Energy, 36, 6-13 (1974).

7. A.N.Tarashchan, Luminescence of minerals, Kiev:Naukova dumka, (1978).

8. N.Kristianpoller and B.Trieman, J.Luminescence, 24, 285 (1981).

9. H.Munekata, S.Murasato and H.Kukimoto, Appl.Phys.Letts, 37, 536 (1980).

10. R.Carius, R.Fischer and E.Holzenkampfer, J. Luminescence, 24, 47 (1981).

11. T.Minami, H.Nanto and S.Takata, J.Luminescence, 24 63 (1981).

12. T.Inoguchi, M.Takeda, Y.Kakihara, Y.Nakata and M.Yosheda, Digest 1974, S.I.D.Int.Symp. (1974).

13. J.D.Schanda, J.Luminescence, 25, 851 (1981).

14. D.A.Weitz, S.Garoff, C.D.Hanson and T.J.Gramila and J.I.Gersten, J.Luminescence, 24, 83 (1981).

15. A.Goetzberger and W.Greubel, Appl.Phys, 14, 123 (1977).

16. W.H.Weber and J.Lambe, App.Optics, 15, 2299 (1979).

17. H.W.Moos, J.Luminescence, 1,2, 106 (1970).

18. Bansi Lal and D.Ramachandra Rao, J.Phys.Chem.Solids, 40, 97 (1979).

19. H.J.Schulz in Current topics in material science, North Holland Publishing Company, Amsterdam (1981) p.7.

20. O.Hidebrand, O.E.Goebel, K.M.Romanek, H.Weber and G.Mahler, Phys.Rev B, 17, 4775 (1978).

21. R.F.Lehney and J.Shah, Phys.Rev.Letts, 37, 871 (1976).

22. E.O.Gobel, W.Graudzus, P.H.Liang, J.Luminescence, 25, 573 (1981).

23. P.M.Selzer in Laser spectroscopy of solids, vol.49, Springer Verlage (1981).

24. W.M.Yen and Selzer, IBID, p.141.

25. D.Curie, Luminescence in crystals, John Wiley & Sons Inc., New York (1963).

26. P.Gorlich, H.Karras, G.Kotitz, R.Lehmann, Phys. Status Solidi, 5, 3 (1965).

27. G.Burns, E.A.Geiss, B.A.Jenkins, M.I.Nathan, Phys. Rev, 139A, 1687 (1965).

28. J.H.Schulzman, L.W.Evans, R.J.Ginther, K.J.Murata, J.Appl.Phys, 18, 732 (1947).

29. P.Goldberg, Luminescence of inorganic solids, Academic Press, London-New York (1966).

30. W.W.Holloway, E.W.Prohofsky, M.Kistigian, Phys.Rev. 139A, 954 (1965).

31. G.H.Dicke, Spectra and energy levels of rare earth ions in crystals, Interscience Publishers, New York (1968).

32. R.A.Passwater, Guide to fluorescence literature, vol.3, Plenum Press, New York (1974).

33. K.R.Laud, E.F.Gibbons, T.Y.Tien, H.L.Stadler, J.Electrochem Soc, 118, 918 (1971).

34. J.L.Merz and P.S.Pershan, Phys.Rev. 162, 217 (1967).

35. V.V.Osiko, Neorg Mater 5, 433 (1969).

36. N.Rabbiner, Phys.Rev, 132, 224 (1963).

37. P.P.Sorokin, Electronique Quantique, C.R.3 Conf. Int. New York (1964) 985.

38. Yu.K.Voronko, B.I.Denker, V.V.Osiko, Phys.tverd.tela, 13, 2193 (1971).

39. V.F.Barabonov, G.N.Goncharov, Dokl.Akad.Nauk, 173, 1408 (1967).

40. I.Huber Schausberger, E.Schroll, Geochim.Cosmochim Acta, 31, 1333 (1967).

41. J.V.Nicholas, Nature, 215, 1476 (1967).

42. L.N.Ovchinnikov, V.G.Mascenkov, Geol.Rud.Mestorozhd, 6, 3 (1965).

43. N.N.Vasilkova, S.G.Solomkina, Typomorph features of fluorite and quartz, Moscow (1965).

44. W.T.Carnall, P.R.Fields, Lanthanide - Actinide Chemistry, 86 (1967).

45. G.H.Dicke, A.B.F.Duncan, Spectroscopic properties of uranium compounds, McGraw Hill, New York (1949).

46. N.Edelstein, W.Easley, R.McLaughlin, Lanthanide - Actinide Chemistry, 203 (1967).

47. M.Fred, Lanthanide - Actinide Chemistry, 1820 (1967).

48. E.Rabinowitch, R.L.Belford, Spectroscopy and photochemistry of uranyl compounds, Pergamon Press, New York (1964).

49. W.A.Hargreaves, Phys.Rev.B, 2, 2273 (1970).

50. J.V.Nicholas, Nature, 215, 1476 (1967).

51. I.Richman, P.Kisiluk, E.Y.Wong, Phys.Rev.155, 262 (1967).

52. D.Bramanti, M.Mancini, A.Ranfagni, Phys.Rev, 133, 3670 (1970).

53. M.L.Kats, Luminescence and electron hole processes in photochemically colored alkali halide compounds, Saratov Univ. (1960).

54. A.I.Komiak, A.N.Sevchenko, M.M.Sidorenko, Izv.Akad. Nauk, Ser Phys, 34, 576 (1970).

55. Ch.B.Lushchik, Proc.Inst.Phys.Ast.Akad.Nauk. Est, SIK, 31, 19 (1966).

56. J.H.Schulman, R.D.Kirk, Solid State Commun. 1, 105 (1964).

57. O.I.Slid, Theory of luminescence center in crystal, Univ edn. (1968).

58. K.Teegarden, Luminescence of inorganic solids, Academic Press, New York (1966), 53.

59. A.N.Tarashcan, A.I.Serebrennikov, A.N.Platanov, Constitution and properties of minerals, 4, 63 (1970).

60. G.Lehmann, Phys, Kondens, Mater, 13, 297 (1971).

61. Sh.Shinoya, J.Luminescence, 1-2, 17 (1970).

62. Ch.S.Kang, P.P.Beverley, R.H.Bube, Phys.Rev, 156 998 (1967).

63. H.E.Gumlich, H.J.Schulz, Phys.Chem.Solids, 27, 187 (1966).

64. Gool W.Van, Philips Res.Repts, Suppl. N 3, 1 (1961).

65. A.G.Fischer, Luminescence of inorganic solids, Academic Press, New York (1966) 541.

66. F.J.Bryant, A.F.Fox, Br.J.Appl.Phys, 16, 463 (1965).

67. J.L.Birman, Proc.Int.Conf.Luminescence, Budapest, (1968) 919.

68. N.Arpiarian, Proc.Int.Conf.Luminescence, Budapest, (1968) 903.

69. E.J.Bowen, Luminescence in chemistry, London (1968).

70. N.S.Poluektov, L.I.Kononenko, Spetrophotometric methods of determination of individual rare earths, Naukova dumka (1968).

71. Yu.K.Voron'ko, V.V.Osiko, A.M.Prokherov, I.A.Shcherbakov, Proc.P.N.Lebedev Phys.Inst, 60, 1-30 (1974).

72. H.P.Weber, T.C.Damen, H.G.Darielmeyer, Appl.Phys.Lett. 22, 534 (1973).

73. B.G.Wybourne Spectroscopic properties of rare earths, Wiley, New York (1965).

74. B.R.Judd, Phys.Rev, 127, 750 (1962).

75. W.T.Carnall, P.R.Fields, K.Rajnak, J.Chem.Phys, 49, 4424 (1968).

76. K.K.Rebane, Impurity spectra of solids, Plenum Press, New York, London (1970).

77. J.Sugar, Phys.Rev.Lett, 14, 731 (1965).

78. J.F.Kielkopf and H.M.Crosswhite, J.Opt.Soc.Am. 60, 347 (1970).

79. H.M.Crosswhite and H.W.Moos, Conf.Opt.Properties of ions in crystals, Wiley Interscience, New York (1967) 3.

80. P.P.Feofilov, Phys.Maths-isdat (1959).

81. V.A.Arkhangelskaya, Opt. and Spectroscopy, 16, 628 (1964).

82. W.Hayes and J.W.Twidell, Proc.Phys.Soc, 79, 1295 (1962).

83. W.Kanzig, Proc.Intern.Conf. on Semicond.Physics, Prague (1960) 705.

84. Z.J.Kiss and R.C.Duncan, Proc.IRE, 50, 1531 (1962).

85. Z.J.Kiss, Phys.Rev, 127, 718 (1962).

86. Ya.E.Kariss and P.P.Feofilov, Optics and Spectroscopy 15, 572 (1963).

87. W.Hayes, G.D.Jones and J.W.Twidell, Proc.Phys.Soc, 81, 371 (1963).

88. F.Seitz, Rev.Mod.Phys, 26, 7 (1954).

89. W.Kanzig, T.O.Woodruff, J.Phys.Chem.Solids, 9, 70 (1958).

90. W.Kanzig, Proc.Int.Confer.Semicond.Phys, Prague (1961) 705.

91. J.Scirro, Phys.Rev, 138A, 650 (1965).

92. A.S.Marfunin, Spectroscopy, luminescence and radiation centres in minerals, Springer Verlag, New York (1979) 302.

CHAPTER II

SPECTRAL STUDIES AND POWER ENHANCEMENT OF A PULSED N_2 LASER

2.10 Introduction

Pulsed laser action in N_2 gas has been observed and described by several authors[1-9]. The high peak power, short duration and short wavelength are important properties that make this device suitable for several applications. Transversely Excited Atmospheric (TEA) Nitrogen lasers of different designs have been reported[10-15] with pulse widths in the nanosecond and subnanosecond regimes and output peak powers of a few Megawatts. Attempts have also been made quite successfully by Dreyfus and Hodgson[16] to generate coherent radiation at 337.1nm using high energy electron beam excitation of N_2.

The mechanism of the laser action in N_2 is unusual as the lifetime of the upper $C^3\Pi_u$ level is about 40 nsec; much shorter than that of the lower $B^3\Pi_g$ level which is about 6 μsec. Population inversion can still be achieved due to the fact that the electron excitation cross section is about twice as large for the upper level as for the lower level. So, by using a very fast discharge,

the system can be inverted. To maintain the necessary electron temperature and make the discharge faster, transverse excitation is used in most cases. As the cross-section of induced emission for the $C^3\pi_u \longrightarrow B^3\pi_g$ transition is large, the population inversion in the system decays very rapidly, and, in most cases, the gain overcomes the loss of photons for the single pass of the active medium. Therefore no mirrors are necessary if the length of the laser exceeds a certain threshold length.

In transversely excited nitrogen lasers only the 337.1nm radiation has been commonly observed. But Kaslin and Petrash[17] has observed an amplification effect in the (0,1) 357.7nm and (1,0) 315.9nm bands of the second positive system of N_2. Later several others have reported the appearance of the 357.7nm line along with the 337.1nm emission of N_2[18,19]. Many researchers have analysed the 337.1nm band of the N_2 laser spectra and have identified a number of rotational lines belonging to the P and R branch transitions in the nitrogen molecule[20-24]. Suchard et al[25] have reported bands due to (0,1), (0,2), (1,2) and (1,3) transitions in the N_2-SI_C laser emission.

In this study, Nitrogen laser emission spectra was analysed and a large number of vibrational bands belonging to the $C^3\pi_u - B^3\pi_g$ second positive system of the N_2 molecule were identified.

Considering the applications of the N_2 laser, there is a definite advantage in using this laser to develop continuously tunable dye lasers. In addition to this major application, Kobayasi et al[26] have used a TEA pulsed N_2 laser with a repetitive frequency of 100 cycles/sec. for the atmospheric pollution study.

Some preliminary two photon absorption studies in alkali halides have been made with this laser and it has been observed that the UV radiation is absorbed resulting in the formation of an exciton which subsequently is trapped at an imperfection in the crystal giving rise to F centres[27]. It is also found that with this laser important free radicals like CH and C_2 in several combustion reactions could be pinpointed to extremely small regions as was shown by Barnes[28].

Finally, it has been observed that a good number of rare earth ions in different crystals absorb this radiation strongly to emit fluorescence in the visible and

infrared regions with good fluorescence yield. The additional advantage of using this laser compared to continuous lasers is that with high peak power of extremely short duration, lifetime measurement of fluorescence of excited states (of rare earth ions) in a number of crystals is a clear feasibility.

It is desirable to increase the output power of transversely excited (TE) nitrogen laser for increasing the fluorescence yield and also for making it ideal for some recently suggested high power applications[29,30]. Subsequent to the earlier attempts of Searles[31] many researchers have tried to enhance the output power of TE N_2 laser by using additives like SF_6, Ar, CF_4, F_2 and BF_3. It is believed that these additives help either in the efficient pumping of the $C^3\pi_u$ state or in the quenching of the $B^3\pi_g$ state of the nitrogen molecule.

Levatter and Lin[32] tried Argon, SF_6 and various members of the Freon and Genitron family (eg. trichloro-fluoro methane, dichlorofluoro methane, chlorotrifluoro methane etc.). Among these additives, SF_6 was found to increase the output power while Argon and members of the Freon and Genitron family showed no observable effect and

some were found to create arcing. A maximum increase of about 1.7 times was observed with 10-20% of SF_6 added to N_2 gas.

Using SF_6 as the additive Suchard et al[25] also observed increase in output power in the first positive as well as the second positive system of N_2 molecule. They observed the 357.6nm (0-1) emission to be more intense than 337.1nm (0-0) emission band of nitrogen. The action of SF_6 is to deactivate the lower level in a short time compared to the rate of spontaneous deactivation from the upper laser level. This was against the result of Willet and Litynski[33] who had attributed the increase in power to a modification of the electron energy distribution by SF_6 or its discharge products, to the one that favours the excitation of the upper laser levels. The maximum power increase reported in N_2-SF_6 mixture is 140% (N_2 = 30 torr and SF_6 = 4 torr) by Mahendale and Bhawalkar[34]. They have also reported 25% increase in the power with BF_3 (7 torr) and N_2 (30 torr)[35].

Various amines such as triethyl amine, tripropyl amine etc. which have low ionization potentials were also tried by many investigators. Using triethyl amine Kurnit et al[36] observed almost 100% increase in the output power.

Long pulse operation of an electron beam sustained (300ns) N_2 laser with CF_4 as additive has been reported by Collier et al[37] in which the deactivation of the $B^3\pi_g$ state was achieved due to irreversible transfer of vibrational energy of N_2 to CF_4 during collisions. A sudden jump in laser wavelength from 337.1nm to 357.7nm for a small increase in CF_4 partial pressure was also reported. At 337.1nm the pulse width was about 100-150ns while at 357.7 emission the pulse width was 70ns. It may be noted that with the usual TE N_2 lasers using SF_6 as an additive the maximum pulse width reported[38] is 70ns. Sumida et al[39] have reported 30% increase in output power with 4% F_2 and 96% N_2 at a total pressure of 120 torr. Variation of N_2 laser power with addition of gases has been studied by Savadatti et al also[40].

Mau-song Chou[41] has observed long pulse laser emissions at 357.7nm, 380.5nm and 405.9nm in the second positive system of N_2 with pulse durations of 150, 300 and 400ns by adding Ne and He into N_2 + Ar mixtures. Experimental studies on the factors affecting the 357.7nm band in a Blumlein N_2 laser has also been reported[42].

It is interesting to look at the role played by these foreign gases in enhancing the power output efficiency

of the N_2 laser, because there are at present a number of conflicting theories which try to explain the function of these gases. The most widely used additive has been SF_6. The pulse width as well as output power at 337.1 shows a significant change and laser transition at 357.7nm also appears in the presence of SF_6.

The problems associated with SF_6 and most other fluorine derivatives is in handling the gas system in a closed discharge under continuous pumping and also the high cost of these gas mixtures. Hence with a view of finding out some new additives, vapours of electronegative and low ionization potential organic and inorganic solvents having saturated vapour pressures of the order a few torrs are used to enhance power.

The details of the N_2 laser the spectral studies made on the N_2 laser emission and the experimental attempt made to increase the power of N_2 laser with additives are described below.

2.20 Details of the N_2 laser

The design of the N_2 laser is shown in Fig.2.1. The laser is excited transversely by a pulse forming circuit which consists of four parallel plate transmission lines,

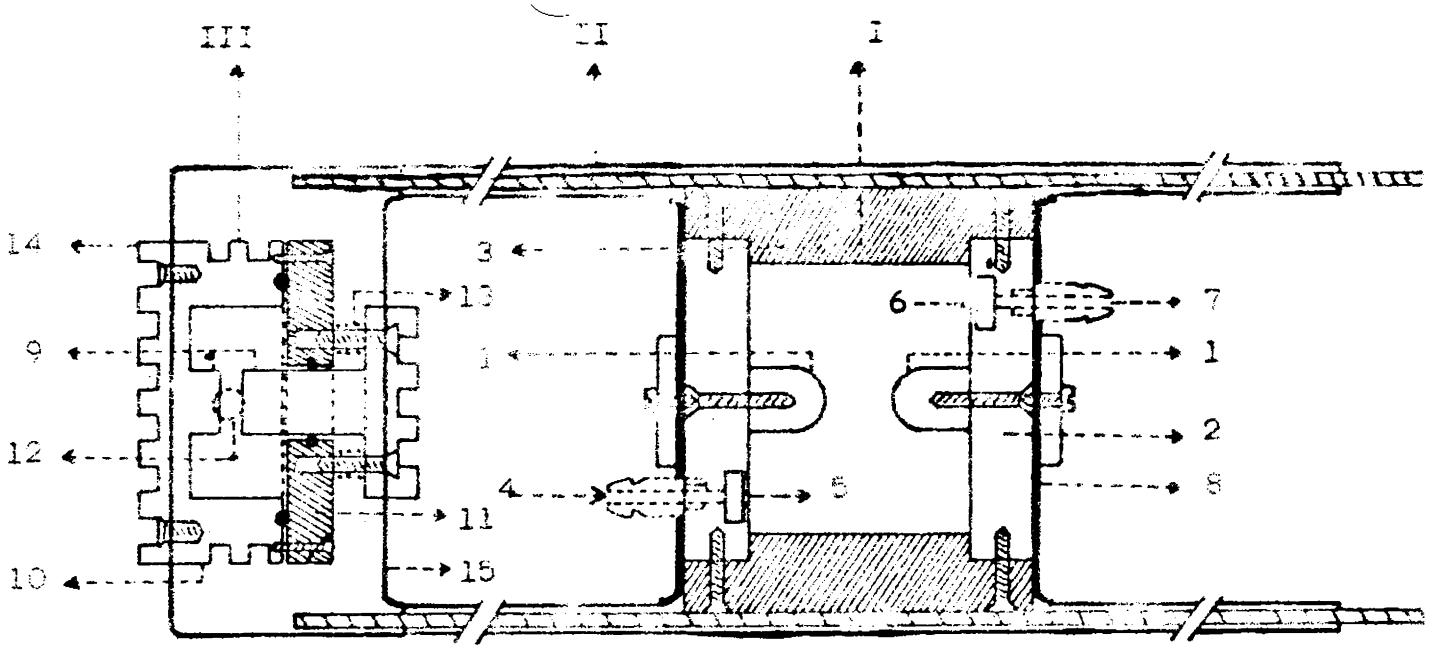

Fig.2.1 Cross sectional view of N_2 laser

I - Laser cavity - 1.Aluminium electrodes, 2. Aluminium side plate 3. Perspex, 4. Gas from cylinder, 5. Gas inlet to the cavity through small holes, 6. Gas outlet from the cavity, 7. To the vacuum pump, 8. Copper strip as connecting leads.
II - Double side copper clad glass epoxy laminate
III - Spark gap - 9. Aluminium electrodes, 10. Aluminium cup on which cathode is machined, 11. Perspex lid, 12. Gas inlet, 13. Spring loaded gap adjusting screw, 14. Cooling Fin, 15. Copper strip as connecting leads.

two above and two below on both sides of the cavity. These transmission lines are charged to ten or more kilovolts by a D.C. power supply. When one pair of the transmission lines is short circuited at its end by a spark gap, a transient voltage occurs transverse to the laser cavity, creating a powerful discharge between the electrodes. The electrons produced in the discharge collide with the N_2 molecules and excite them to the upper energy levels. With suitable E/P values (of the order of 25 volt/cm/torr) the N_2 molecules could be taken to the upper $C^3\pi_u$ state from where it can come down to the $B^3\pi_g$ state emitting the 337.1nm radiation. Uniform distribution of N_2 molecules inside the cavity, and hence better shot to shot reproducibility is achieved by letting in and pumping out the gas through 10 ports transverse to the cavity.

The transmission lines are made out of Formica double side copper clad glass epoxy laminates (CFG6/2DS) of thickness 1.6mm. The laser cavity has an effective length of 40cm. The electrodes are made of Aluminium and the cavity is closed at one end by an Aluminium coated mirror and the other end by a quartz window. The spark gap is pressurised with 1-2 atmosphere of N_2 gas. This enables to obtain a fast discharge inside the laser cavity.

The electrodes of the spark gap are of Aluminium and the physical size of the spark gap is minimised to reduce its inductance.

The capacitance of the transmission line is

$$C = \frac{1.11 \times 2E \times L \times l}{4\pi S} = 11.8nf$$

where E = 4.7, the dielectric constant of the glass epoxy laminate, L = 40cm, the length of the cavity, l = 57cm, the length of the transmission line and S = 1.6mm, the thickness of the dielectric. The value of C gives a stored energy of 3.2 joules at 20KV. The characteristic impedance of this double parallel plate transmission line S is given by

$$Z = \frac{Z_o}{2\sqrt{E}} \times \frac{S}{L} = 0.348$$

where Z_o = 377, the impedance of free space.

Travelling wave excitation of the gas is achieved by keeping the electrodes of the cavity slightly tilted. In this mode of excitation, the electrical discharge strikes at one end of the cavity and moves towards the other end with the velocity of light. Spontaneous emission produced

at one end gets amplified along the laser axis and comes out of the cavity after a single pass; ie, without a feed back. This is possible owing to the short lifetime (10-20 nsec) of the $C^3\pi_u$ state of N_2 molecule.

2.30 Parametric measurements

The pulse width of the N_2-laser is measured using a Hewlett Packard hP_2-4207, silicon pin photodiode of rise time $\simeq$ 0.3ns and a 100MHz Tektronix Model 466 DM44 storage oscilloscope. The whole circuitary used for pulse width measurement is shown in Fig.2.2. It is found that the pulse width at FWHM is 8ns and at base is 17-18ns. Typical output trace is shown in Fig.2.3.

The average output power of the laser is measured using Scientech Model 38-0101 volume absorbing 1 inch disc calorimeter (thermopile). The average power is measured at 12KV with a spark gap pressure of 1.5 atmospheres of N_2 and a cavity pressure of 60 torr. The energy per pulse is obtained by dividing the average power by the repetition rate while the peak power is obtained by dividing the energy per pulse by the pulse width at FWHM. The laser is found to give a peak power of 225KW at 12KV, 60 torr.

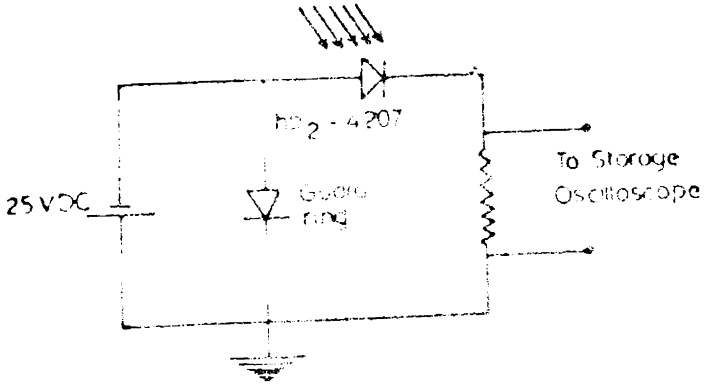

Fig.2.2 Photodiode circuit for pulse width measurement

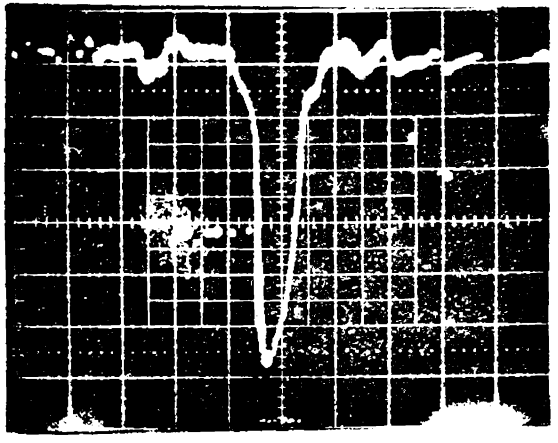

Fig.2.3 N_2 laser pulse shape

Sweep speed – 10 ns/DIV

gain – 50 mv/DIV

2.40 Spectral studies of N_2 laser emission

The laser emission spectrum is charted using a 0.5M Jarell Ash Ebert Scanning monochromator (Model 82-000), an EMI Model 9683 KQB photomultiplier tube and Omniscribe Model, B127-IIX-t recorder. The grating used is the one blazed at 190nm and has a linear dispersion of 1.6nm/mm in the first order. The PMT has a fairly constant quantum efficiency in the 300-400nm spectral range where the present investigations were carried out. The PMT was operated at 1350V d c derived from an EMI model PM28B high voltage power supply and the output was taken across a 450Ω resistor and fed to the recorder.

The emission spectra is charted with sufficient resolution and is found to consist of various bands in addition to the 337.1nm. A typical record of the emission spectrum at 12KV charging voltage charted for a double Non Blumlein N_2 laser[43] is shown in Fig.2.4. Care was taken not to saturate the (0,0) 337.1nm band while recording. Table 2.1 gives a listing of the various bands observed, their relative intensities and assignments. Although the second most intense band arising from the $C^3\pi_u - B^3\pi_g$ second positive system of the N_2 molecule is the (0,1) band with a relative intensity of 7.4%, two other bands with relative intensities of 29% and 8.2% were observed at 331.83 and 340.85nm respectively.

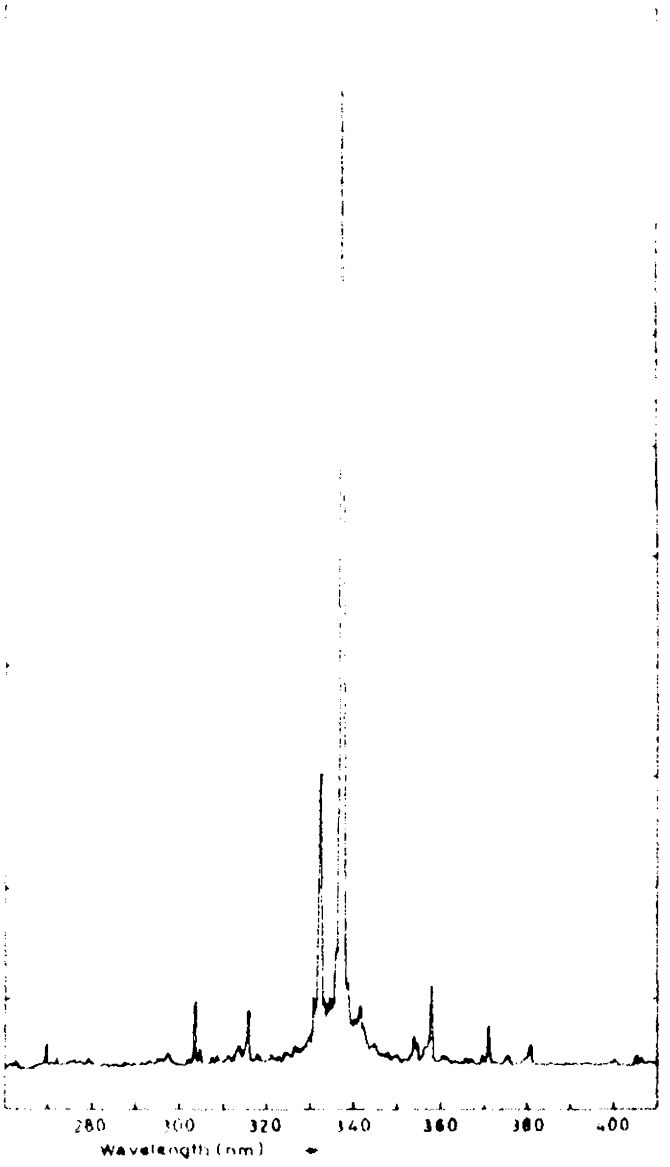

Fig.2.4 N_2 laser emission spectra at 12KV
Scanning speed - 250Å/Min.
Chart speed - 2.5 cm/Min.

Table 2.1

Assignments and relative intensities of the vibrational bands of N_2 laser spectra

Laser emission wavelength (nm)	Relative intensity (%)	Assignment
337.13	100	(0,0) band of $C^3\pi_u$-$B^3\pi_g$ N_2 second positive system
331.83	28.34	Transition from one of the mixed vibrational levels of the C and C' states of the N_2 molecule
340.85	8.16	(3,11) band of $B^3\pi$-$X^2\pi$ NO β system
357.69	7.36	(0,1) band of $C^3\pi_u$-$B^3\pi_g$ N_2 second positive system
303.49	7.04	(0,7) band of $B^2\pi$-$X^2\pi$ NO β system
371.05	5.91	(2,4) band of $C^3\pi_u$-$B^2\pi_g$ N_2 second positive system
315.93	5.03	(1,0) band of $C^3\pi_u$-$B^3\pi_g$ N_2 second positive system
380.49	$\leq$ 2.0	(0,2) band of $C^3\pi_u$-$B^3\pi_g$ N_2 second positive system
405.94	$<$ 2.0	(0,3) band of $C^3\pi_u$-$B^3\pi_g$ N_2 second positive system
375.54	$<$ 2.0	(1,3) band of $C^3\pi_u$-$B^3\pi_g$ N_2 second positive system
399.84	$<$ 2.0	(1,4) band of $C^3\pi_u$-$B^3\pi_g$ N_2 second positive system
353.67	$<$ 2.0	(1,2) band of $C^3\pi_u$-$B^3\pi_g$ N_2 second positive system

To establish whether the observed bands were due to stimulated or spontaneous emission, the laser spectra were recorded with the monochromator at 1.5, 5.0 and 8.2 m from the laser output window with the laser operated at 60 torr N_2 and 8KV charging voltage. The 1180 groves/mm grating used in the monochromator was 500nm blazed (The grating was changed to rule out the possibility of ghosts due to gratings appearing in the spectrum). The entrance and exit slitwidths were 240 and 640 μm respectively. The variation in the relative intensity of the various bands with distance from the laser head is shown in Fig.2.5. The reduction in intensity of the 331.83 and 340.85nm bands as the monochromator to laser head separation was varied from 1.5 to 8.2 m was only 1.9 and 2.4% respectively. But for all the other bands there was a larger reduction in intensity for the same change in separation. For example, the 357.69nm band reduced in relative intensity by 12.7% at 8.2 m. Thus it can be assumed that amplification effect and stimulated emission have taken place at the 331.83 and 340.85nm bands in the nitrogen discharge and that the other bands appearing in the output are due to spontaneous emission.

331.83nm band

Though many new vibrational bands have been identified in the nitrogen laser spectra, the most important

among them was the 331.83nm band. This band was observed in the emission spectrum with the maximum relative intensity of $\backsim$ 29%. The band was seen degraded to the red region unlike the $C^3\pi_u - B^3\pi_g$ bands degraded to violet, with its peak at 331.83nm and extending from 331.67 to 332.45nm. The spectral width at FWHM of this band was 0.42nm. Fig.2.6 is a high resolution scan of the 331.83nm band along with the (0,0) 337.13nm band. Considering the accuracy of the measurement made, this band could not be identified with any reported bands belonging to the second positive system or any other N_2 systems or to NO, CO or CN systems or to impurities like Al or C that may be present in the discharge channel[44].

In the study of the atomic flame spectra of aliphatic amines in active nitrogen, Pannetier et al[45] observed a band at 325.92nm and interpreted it as the (5,5) band of the $C^3\pi_u - B^3\pi_g$ second positive system of Nitrogen. Tanaka and Jursa[46] also observed four weak red degraded triplet bands, with term values higher by 140cm^{-1} than Pannetier et al[45] and believed to originate from the $C^3\pi_u$ (V'= 5) level. But, bands with V'> 4 are not usually observed in the $C^3\pi_u - B^3\pi_g$ second positive system due to predissociation in the upper state[47]. Based on the study

of the strong "non-crossing rule interaction" observed between the levels of the $C^3\Pi_u$ and $C'^3\Pi_u$ states, Carroll and Mulliken[48] interpreted the Pannetier level as mostly C and the Tanaka-Jursa level as mostly C′. They also examined the vibrational structure of the region of interaction, considering the predissociation of the C state by the C′ state and found that the V = 0 level of the C′ state was mixed with the C state and that these mixed vibrational levels showed different degrees of C and C′ character. Thus the 331.83nm band observed in the present investigation can only be a transition originating from one of the mixed vibrational levels of the C and C′states.

The level to which a gas molecule is excited in a discharge depends mainly on the energy transferred by the electrons and ions present while the rise time of this discharge is a function of the laser cavity and spark gap inductances. Thus the appearance of this new band, originating from one of the mixed vibrational levels of C and C′ states in the N_2 laser spectra in contrast to earlier reports, can be attributed to the difference in the laser cavity and spark gap inductances of the discharge circuit.

It is possible to enhance the stimulated emission intensity of the above band by using narrow band dielectric coated rear mirrors for the laser cavity and providing

suitable discharge conditions. All the other bands appearing in the spectrum have been previously identified and are discussed in detail in[43].

2.50 Power enhancement of N_2-laser

The N_2 laser is found to operate quite satisfactorily for continuous operations. An attempt is made to increase the power output of this laser using some additives. Of these, 70% increase in output power is observed with 1-2,Dichloroethane, 45% with Carbontetrachloride and 42% increase with Thionyl chloride.

2.51 Experimental set up used for adding additives to N_2 gas

The gas input assembly to the laser tube is modified, as shown in Fig.2.7 to monitor the additives. The partial as well as the total pressure is read on the same manometer. Needle valves are used to control the partial pressures of N_2 and the additive. The variation in the average power of the laser is measured using a Scientech calorimeter. The pulse shape is recorded on a 100MHz Tektronix Storage Oscilloscope using a hp_2-4207 photodiode of rise time $\simeq$ 0.3ns.

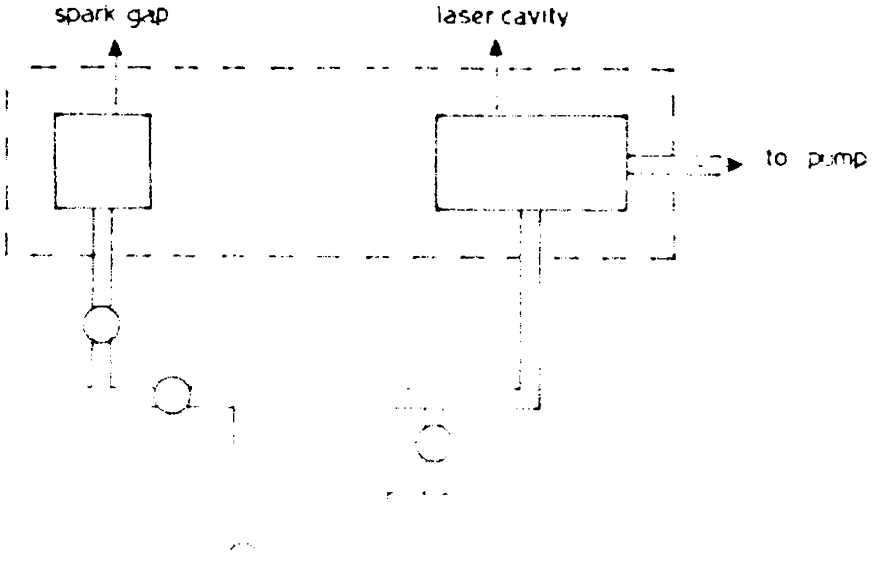
spark gap
laser cavity
to pump

2.52 Power variation with 1,2-dichloroethane (CH_2Cl-CH_2Cl)

Keeping the N_2 gas pressure fixed, the additive pressure was increased slowly upto 4 torr. The experiment then was repeated at different N_2 pressures from 30-150 torr. The repetition rate was kept constant throughout the experiment. The energy per pulse value for different Nitrogen pressures for pure nitrogen and 2,3 and 4 torrs of 1,2-Dichloroethane is shown in Fig.2.8. A maximum increase of about 71% was observed with 140 torr N_2 and 4 torr CH_2Cl-CH_2Cl at a repetition rate of 25 pps. Moreover, the additive assisted in the formation of a uniform discharge inside the laser tube and also helped to reduce the arcing usually observed at high pressures. In the pressure range 50-70 torr of N_2, no appreciable effect was observed while at pressures below 50 torr the output power gradually decreased.

The emission spectra was also recorded using a 0.5 meter Jarrell-Ash monochromator. The increase in the output power was found to be only due to the increase in the 337.1nm emission intensity and not due to the appearance or increase in intensity of any other line. The usefulness of this additive at higher N_2 pressures can be due to its high thermal conductivity and its

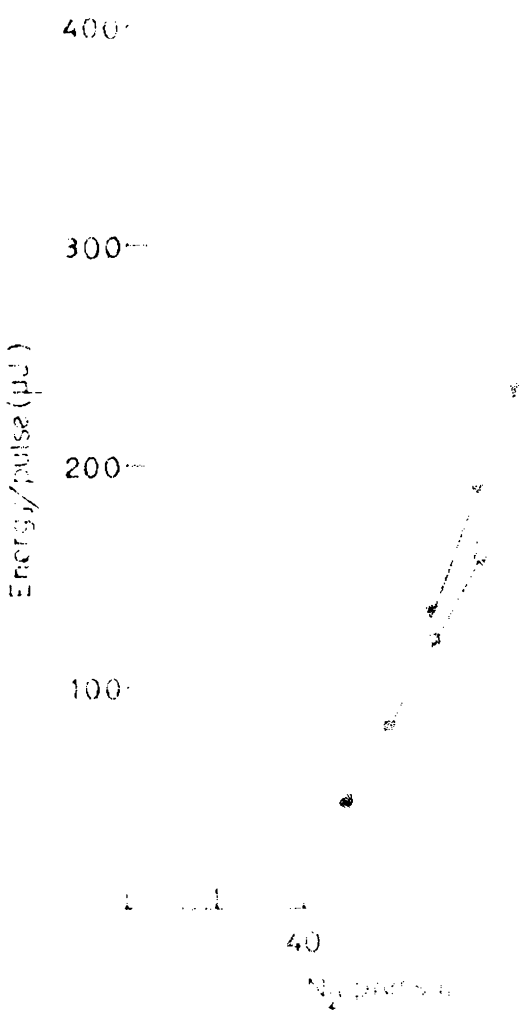

Fig.2.8 Variation of energy/pulse for [illegible]
● ● N [illegible]
△ △ N_2^+ [illegible]

efficiency in depopulating the lowest vibrational level of the $B^3\Pi_g$ state. The pulse width of the laser emission with the additive was found to be slightly larger than that with nitrogen alone.

2.53 Power variation with carbon tetrachloride (CCl_4)

Keeping N_2 pressure at a fixed value ($\simeq$30 torr) the pressure of CCl_4 was varied to 2,4,6 torr and the average power was measured using the calorimeter. Then the nitrogen pressure was varied in steps of 10 upto 150 torr and the whole experiment was repeated. The repetition rate was kept fixed at 25 pps throughout the experiment. The energy per pulse Vs. N_2 pressure for 2 torr and 4 torr of CCl_4 are shown along with that of N_2 alone in Fig.2.9. At 6 torr pressure of CCl_4, the output energy per pulse was lesser than that observed at a pressure of 4 torr. A maximum increase of about 46% was observed with 120 torr of N_2 and 4 torr of CCl_4.

Study of the laser emission spectra with the additive CCl_4 did not show any additional lines. It can therefore be inferred that the power increase was basically due to the increase in the 337.1nm radiation intensity. In this case also the pulse width was found to be slightly greater than that with nitrogen alone.

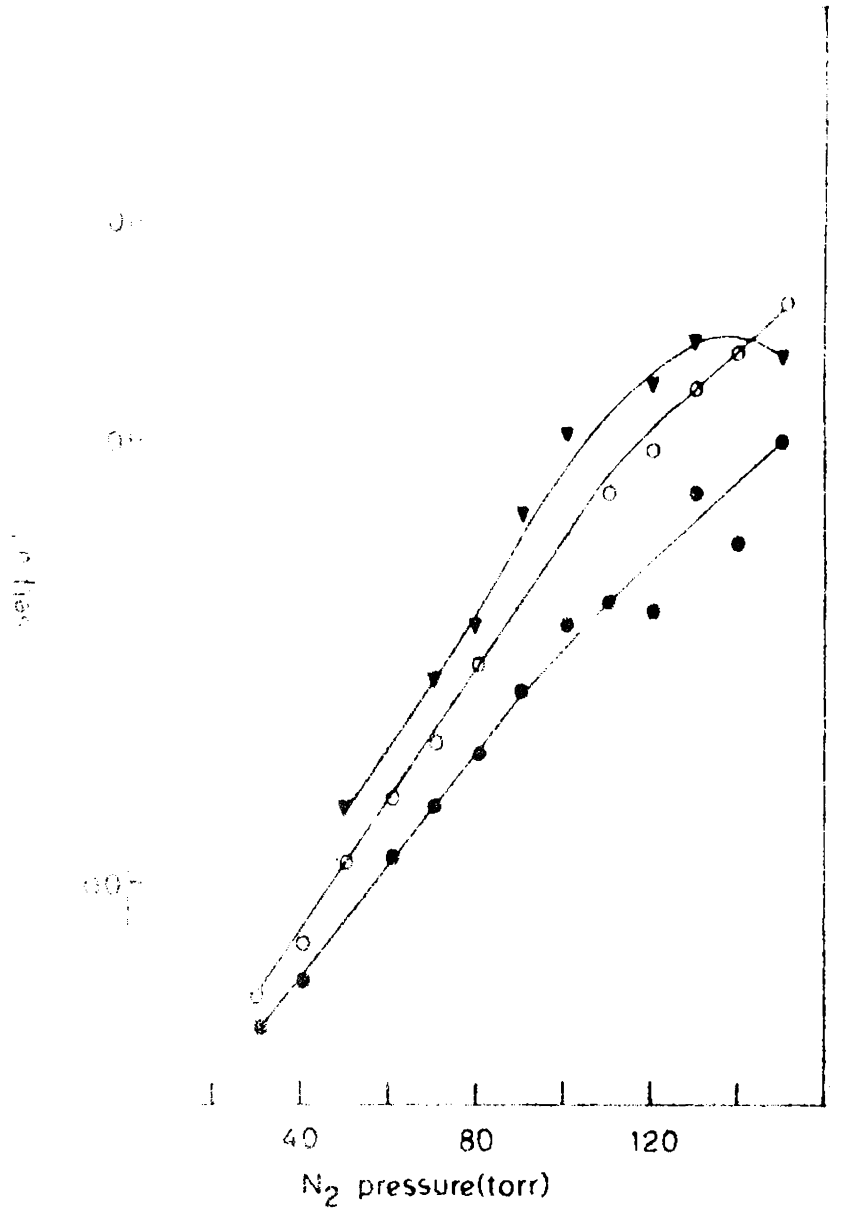

Fig. 1 Variation of energy/pulse with N_2 pressure for N_2 alone and N_2 + carbon tetrachloride.

O—O N_2 alone O—O N_2 + 2 Torr additive

▲—△ N_2 + 4 Torr additive.

2.54 Power variation with Thionyl Chloride ($SOCl_2$)

With Thionyl Chloride at 6 torr, the N_2 pressure was varied from 30 to 150 torr and the increase in output energy per pulse obtained is plotted in Fig.2.10. A maximum increase of 41.8% was observed at 90 torr of N_2. The emission spectra did not show any additional lines and the pulse width was also found to vary only slightly.

2.55 Other additives

Many other additives like Dichloromethane, Trichloroethane, Acrylonitrile, Chlorobenzene, Chloroform and Triethyl amine were also tried along with nitrogen. Dichloromethane did not appreciably increase the output power. A maximum increase of about 20% is observed with 140 torr of N_2 and 3 torr dichloroethane. Beyond a partial pressure of 3 torr, it creates arcing at low N_2 pressures.

With Trichloroethane no arcing could be observed, but there was a reduction in power.

Acrylonitrile and Chlorobenzene did not produce any observable effect. Chloroform did not increase the power and arcing starts even below 1 torr of $CHCl_3$.

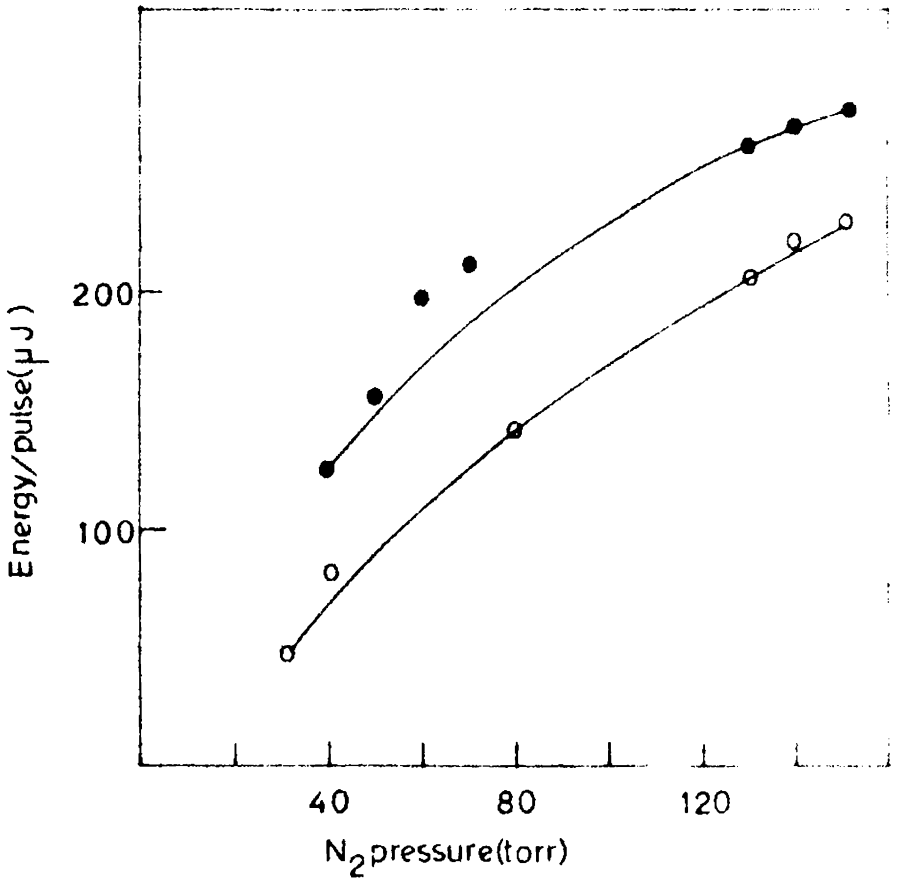

Fig.2.10 Variation of energy/pulse with N_2 pressure for N_2 alone and N_2 + Thionyl-chloride.

O—O N_2 alone ●—● N_2 + 6 Torr additive.

Two torr of Triethyl amine with 40 torr N_2 gave about 91.5% increase in output power. But later when the experiment was repeated after distilling the additive, the output power did not show any significant increase or decrease.

Various mixtures of these additives were also tried along with nitrogen. Triethyl amine and 1-2 Dichloro-ethane, POPOP and Hexane, Carbontetrachloride and triethyl amine were studied at different partial as well as total pressures. No such combination could improve the discharge characteristics or the output power.

2.60 Results and discussion

Power increase in N_2 laser using 1,2-Dichloro-ethane, Carbon tetrachloride and Thionyl Chloride as additive is reported here. The percentage of increase observed in the present study using these three additives is shown in Fig.2.11. It can be seen that 1,2-Dichloro-ethane (CH_2Cl-CH_2Cl) is more effective in increasing the output power at higher N_2 pressures. Usually, when N_2 lasers are operated in the 120-150 torr range one can see the discharge as having a flame like appearance. The observation of a better uniform discharge and increase in the output power in the 80-150 torr pressure range can be

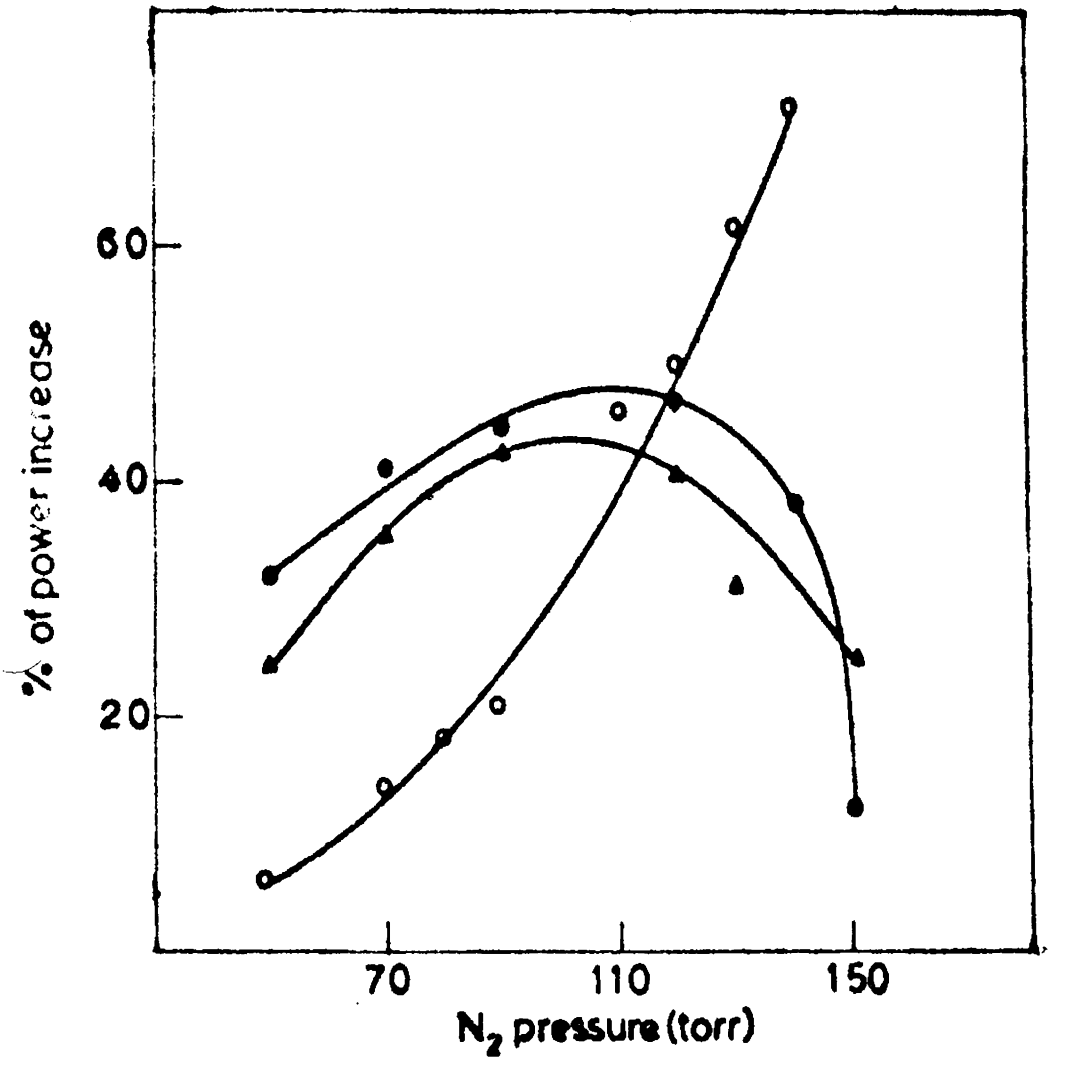

Fig.2.11 Percentage of power increase with additives for different N_2 pressures.

O—O 1,2-Dichloroethane + N_2

●—● Carbontetrachloride + N_2

▲—▲ Thionyl chloride + N_2

attributed to an increase in thermal conductivity of N_2 molecules due to the addition of 1,2-Dichloroethane. The maximum increase in output is obtained at 140 torr of N_2.

In contrast, the percentage of increase using carbon tetrachloride and Thionyl chloride is somewhat uniform throughout the pressure range 50-150 torr, with maximum efficiency of around 90 torr. So, to a first estimate we attribute the nature of increase in power to the one that is due to the fast deactivation processes made possible from the $B^3\pi_g$ state by vibrational quenching and not due to any improvement in the excitation cross section of the $C^3\pi_u$ state. This deactivation process takes place in a time fast compared to the rate of spontaneous deactivation of the upper level. Thus CCl_4 and $SOCl_2$ effectively 'unblocks' the self terminating feature of conventional N_2 lasers to a certain extent. The difference in discharge behaviour for different additives may be due to some being easily ionizable.

Though power enhancement could be achieved with the above additives the pulse width was found to increase with additives. Besides it is found to be very difficult with the present set up to control flow of additives at a uniform pressure for more than half an hour. Hence for the

fluorescence studies carried out with the N_2 laser no additives were used along with N_2 gas.

REFERENCES

1. Heard, Nature, 200, 667 (1963).

2. D.A.Leonard, Appl.Phys.Lett. 7, 4 (1965).

3. E.T.Gerry, Appl.Phys.Lett. 7, 6 (1965).

4. M.Geller, D.E.Altman and T.A.De Temple, Appl.Opt. 7, 2232 (1968).

5. D.Basting, F.P.Schafer and B.Steyer, Opto Electron. 4, 43 (1972).

6. J.C.Small and R.Ashari, Rev.Sci.Instrum. 43, 1205 (1972).

7. B.W.Woodward, V.J.Ehlers and W.C.Lineberger, Rev. Sci.Instrum. 44, 882 (1973).

8. B.Godard, IEEE J.Quantum Electronics, 10, 147 (1974).

9. J.P.Girardeau Montant and C.Girardeace Montant, Nouv.Rev.Opt. 5, 179 (1974).

10. E.E.Bergmann, Rev.Sci.Instrum, 48, 545 (1977).

11. E.E.Bergmann, App.Phys.Letts, 31, 661 (1977).

12. V.Hasson et al, Appl.Phys.Letts, 28, 17 (1976).

13. Herden, Phys.Lett. 54A, 96 (1975).

14. B.S.Patel, Rev.Sci.Instrum. 49, 1361 (1978).

15. R.Cubeddu and S.M.Curry, IEEE J.Q.E, QE-9, 499 (1973).

16. R.W.Dreyfees and R.T.Hodgson, Appl.Phys.Lett. 20, 195 (1972).

17. V.M.Kaslin and G.G.Petrash, Sov.Phys. JETP, 27, 561 (1968).

18. W.A.Fitzsimmons, L.W.Anderson, C.E.Riedhauses and J.M.Vrtilek, IEEE J.Quantum Electronics, QE-10, 624 (1976).

19. J.Itani, K.Kagawa and Y.Kimura, Appl.Phys.Letts. 27, 503 (1975).

20. T.Kasuya and D.R.Lide, Appl.Opt.6, 69 (1967).

21. J.H.Parks, D.R.Rao and A.Javan, Appl.Phys.Letts. 13, 142 (1968).

22. M.Gallardo, C.A.Massone and M.Garavaglia, Appl.Opt. 7, 2418 (1968).

23. A.Petit, F.Launay and J.Rostas, Appl.Opt. 17, 3081 (1978).

24. J.P.Singh and S.N.Thakur, Appl.Opt. 19, 1967 (1980).

25. S.N.Suchard, L.Galvan and D.G.Sutton, Appl.Phys.Letts. 26, 521 (1975).

26. T.Kobayasi, M.Jakemura and H.Shimutu, Proc.Quantum Elec.Conference Montreal (1972).

27. Kirchiro Kagawa and Toshizo Nakaya, J.Phys.Soc.Japan, 38, 901 (1975).

28. R.H.Barnes, C.E.Moeller, Kimcher J.F. and C.M.Verfer, Appl.Opt. 12, 2531 (1973).

29. V.S.Letokhov, Science, 180, 451 (1973).

30. B.B.Snavely, VIII International Quantum Electronics Conf., Sanfranscisco (1974).

31. S.K.Scarles, VIII International Quantum Electronics Conf., Sanfranscisco (1974).

32. J.I.Levatter and Shao Chin Zin, Appl.Phys.Letts, 25, 703 (1974).

33. C.S.Willett and D.M.Lityanski, Appl.Phys.Letts, 26, 118 (1975).

34. S.C.Mehendale and D.D.Bhawalkar, Laser Division Technical Report, BARC.

35. S.C.Mehendale and D.D.Bhawalkar, J.Appl.Phys, 53, 6445 (1982).

36. N.A.Kurnit et al, IEEE J.Quantum Electron, QE-11, 174 (1975).

37. P.Collier, G.Thiell and P.Cotton, Appl.Phys.Letts, 32, 739 (1978).

38. O.Judd, IEEE J. Quantum Electron, QE-12, 78 (1976).

39. S.Sumida et al. Appl.Phys.Letts, 34, 31 (1979).

40. M.I.Savadatti, B.S.Kunabenchi and M.R.Gorbal, Indian J.Phys. 54, 204 (1980).

41. Mau-Songchou and Gerald A.Zawadzkas, IEEE J.Quantum Electron, QE-17, 77 (1981).

42. Tetsuya Mitani, Appl.Phys. 52, 3159 (1981).

43. N.Subhash, Ph.D. Thesis, Cochin University (1981).

44. P.W.B.Pearse and A.G.Gaydon, The identification of molecular spectra, Chapman & Hall, London (1976).

45. G.Pannetier, L.Marsigny and H.Guenebaut, C.R.Acad. Sci, 252, 1753 (1961).

46. Y.Tanaka and A.S.Jursa, J.Opt.Soc.Am. 51, 1239 (1961).

47. A.Lofthus and P.H.Krupenie, J.Phys.Chem.Ref.Data 6, 113 (1977).

48. P.K.Carroll and R.S.Mulliken, J.Chem.Phys. 43, 2170 (1965).

CHAPTER III

FLUORESCENCE SPECTRA OF PURE ALKALINE EARTH FLUORIDES (CaF_2, SrF_2 and BaF_2)

3.10 Introduction

The alkaline earth fluoride compounds have been utilised as a matrix for trivalent cation dopants in an extensive number of experiments. They are found to be the best host crystals for rare earth ions and are widely used as laser crystals[1] after doping them with rare earths. Alkaline earth fluorides (CaF_2, SrF_2 and BaF_2) are also useful in many fields of application, for example, radiation dosimetry[2,3] and photochromic effects[4,5]. Moreover, these crystals are used as windows for UV lasers[6] as these are found to have little absorption in the UV and optical regions. They are widely used as low-loss components on UV excimer lasers. Therefore several of the alkaline earth halides possessing the fluorite structure have been studied fairly extensively. These fluoride crystals have recently been the objects of numerous spectroscopic investigations by different groups of authors.

Studies of intrinsic defects in alkaline earth fluorides have been carried out by several authors with additive coloration[7], X-rays[8,9], electron[10] and neutron[11]

irradiation at low temperatures. Ionizing radiations are much less effective even at low temperatures on the production of intrinsic point defects (eg. F,V_K,H) in undoped alkaline earth fluorides. The F centre (an electron trapped in a fluorine vacancy) in additively coloured crystals has been identified by Arends[7] using ESR techniques. Further, a V_K centre (the self trapped hole), a V_H centre (a hole trapped at an interstitial fluorine site called an H centre) and a V_{KA} centre (the impurity associated hole) induced by X-ray irradiation at 77K in Tm doped alkaline earth fluorides have been investigated in detail by Beaumont et al[12] through optical, ESR and thermoluminescent methods.

The thermoluminescence of rare earth doped alkaline earth fluorides below room temperature has been investigated by many workers[13-18]. In particular, the thermoluminescence of rare earth doped CaF_2 crystals irradiated with X or γ rays at 77K has been studied systematically by Merz and Pershan[13,14]. The kinetics of the thermoluminescence build up in CaF_2 had been well studied by Aramu[19] and Atobe[20]. Atobe[21] has also studied the growth of F band in undoped CaF_2 by reactor irradiation at low temperatures. He has also shown that there is a close correspondence between annealing steps of the F band intensity and glow peaks in the thermoluminescence process for neutron irradiated SrF_2 crystals[22].

Using positron spectroscopy, the study of charge transitions of rare earth ions in CaF_2 has been done by Arefev[23]. An investigation of the relaxation of the absorption of pure and doped CaF_2 crystals has been done after irradiating with a nanosecond pulse of 200 KeV electrons at temperatures from 100 to 520K by Lisitsyn[24], and has estimated the energy of formation of radiation defects in CaF_2.

Knowledge of the behaviour of the pure materials with temperature, pressure and excitation energy can provide a basis for an understanding of the behaviour of the doped and mixed crystals. Some temperature dependent Raman measurements and the pressure dependence of the optic phonon frequencies in some alkaline earths have been already reported[25,26]. Also room temperature infrared transmission, reflection measurements and emission measurements have been made on CaF_2, BaF_2, SrF_2 and $SrCl_2$[27,28,29]. Rehn[30] has measured the bulk loss coefficient in two CaF_2 samples between 200 and 400nm using the prism technique and has observed a strong peak at 305nm.

The photoluminescence study of these alkaline earth fluorides are also done by several researchers[31,32,33]. Beaumont et al[12] have observed a broad asymmetric emission

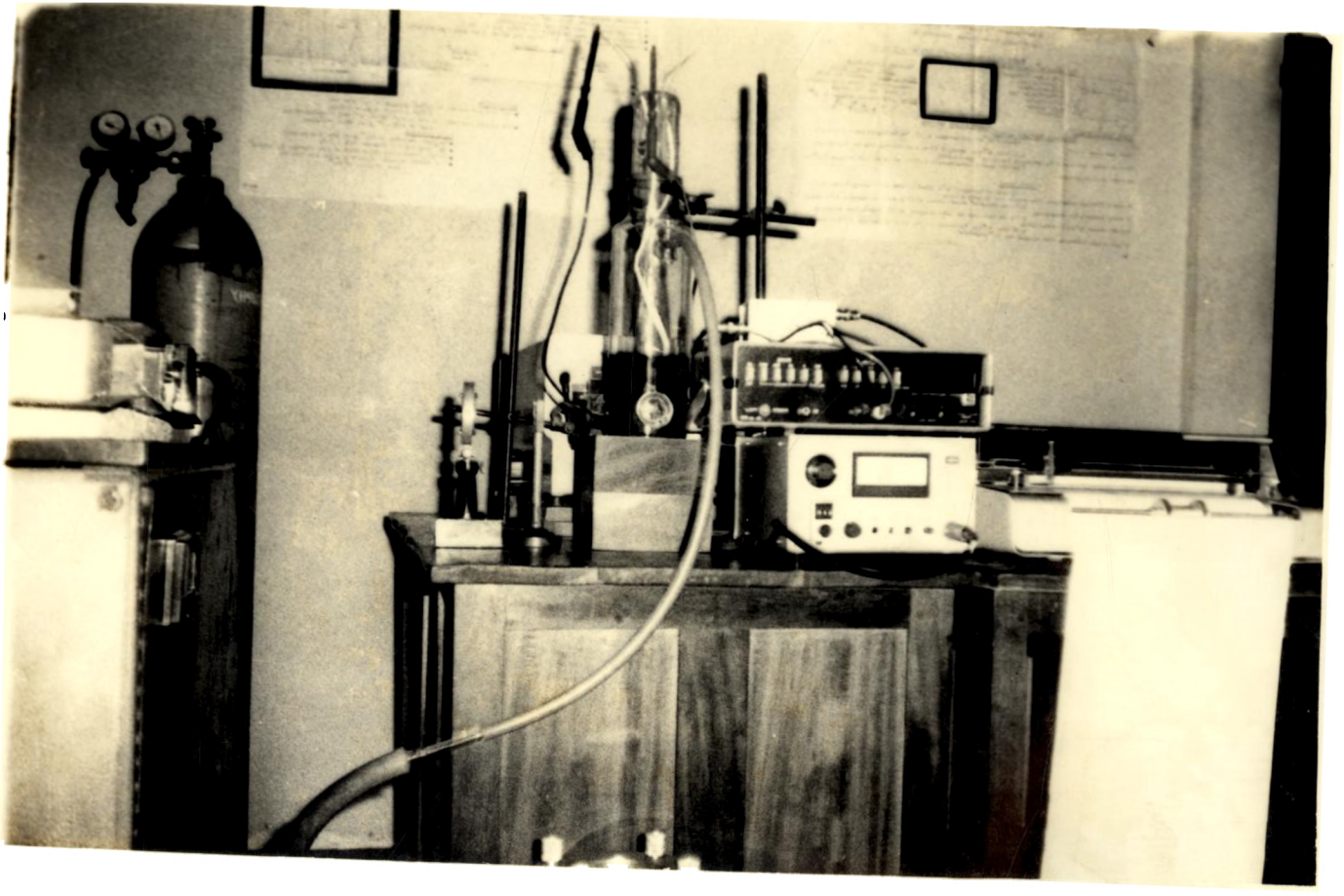

Fig 3.1A Exptl. set up for fluorescence spectrum recording

band near 300nm in the undoped and Tm doped CaF_2, SrF_2 and BaF_2 under X-ray irradiation at 77K. They have shown that a similar emission band occurred in the recombination luminescence of the V_K centre (the self trapped hole). This intrinsic luminescence has been well studied in the alkali halides by Tanimura et al[34]. In the undoped alkaline earth fluorides, this instrinsic luminescence and the perturbed luminescence of the V_K centre have been detected on F centre annealing[35]. This band has also been observed under X-ray irradiation in the alkaline earth fluorides doped with 3d ions[36,37].

Alonso[36] has studied the influence of 3d ions on the production efficiency of intrinsic defects in CaF_2. He has studied the influence of 3d impurities on the production efficiency of V_K and F centres in low temperature X irradiated fluorite crystals. For this, they have compared the optical absorption spectra of pure CaF_2 and CaF_2 doped with Mn, Fe, Co and Ni before and after X irradiation at 15K.

In the present work the emission spectra from pure crystals of CaF_2, SrF_2 and BaF_2 under N_2 laser irradiation showed an intense band in the ultraviolet and a weak band in the blue region at both liquid nitrogen and

room temperatures. These emission bands are observed for the first time. Their excitation spectra are also taken to identify the absorption levels. The emission bands are concluded to be due to the presence of some kind of colour centres.

Several authors have reported the formation of F and V centres and the recombination luminescence of these centres in the alkali halides by two photon absorption on N_2 laser irradiation[38,39]. However, to the author's knowledge, formation of such colour centres have not been reported in the alkaline earth fluorides on N_2 laser irradiation and in the present study also the power of the N_2 laser is not enough to get a multiphoton excitation. So the two new emission bands observed by the authors are interpreted as due to the excitation of some quasi molecular complexes formed near the anion and cation vacancies present in the crystal. These emission bands are found to influence the emission characteristics of rare earths in these hosts considerably.

3.20 Experimental details

Experimental set up used for recording the emission spectra of the crystals is shown in Fig.3.1A and 3.1B. This set up is built around a Jarrell-Ash 0.5m plane grating

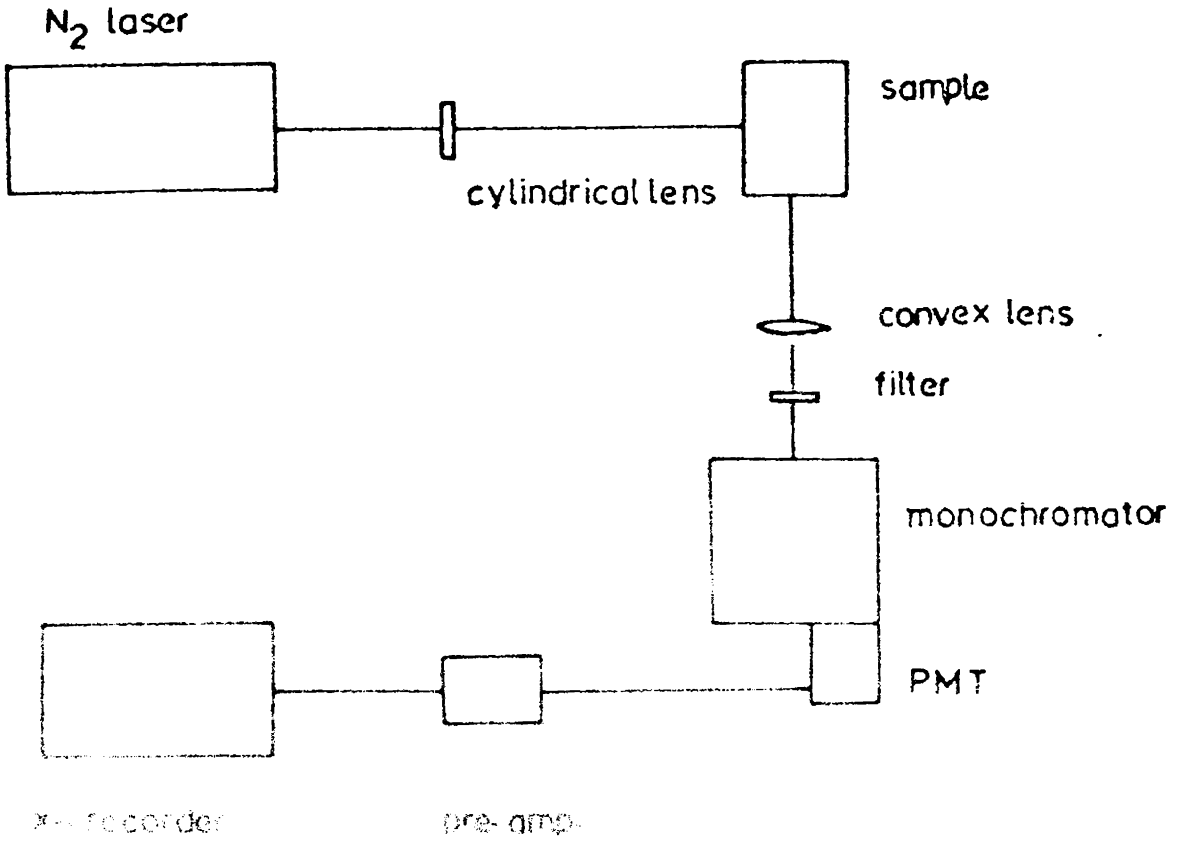
N_2 laser
sample
cylindrical lens
convex lens
filter
monochromator
PMT
pre-amp.

monochromator. The N_2 laser beam is focused on to the crystal and the fluorescence emitted is collected in a direction perpendicular to that of the laser beam, and focused on to the slit of the monochromator. The diffracted light is detected by a photomultiplier tube attached directly in front of the exit slit and the photocurrent produced in it is recorded by a pre-amplifier and a strip chart recorder. Wavelength scanning is accomplished by a variable speed DC motor attached to the grating drive shaft.

3.21 Source

The excitation source used in the present study is a 225KW N_2 laser of pulse width $\sim$ 8 nsec (FWHM). The details of the laser are given in chapter I. In all the experiments the N_2 laser was operated at 10KV and at a nitrogen pressure of 60 torr. The repetition rate was kept constant at 25 pps throughout the experiment. The laser beam was focused on to the crystal with a power density of 1.5 Mw/cm^2.

3.22 Illumination and collection optics

The illuminating optics for the laser beam consists of two cylindrical quartz lenses. The laser

beam has a rectangular image of size 1.5cmx0.75cm and this beam is focused vertically by the first cylindrical lens. The second cylindrical lens was used to convert the beam into a rectangular shape suitable to the crystal size of about 1cmx0.4cm. With the combination of the two cylindrical lenses the intensity of the whole laser beam could be collected with minimum loss. The final beam falling on the crystal placed in the low temperature is found to have a cross section 0.4cmx0.3cm.

The collection optics for the fluorescence consists of a single convex lens of focal length 5 cms. This lens collects the emission light from the crystal and is focused on to the slit of the monochromator. A filter (L.W.P. 337.1nm, CVI) is also used to reduce the background light caused by the scattered 337.1nm radiation of the source. All the background light is minimised by carrying out the experiments in a dark room and also by using baffles and screens.

3.23 Low temperature cell, crystal mounting and cooling

Single crystals of pure and doped CaF_2, SrF_2 and BaF_2 were obtained from Optovac Inc. and are of the dimensions 10mmx4mm. Most of the work is done by cooling

the crystals to liquid nitrogen temperature. For this, the crystals are mounted inside a demountable cold finger of a dewar. The design of this liquid nitrogen cryostat is shown in Fig.3.2.

This low temperature cell consists of an outer glass vessel and an inner glass tube. The inner tube terminates in a glass to metal (covar) joint and a copper crystal holder mounted to the covar tube. The crystal holder is made push fit to the covar tube and is sealed vacuum tight using M-seal (Toughset-B). This seal is found to be very strong, leak-proof and is successfully used for low temperature measurements. It can also be used for high temperature measurements upto 600K. Coolants like LN_2, ice-salt mixture, LO_2 etc. can be taken inside the inner tube of the dewar. There are six electrical leads sealed on to the cell with araldite for temperature measurements. The cell is evacuated by connecting it to a rotary diffusion combination through a side tube. The inner glass tube and the outer glass vessel are separable with a B24 joint at the neck. This cell has four quartz windows at right angles to each other and this enables to make reflection, transmission, and fluorescence measurements. These windows are mounted using araldite to the outer tube.

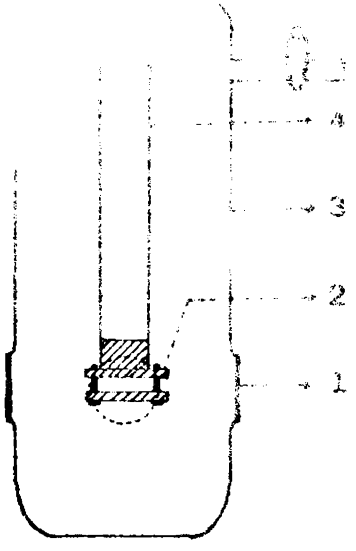

Low temperature cell

Fig.3.2 Low temperature cell
1 - quartz window
2 - crystal holder
3 - outer jacket
4 - inner tube

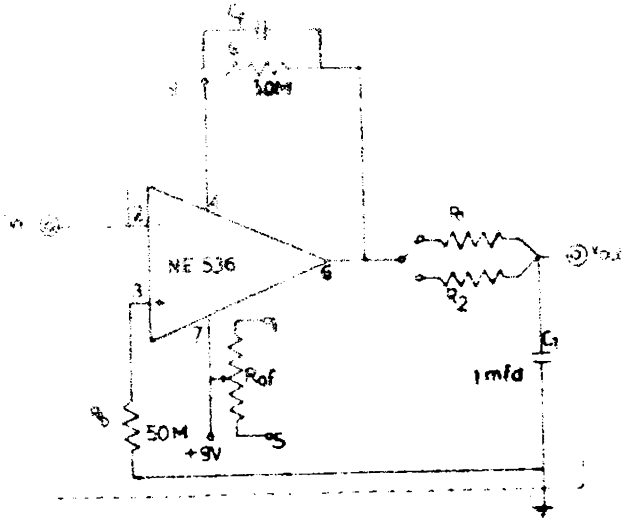

Fig.3.3 Pre-amplifier circuit

The crystal holder consists of two flat round copper discs which can be tightened with the crystal in between, using four brass screws. The crystal holder has a diameter of 2" and thickness 2mm and therefore would not obstruct the fluorescence light beam from the crystal. The top disc is machined from a copper rod of 2" diameter and at the centre of the top disc is a cylindrical projection of 2cm diameter and 1cm length which is made push fit to the glass metal tube of the low temperature cell.

The cell is used for fluorescence measurements at LNT and room temperature. It can be evacuated to a pressure of 2×10^{-5} torr. The bottom of the cell is flat which makes it easier to handle.

3.24 Spectrometer

For the wavelength scanning of the fluorescence sample, a high resolution scanning instrument is needed. This is accomplished by a Jarrell-Ash 0.5 meter Ebert Scanning Spectrometer (Model 82-000). This instrument provides a smooth scanning motion in eight speeds ranging from 2Å/minute to 500Å/minute and has a maximum resolution of 0.2Å. The monochromator covers a spectral range of 2000Å to 16000Å with the three gratings blazed at 1800Å, 5000Å and 7500Å. The spectral limit of this scanning

spectrometer can be extended from 2000Å to 1780Å by flushing the instrument with nitrogen. The reciprocal linear dispersion at exit slit is 16Å/mm.

3.25 Photomultiplier tube

The output from the monochromator is detected by an EMI photomultiplier tube (Model No.9683KQB) with S-20 cathode. This PMT has a fairly constant quantum efficiency in the 300-800nm spectral range where the present investigations are carried out. The PMT is operated at 1350V DC derived from an EMI model PM28B high voltage power supply. The tube has an RF shielded housing which is air cooled. The tube is directly mounted at the exit slit of the monochromator. The output of the PMT is amplified by a pre-amplifier before feeding to the chart recorder.

3.26 Pre-amplifier (Current to voltage converter)

Very low intensity light emission from the low efficiency phosphors should be amplified using noise free high gain amplifiers. For this purpose, a simple, inexpensive low noise amplifier having negligible drift using a simple integrated circuit operational amplifier is fabricated. The circuit of the amplifier is shown in Fig.3.3.

In this circuit a FET input operation amplifier NE 536 connected in the current to voltage configuration is used. Since this integrated circuit has a very large input impedance (10^{14} ohms) it does not load the large resistance R_f (50 M ohms) connected in the feed back circuit. The circuit performance is unaffected by the resistance R_b (50 M ohms) used to compensate the bias current, since the PMT has an output impedance greater than 10^{12} ohms. The low leakage low value condenser C_f suppresses possible oscillations. The RC filter circuit at the output of the amplifier is so chosen to have a time constant appropriate with the type of signal detected with the system.

Amplifier has a conversion gain of 5×10^7 or 1 volt/20nA. When used with a 10mV strip chart recorder the system is capable of measuring clearly a change in PMT current as low as 2 pico amperes with very low noise level. The PMT dark current could be compensated by adjusting the offset potentiometer R_{of}. The details of the working of the amplifier is reported elsewhere[40].

3.27 Recorder

The amplified output of the PMT is fed to an X-t recorder, Omniscribe Model, B127-11. The sensitivity of the recorder is 0.5 mV/cm. In order to have sufficient

resolution, the emission is scanned at a speed of 125Å/min with the X-t recorder operated at 2.5Å/min. The combination gave 50Å/cm on the chart paper.

3.30 Observations

The emission spectra of pure CaF_2, SrF_2 and BaF_2 taken at LNT and RT are shown in Figs.3.4, 3.5 and 3.6. A broad intense band appears in all the spectra in the ultra-violet region (370nm-380nm). This band overlaps the three weak vibrational bands of Nitrogen (370nm, 375nm and 380nm) which are clearly detectable with the high sensitive detecting system used for the investigations. The N_2 band positions are observable as shoulders on the room temperature spectra and these bands as well as the 357nm band of Nitrogen seen in the spectra serve as internal wavelength standard. The appearance of the N_2 bands are due to the scattering from the crystal being amplified by the amplifier. These vibrational bands of Nitrogen has been observed in the N_2 laser emission spectrum and is reported elsewhere[41].

At low temperature, the intensity of the 370nm band becomes large and totally masks the N_2 bands. In spite of this overlap, there is no ambiguity regarding the shape

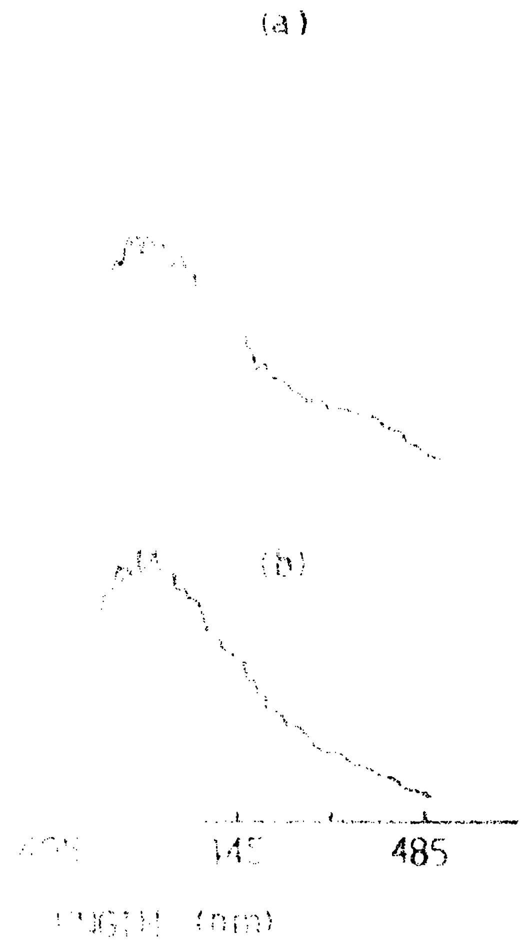

...spectra of pure CaF_2
... (b) at LNT

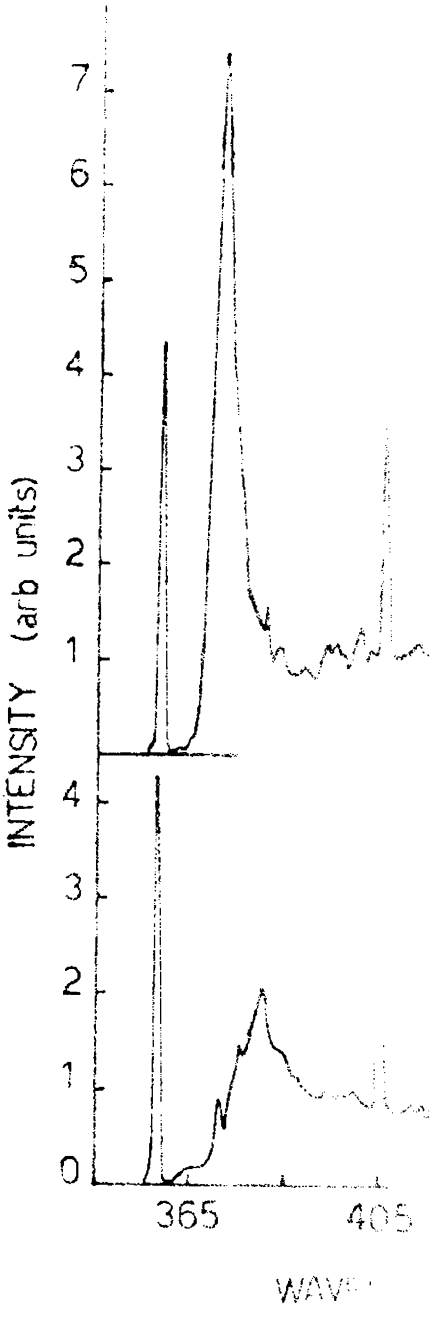

Fig.3.5 Emission
(a) at n

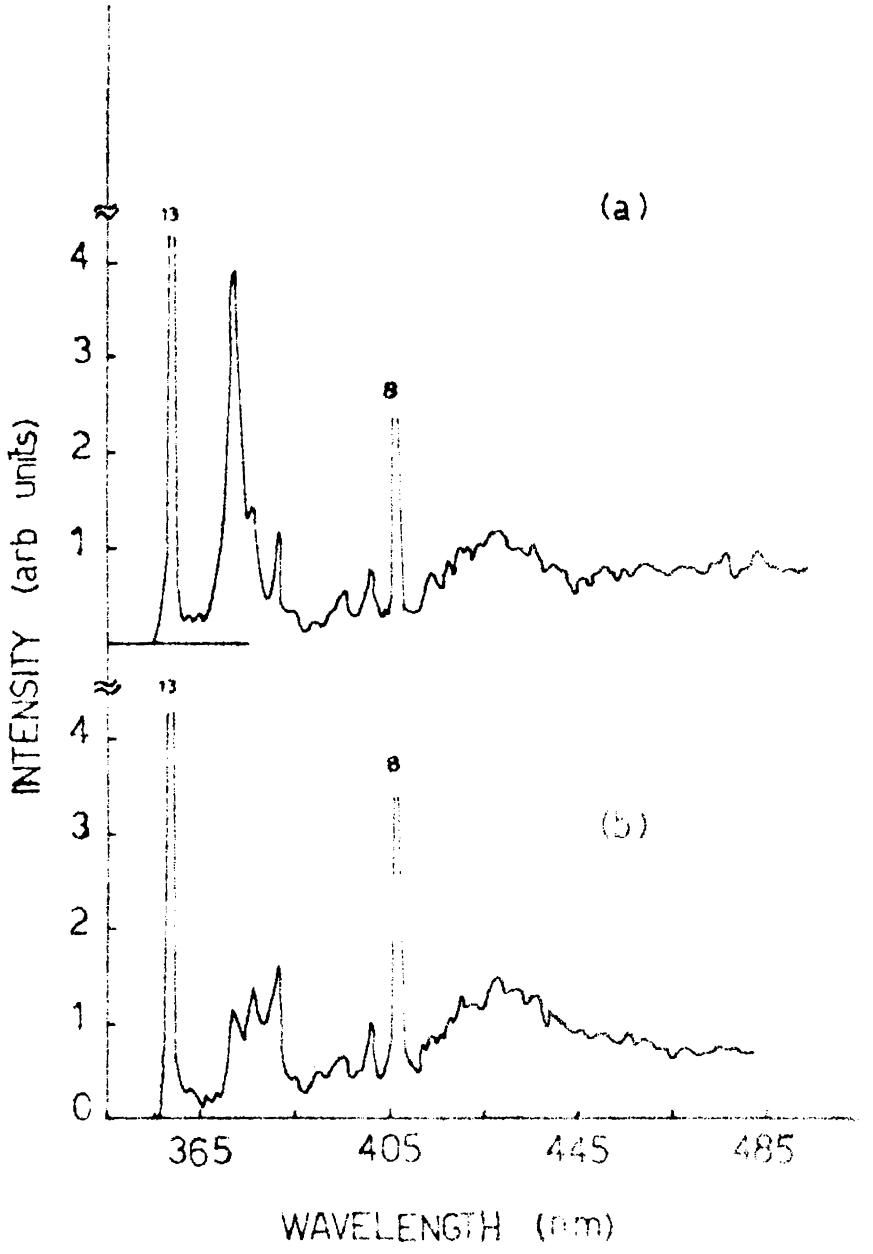

Fig. 3.6 Emission spectra of pure BaF_2
(a) at RT (b) at LNT

and half intensity width of this ultraviolet band. At 80K the half intensity width of this UV band is found to be 64Å, 47Å and 35Å for CaF_2, SrF_2 and BaF_2 respectively. The band maxima observed in all the cases coincided with the 370nm band of N_2 and this gave some difficulty in exactly fixing the band maxima. However, this has not presented any special difficulty in the overall interpretation of the band.

Besides the 370nm band, another broad band appears at 420nm for CaF_2 and BaF_2. Unlike the 370nm band the intensity of the 420nm remains the same at 300K and 80K. This band has greater intensity in CaF_2, and does not appear in the spectra of SrF_2 at both the temperatures.

The excitation spectra of pure CaF_2 (Fig.3.7) show absorption peaks at 305nm and 350nm corresponding to the 370nm emission and 420nm emission respectively. The excitation spectra of the crystals could not be taken at LNT. However the absorption peak though very low in intensity could be clearly detected at room temperature. Decay times of the emission bands at 370nm and 420nm are found to be less than 10 μs.

Fig. 3

3.40 Results and discussion

Because of the large energy gap ($\sim$ 10eV)[42] of the alkaline earth fluorides high energy excitations like X-ray irradiation are required for a band to band transition in these crystals. Such excitations produce colour centres and their recombination will give rise to UV and near UV emissions as observed by Kozo Atobe[36] and Alonso[37]. A similar phenomenon is observed under UV irradiation for LiI crystals having a relatively low energy gap[43]. Colour centres are also produced by a two photon absorption for the alkali halides by N_2 laser irradiation[38]. In KBr and KCl F centre and V centre are produced by two photon absorption from N_2 laser. The V_K centre produced is reported to have a strong absorption at 337.1nm[44]. However, for the alkaline earth fluorides investigated here the possibility of multiphoton excitation under pulsed N_2 laser irradiation with the available power density of 1.5Mw/cm^2 can be safely excluded as a mechanism for the creation of colour centres.

In the absence of a band to band transition, the observed spectra can be interpreted as only due to the excitation of some complex molecules formed near the anion and cation vacancies in the crystal. Pick[45] has already

reported the formation of a colour centre in alkali halides by the association of F centres with complexes of a divalent cation plus a charge compensating cation vacancy. The optical absorption bands for F_{Z1}(Ca), F_{Z1}(Ba) and F_{Z1}(Sr) centres in alkali halides are found to be almost the same. It should be noted that in present study also the emission bands observed appear at the same positions for CaF_2, SrF_2 and BaF_2 though with different relative intensities and half-widths.

In pure alkaline earth fluorides absorption at 350nm due to colour centres has been already reported by Harrington et al[46] on exciting with the UV line of Ar^+ laser. The excitation spectra taken by the authors also showed absorption peaks at 305nm and 350nm corresponding to the emission bands at 370nm and 420nm respectively.

Considering all the above facts, one may postulate that the observed spectra in pure alkaline earth fluorides are due to the excitation of colour centres formed by quasi-molecular complexes near the anion and cation vacancies present in the crystal.

3.41 Model of the suggested complexes

Cation and anion vacancies in the crystal can be thought of as ionised V centre (V_c^-)V centre without a trapped

hole) and ionised F centre (F^+, F centre without trapped electron). One may therefore postulate the existence of a vacancy complex (V^-F^+) formed by the neighbouring anion and cation vacancies. Cation R^{++} and anions F^-, on relaxation towards (V^-F^+) will form a molecular ground state $(RF)^+$. The emission band observed in the UV region is assumed to be due to the excitation of complex $(RF)^+$. Ground state of $(RF)^+$ is X' state arising from the electron configuration $(\sigma 3P)^2$ $(\pi 3P)^4$ $(\pi 2P)^4$ $(\sigma 2P)^2$ $(\pi 3P)$. Excitations of outer electron to various orbitals give rise to a number of energy states viz., $A^3\pi$, $B^1\pi$, $C^3\Sigma$, $D^1\Sigma$, $E^3\pi$, $F^1\Sigma$. Schematic energy level diagram of $(CaF)^+$, $(SrF)^+$ and $(BaF)^+$ is shown in Fig.3.8. Energy levels of $(RF)^+$ molecule will get lowered as mass of cations (Ca^{2+}, Sr^{2+}, Ba^{2+}) increases and for heavier masses, a large number of bound states will appear. As a result, 337.1nm absorption may excite $(CaF)^+$, $(SrF)^+$ and $(BaF)^+$ to $C^3\Sigma$, $D^1\Sigma$ and $E^3\pi$ states with corresponding emission in the longer wavelength side due to Stoke's shift. Intensity and halfwidth of the UV band shows clear cation mass dependence. In the case of CaF_2 this band has maximum intensity and maximum band width and will be minimum in the case of BaF_2. This shows that as the mass of R^{2+} increases, the change in the internuclear distance in the excited state and ground state decreases. Thus the 370nm band shows a mass dependency.

This also supports the assignment of UV band to the excitation of $(RF)^+$ molecule.

The intensity of the UV band is found to decrease with increase in temperature. This is because as the temperature is raised there will be diffusion of vacancies ie, V^- and F^+ centres will be isolated thereby decreasing the efficiency of $(RF)^+$ complex formation. Hence at RT the intensity of UV band will be very low.

In alkaline earth fluorides, anions F^- in the vicinity of V^- centre will form a complex F_2^{---} with bonds bent towards cation vacancies. The nature of these complexes and the excited states of these complexes have been well studied in alkali halides[47]. The emission at 420nm is attributed to the excitation of F_2^{---} complex formed near the independent cation vacancy. Fig.3.9 gives the schematic energy level diagram for F_2^{---} complexes. In the case of homonuclear molecule F_2^{---} an additional selection rule $g \not\longleftrightarrow g$, $u \not\longleftrightarrow u$ and $g \longrightarrow u$ restricts the number of possible transitions. The absence of this band in SrF_2 can only be attributed to the additional restriction imposed on the overall, selection rule of the homonuclear F_2^{---}. The temperature dependence of this band will be very less between 80K and 300K as the F_2^{---} complex formation is independent of temperature. The 420nm band is much broader

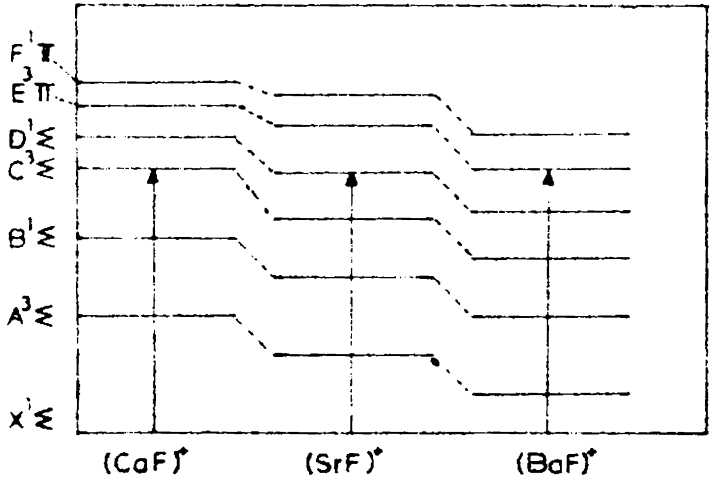

Fig.3.8 Schematic energy level diagram of $(RF)^+$complexes

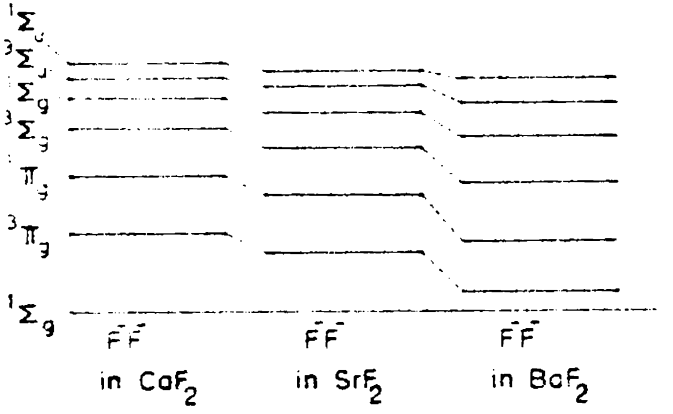

Fig.3.9 Schematic energy level diagram of F_2^{--} complexes

when compared to the 370nm band. This band has a greater intensity for CaF_2.

Thus it is concluded that the two prominent bands observed from the pure crystals of CaF_2, SrF_2 and BaF_2 are due to the centres formed by quasi molecular complexes like $(RF)^+$ and F_2^{---} in the crystal.

REFERENCES

1. G.B.Garret, in Proceedings of the 3rd International Congress on Quantum Electronics (Columbia University, New York, 1964), 2, 971 (1964).

2. M.J.Marrone and F.H.Attix, Health Phys. 10, 431 (1964).

3. K.V.Ettinger, S.A.Durrani and C.Christodoulides, Rad. Eff. 5, 99 (1970).

4. D.L.Staebler and Z.T.Kiss, Appl.Phys.Lett. 14, 93, (1969).

5. D.L.Staebler and S.E.Schnatterly, Phys.Rev. B3, 516 (1971).

6. John E.Harry, Industrial lasers and their applications, Mc Graw Hill, London (1974) 28.

7. J.Arends, Phys.Stat.Solid, 7, 805 (1964).

8. R.G.Bessent, W.Hayes, J.W.Hody and P.H.S.Smith, Proc. R.Soc.London, SerA, 309, 69 (1969).

9. W.Hayes and R.F.Lambourn, J.Phys.C, 6, 11 (1973).

10. P.J.Call, W.Hayes, J.P.Stott and A.E.Hughes, J.Phys.C, 7, 2417 (1974).

11. Y.Kazumata, Phys.Stat.Solidi, 34, 377 (1969).

12. J.H.Beaumont, W.Hayes, D.L.Kirk and G.P.Summers, Proc.R.Soc. London, SerA, 315, 69 (1970).

13. J.L.Merz and P.S.Pershan, Phys.Rev, 162, 217 (1967).

14. J.L.Merz and P.S.Pershan, Phys.Rev, 162, 235 (1967).

15. F.K.Fong, Progress in solid state chemistry, ed. H.Reiss, NPergamon, New York (1967).

16. C.M.Sunta, V.N.Bapat and S.P.Kathuria, Proc.Third. Int.Conf.Lumin. Dosim. Riso Rept. 249 (Denmark: Danish Atomic Energy Comm) p.392.

17. K.S.V.Nambi, N.N.Bapat and S.M.D.Rao, J.Phys.C, 12, L745 (1979).

18. K.Atobe, Phys.Letts., 71, no.2,3, 249 (1979).

19. F.Aramu, Lett, Nuovo Cimento, 25, Ser2, No.3, 75 (1978).

20. K.Atobe, Annu.Rep.Res. React.Inst. (Kyoto Univ. Japan) 11, 28 (1978).

21. K.Atobe, Annu.Rep.Res.React.Inst. (Kyoto Univ, Japan), 11, 134 (1978).

22. K.Atobe, Phys.Status Solidi, 50, No.1, p.77 (1978).

23. K.P.Arefev, Sov.Phys.Solid State, 19, No:12, 2099 (1977).

24. V.M.Lisitsyn, Sov.Phys.Solid State, 20, No.9, 1509 (1978).

25. D.G.Mead, J.Phys.C, 10, No.7, 1063 (1977).

26. J.R.Ferraro, M.Horan and A.Qualtrochi, J.Chem.Phys. 55, 664 (1972).

27. A.Mitsuishi, Y.Yamada and H.Yoshinaga, J.Upt.Soc.Am, 52, 14 (1962).

28. P.Denham, P.L.Morse and G.R.Wilkinson, Proc.R.Soc.A, 317, 55 (1970).

29. K.Hisano, N.Chama and O.Matumura, J.Phys.Soc.Japan, 33, 430 (1965).

30. V.Mehn, Laser induced damage in optical materials, Boulder Co, USA, 4 (1977).

31. Bansi Lal and D.Ramachandra Rao, Chem.Phys.Letts. 53, 250 (1978).

32. P.J.Alonso, V.M.Orera and R.Alcald, Phys.Stat.Solidi, 99, 585 (1980).

33. A.Sivaram, H.Jagannath, D.Ramachandra Rao and Putcha Venkateswarlu, Phys.Chem.Solids, 40, 1007 (1979).

34. K.Tanimura, M.Fujita, T.Okada and T.Suita, Phys. Lett. A50, 301 (1974).

35. Kozo Atobe, J.Chem.Phys, 71(6), 2588 (1979).

36. P.J.Alonso and R.Alcala, J.Luminescence, 21, 147 (1980).

37. J.Casas Gonzalez, P.J.Alonso, H.W.den Hartog and R.Alcala, J.Luminescence, 22, 139 (1981).

38. M.Geller, D.E.Altman and T.A.Detemple, Appl.Phys. Lett, 11, 221 (1967).

39. Kirchiro Kagawa, J.Phys.Soc.Jpn, 41, no:2, 507 (1976).

40. S.M.Pillai, C.Raghavan, Sudha Kartha and C.P.G.Vallabhan, J. of Instrument Society of India, 12, 7 (1982).

41. N.Subhash, Sudha C.Kartha and K.Sathianandan, Appl. Optics, 22, 3612 (1983).

42. Dwieght E.Gray, American Institute of Physics Handbook, 3rd ed, Mc-Graw Hill Book Company, New York (1972) 9-18.

43. S.Hashimoto, K.Nakagawa, Z.Nackawa, and T.Murata, J.Phy.Soc. Japan, 45, no:3, 944 (1978).

44. C.J.Delbecq, Phys.Rev, 121, 1043 (1961).

45. H.Pick in Optical props of solids, ed. by F.Abele's, North Holland Publishing Company, London (1972) 707.

46. J.A.Harrington, B.L.Lobbs, M.Braunstein, R.K.Kim, R.Steqrns and R.Braunstein, Appl.Opt., 17, 1541 (1978).

47. Karasawa and Hirai, J.Phys.Soc. of Jpn, 40, no:3 (1976).

CHAPTER IV

FLUORESCENCE OF Ho^{3+} IN CaF_2

4.10 Introduction

The development of the solid state laser has generated widespread interest in the spectroscopy of ions in crystals. Among the candidates for laser materials, the lanthanide series of range earth ions is particularly promising because of the multitude of sharp energy levels lying in the visible and infrared. These ions are easily incorporated into cubic hosts of optical quality such as CaF_2, and laser oscillations have been obtained for many of these systems. The most extensively used activator ion in laser crystals is trivalent Neodymium. In the second place is Holmium followed by Erbium and Thulium[1]. The study of fluorescence phenomena in rare earth doped alkaline earth fluorides has also received considerable attention because of the possibility of using rare earth ions in crystals as new lasants. Extensive work in this direction has been carried out using Ar^+ laser[2] and other high energy radiations as sources of excitation.

A great deal of research on the concentration and temperature quenching of fluorescence and lifetime

of Ho^{3+} ion in crystals are undertaken by several researchers. The SLJ states of the lowest configuration of Ho^{3+}, $4f^{10}$, have been fairly well established by various studies made from Holmium salts and Ho^{3+} as impurity in various matrices. The Holmium salts studied so far are $HO_2(SO_4)_3$[3,4], $HOCl_3$, HO_2O_3[5,6], $HO_2(C_2H_5SO_4)\ .9H_2O$[7] and $HOFeO_3$[8]. The fluorescence and absorption spectra of Ho^{3+} in $LaCl_3$ have been studied in detail by Duke and Pandey[9] while a comprehensive theoretical interpretation of Ho^{3+}:$LaCl_3$ is given by Rajnak and Krupke[10]. The other crystals containing Ho^{3+} that are studied so far are CaF_2[11], YGaG, YIG[12], $CaWO_4$[13], YPO_4[14], $YAlO_3$[15], $LiTmF_4$[16] and also tellurites, Calibo and phosphate glasses[17]. The absorption as well as fluorescence of Ho^{3+} in LaF_3 have been extensively studied by Caspers et al[18] and have established the complete energy level scheme upto 26,000 cm^{-1}.

The absorption, the luminescence and relaxation spectra of a series of fluorite crystals with different Ho^{3+} concentrations have been recorded and investigated[19]. The line groups observed in the luminescence spectrum that are in resonance with absorption lines were identified as due to transitions between the excited ($^5F_4$,$^5S_2$), ($^5F_5$,$^5I_6$) and $^5I_7$ states and $^5I_8$ ground state. The non resonance line groups in the luminescence spectrum were

identified as transitions between excited terms. A detailed optical study of $CaF_2:Ho^{3+}$ has been carried out by Schelsinger[20]. Linear stark effect in f-f spectra of Ho^{3+} ions in fluorite crystals is also studied[21] and reports that due to the presence of defects and the centres there is no appreciable stark effect for lines of the electric dipole type. Using selective laser excitation, the crystallographic sites arising from fluoride compensation of Ho^{3+} doped in CaF_2 have been investigated by Seelbinder[22]. Fluorescence and lifetime studies of $CaF_2:Ho^{3+}$ have been carried out using Ar^+ laser excitation and four fluorescence groups in the wavelength region 477.5-759.0nm have been recorded. The concentration range studied is from .01 to .1% wt of Ho^{3+}. In $CaF_2:Ho^{3+}$ laser oscillation has been identified at 551.2nm wavelength in the visible region[23] and also at 2.092μm in the infrared region[24].

4.20 Rare earth ions in CaF_2 lattice

The CaF_2 lattice can be visualised as a cubic array of F^- ions with a Ca^{2+} at every other body centre position. When rare earth ions are added, they enter the lattice substitutionally for Ca^{2+} ions, but they are more stable in the trivalent state. This additional positive

charge requires some form of charge compensation and several different kinds of compensators have been identified by optical and magnetic resonance experiments. The type and symmetry compensation is strongly dependent on the starting materials used to grow the crystals, the method of growing and thermal treatments given to the crystals. One of the most common type of charge compensators is interstitial fluorine ion in the adjacent body centre position leading to tetragonal (C_4V) symmetry at the rare earth site. There have been a number of experiments with trivalent rare earth ions doped into fluoride lattices which show that the population of rare earth ions in the different crystallographic sites caused by charge compensation is a function of both the specific rare earth dopant ion and the specific lattice.

At higher concentrations of the dopant, the site behaviour becomes more difficult to describe. Naberhuis and Fong[25] developed a model which predicted the presence and importance of $(R^{3+}-F^{-})_2$ dimers, in the crystal equilibrium at higher concentrations. Their theory also predicted that trimers and higher order clusters would not be present in significant numbers.

In the present work, a detailed study of the fluorescence of Ho^{3+} in CaF_2 lattice has been carried

out for different concentrations of Ho^{3+} at both room and liquid nitrogen temperatures. The N_2 laser excited fluorescence of $CaF_2:Ho^{3+}$ and the variation of fluorescence emission and lifetime with concentration is studied to get information about the different relaxation and quenching processes present in the crystal. Absorption spectra and excitation spectra are also taken to identify the absorption levels.

4.30 Experimental details

Laser systems with energy densities (per unit frequency interval per unit solid angle) many orders of magnitude higher than any thermal source, are ideal excitation sources for the measurement of fluorescence decay. The fluorescence spectra of $CaF_2:Ho^{3+}$ is charted with Xe lamp excitation and N_2 laser excitation. The lifetime of the fluorescence group in the region 530.0-550.0nm under N_2 laser excitation is measured with the help of a photomultiplier, a box car averager and a chart recorder.

4.31 Fluorescence spectra

The fluorescence spectra of $CaF_2:Ho^{3+}$, on exciting with a Xenon lamp at 285.0nm is shown in Fig.4.1.

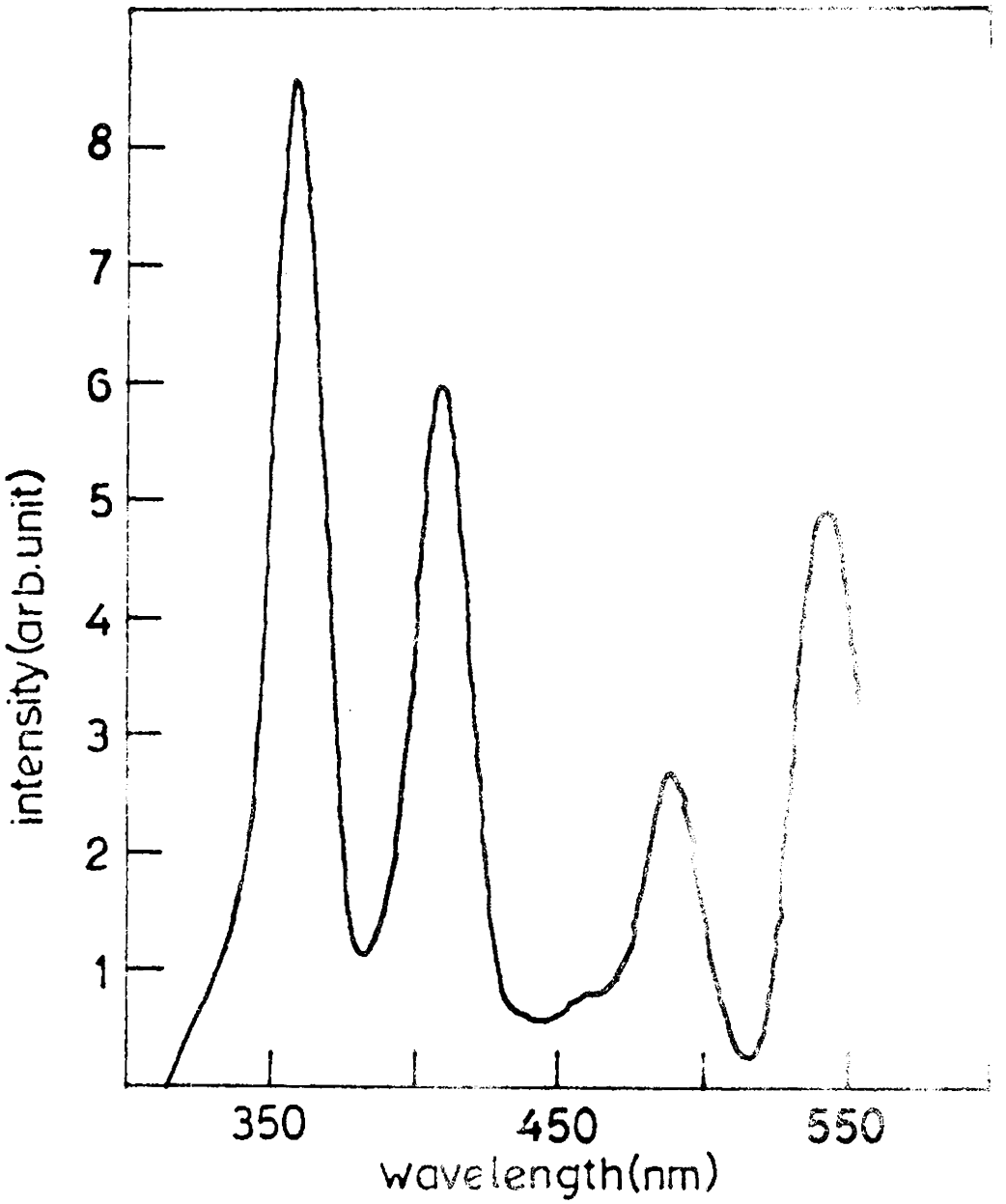

Fig.4.1 Xe lamp excited fluorescence spectra of $CaF_2:Ho^{3+}$ (1%) at RT.

There are four groups of fluorescence emission and they are at 360nm, 410nm, 485nm and 549nm. One more fluorescence group was observed at 645nm on excitation with 415nm. These emissions are due to the different radiative transitions between the various levels of Ho^{3+} in CaF_2. The wavelength, their corresponding transitions and relative intensities are given in table 4.1. The fluorescence spectra of CaF_2 doped with Ho^{3+} when excited by an N_2 laser is also taken using the same experimental set up described in chapter III. CaF_2:Ho^{3+} crystals with three different Ho^{3+} concentrations (0.2%, 0.4% and 1%) obtained from Optovac Inc. and having the same dimensions (10mmx4mm) were irradiated with an N_2 laser (1.5 Mw/cm^2) and the fluorescence emission spectra were recorded both at RT and LNT using a 0.5m Jarrell-Ash Monochromator, an EMI photomultiplier and an X-t recorder. The grating used was the one blazed at 5000Å. Both the exit and entrance slit widths of the monochromator were kept at 600 μm so that a resolution of nearly 4.8Å was achieved. The scanning speed used in all the cases were 125Å/min. The chart speed was 50Å/min. Care was taken to keep the experimental conditions the same for all the experiments. The fluorescence spectra of CaF_2:Ho^{3+} when excited by the N_2 laser gave distinct emission peaks at 530nm region.

Table 4.1

Different fluorescence groups of $CaF_2:Ho^{3+}$

Emission wavelength (nm)	Energy (cm^{-1})	Transitions	Intensity (arb.units)
360	27777		94
410	24390	$(^5F_1, ^5G_6) \rightarrow {}^5I_8$	68
485	20618	$^5F_3 \rightarrow {}^5I_8$	35
549	18214	$(^5F_4, {}^5S_2) \rightarrow {}^5I_8$	57
645	15503	$^5F_3 \rightarrow {}^5I_7$	12

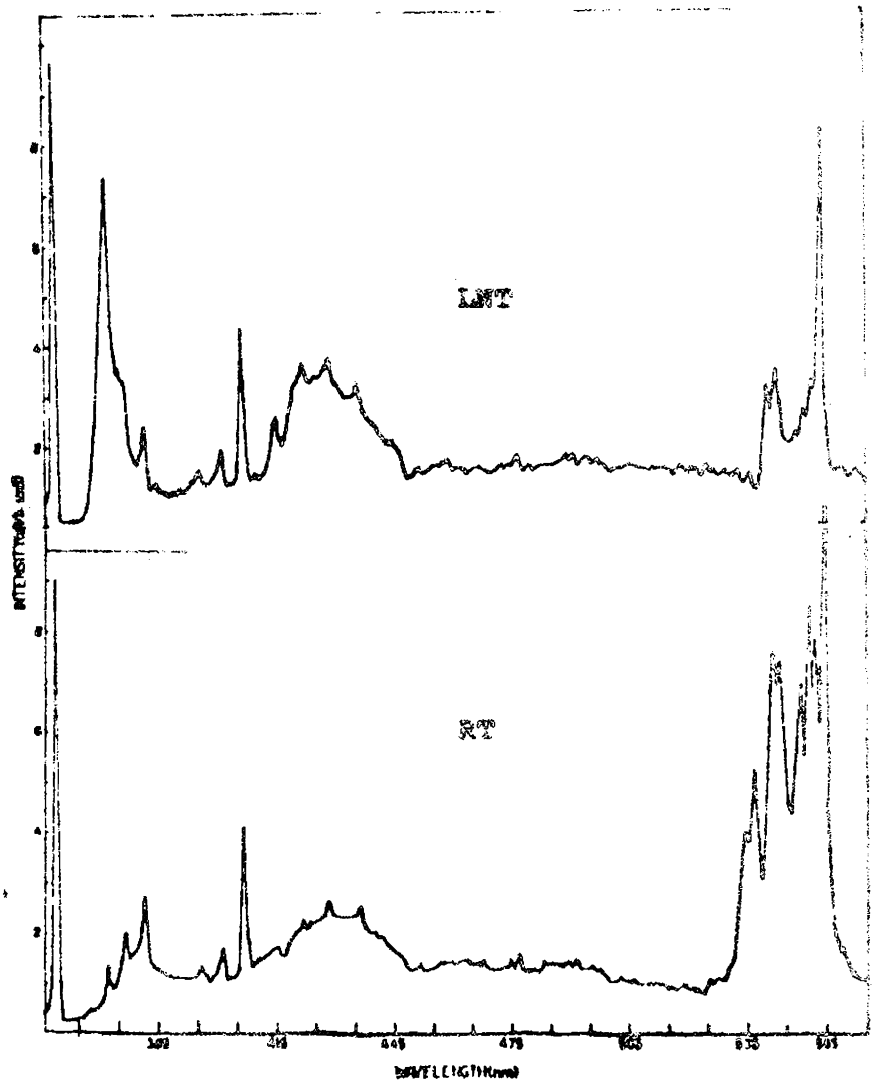

Fig.4.2A N_2 laser excited fluorescence spectra of $CaF_2:Ho^{3+}$ (0.2%)

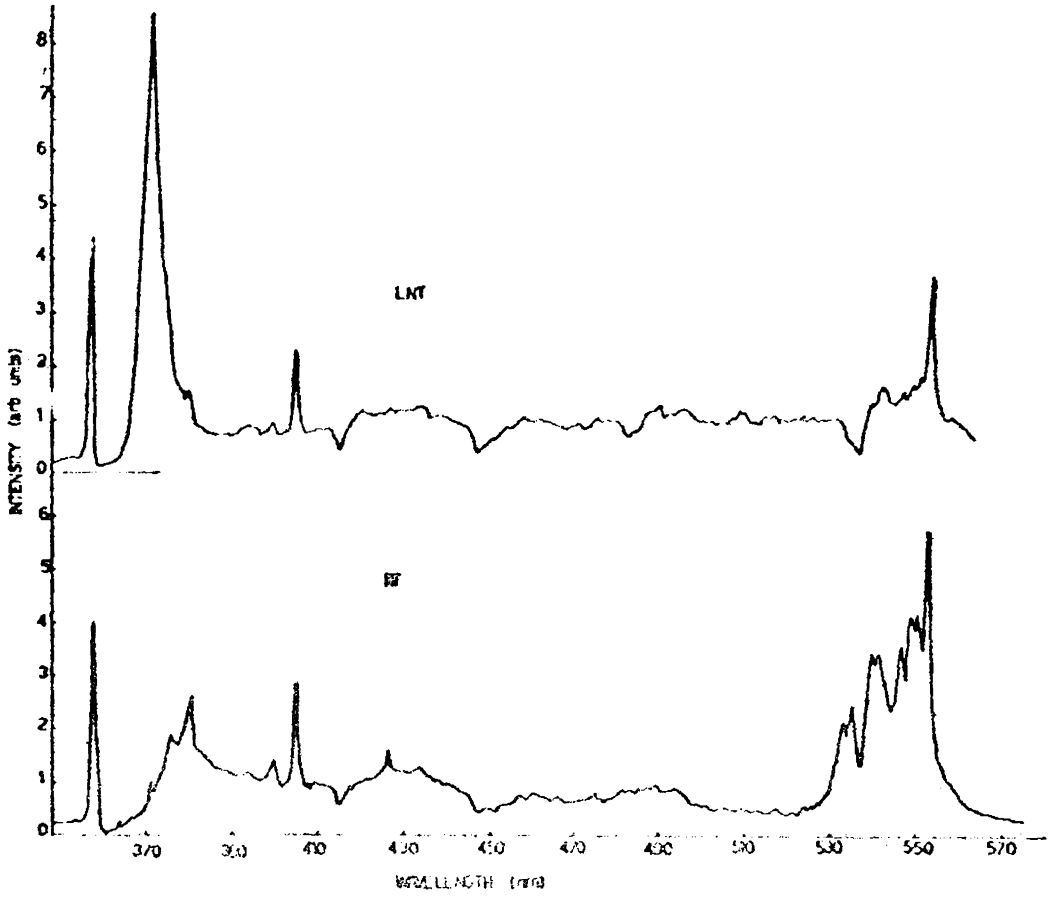

Fig.4.2B N_2 laser excited fluorescence spectra of $CaF_2:Ho^{3+}$ (0.4%).

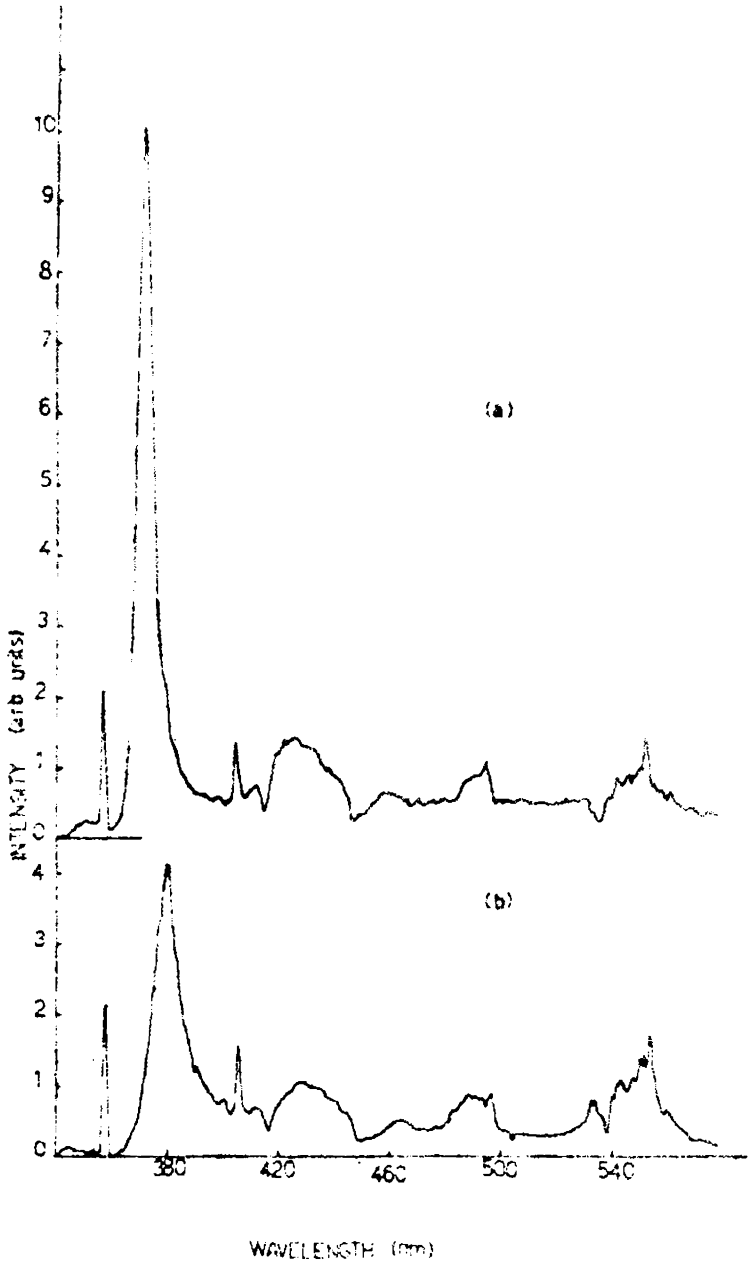

Fig.4.2C N_2 laser excited fluorescence spectra of $CaF_2:Ho^{3+}$ (1%).
(a) at LNT (b) at RT.

Figs.4.2A, 4.2B and 4.2C show the fluorescence spectra of $CaF_2:Ho^{3+}$ at three different concentrations. The spectra were found to contain the vibrational bands of N_2 also due to scattering. These bands have been already identified and reported in chapter II.

4.32 Excitation spectra

The excitation spectra of $CaF_2:Ho^{3+}$ for two different concentrations (0.4 and 1% of Ho^{3+}) were taken on an Aminco Bowman spectrofluorometer. The sensitivity and the PMT load were adjusted for optimum conditions. The crystals were placed in a quartz cell and placed in front of the xenon source and the spectra were charted at room temperature. The excitation spectra are shown in Figs.4.3A and 4.3B.

4.33 Absorption spectra

The absorption spectra of the crystals were taken on a Cary-14 spectrometer. The spectrometer has a resolution of 1Å. The spectra were charted both at RT and LNT at a speed of 25Å/cm. The absorption spectra for 1% Ho^{3+} in CaF_2 is shown in Figs.4.4A and 4.4B. The absorption coefficients were determined by dividing

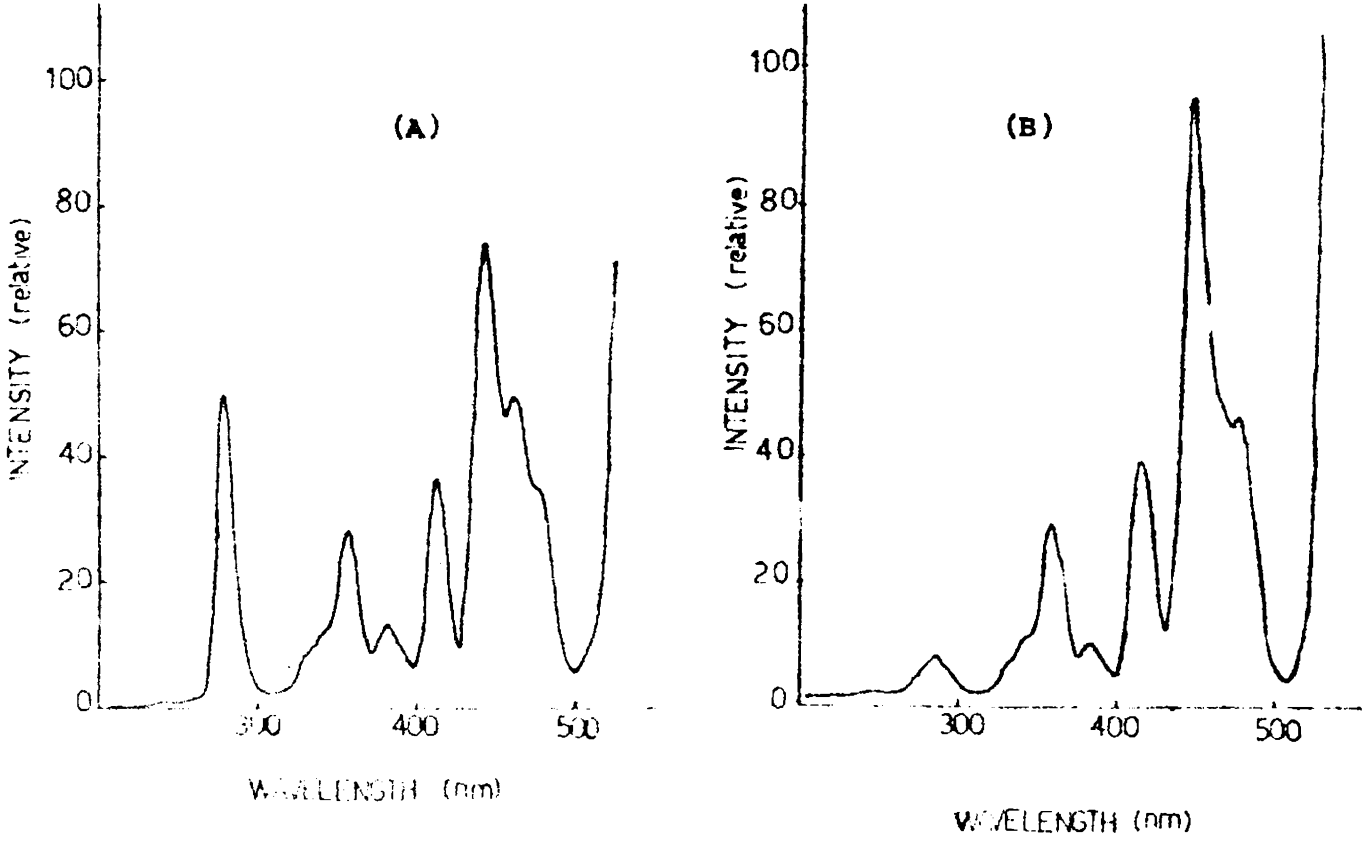

Fig.4.3 Excitation spectra of $CaF_2:Ho^{3+}$ at 530nm
(A) - for 0.1% of Ho^{3+}, (B) - for 1% of Ho^{3+}

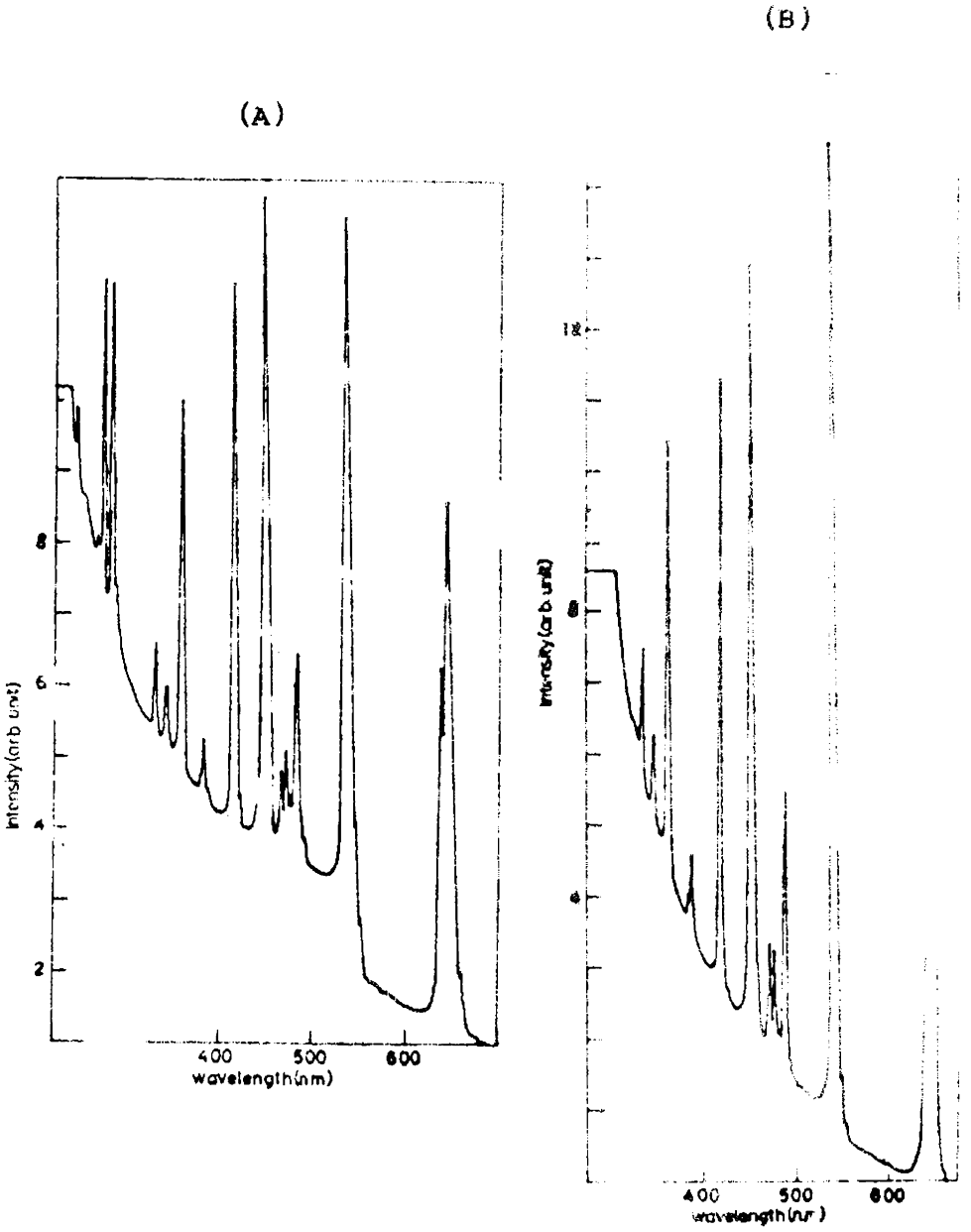

Fig.4.4 Absorption spectra of $CaF_2:Ho^{3+}$ (1%).

(A) - at RT (B) - at LNT.

the peak height of the absorption lines by the thickness of the crystal.

4.40 Fluorescence lifetime spectrometer

To measure the decay times of the fluorescence emission a fluorescence lifetime spectrometer was set up. The transient fluorescence signals are directly monitored by a photomultiplier tube and the resulting electrical signals after proper amplification are processed using a box car averager and charted using a recorder. The experimental set up is given in Fig.4.5. The present set up can be used for measuring decaytimes in the range from 10 μsec to several seconds. The experimental set up, though assembled for the measurement of fluorescence decay times of solids, can also be used for the study of liquids and gases with slight modifications. The main parts of this experimental set up are (i) Excitation source, (ii) Monochromator and (iii) Signal processing electronics.

4.41 Excitation source

A pulsed N_2 laser operating at a pressure of 60 torr at a charging voltage 10KV is used for exciting the fluorescence. The details of the N_2 laser has been

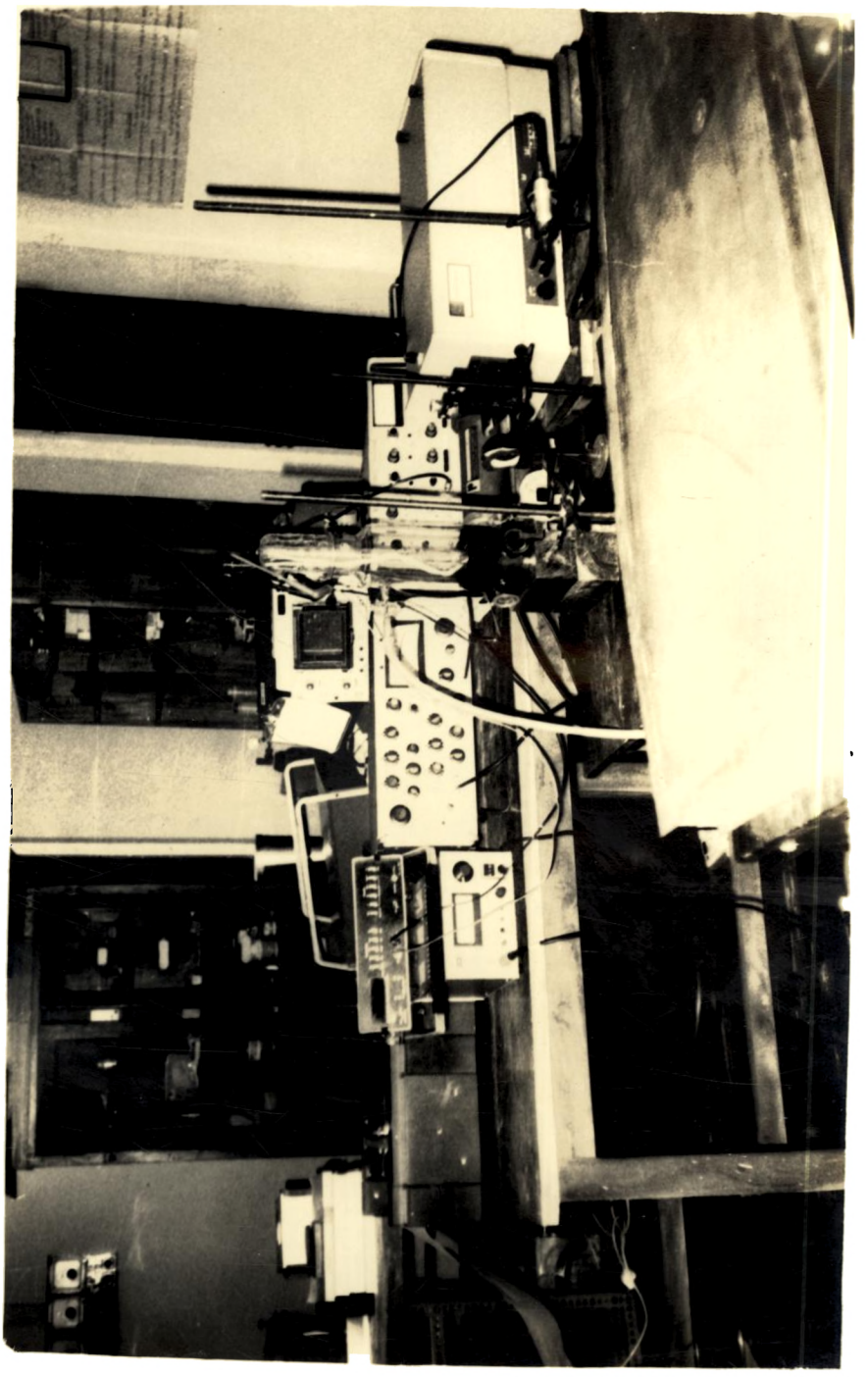

after 108

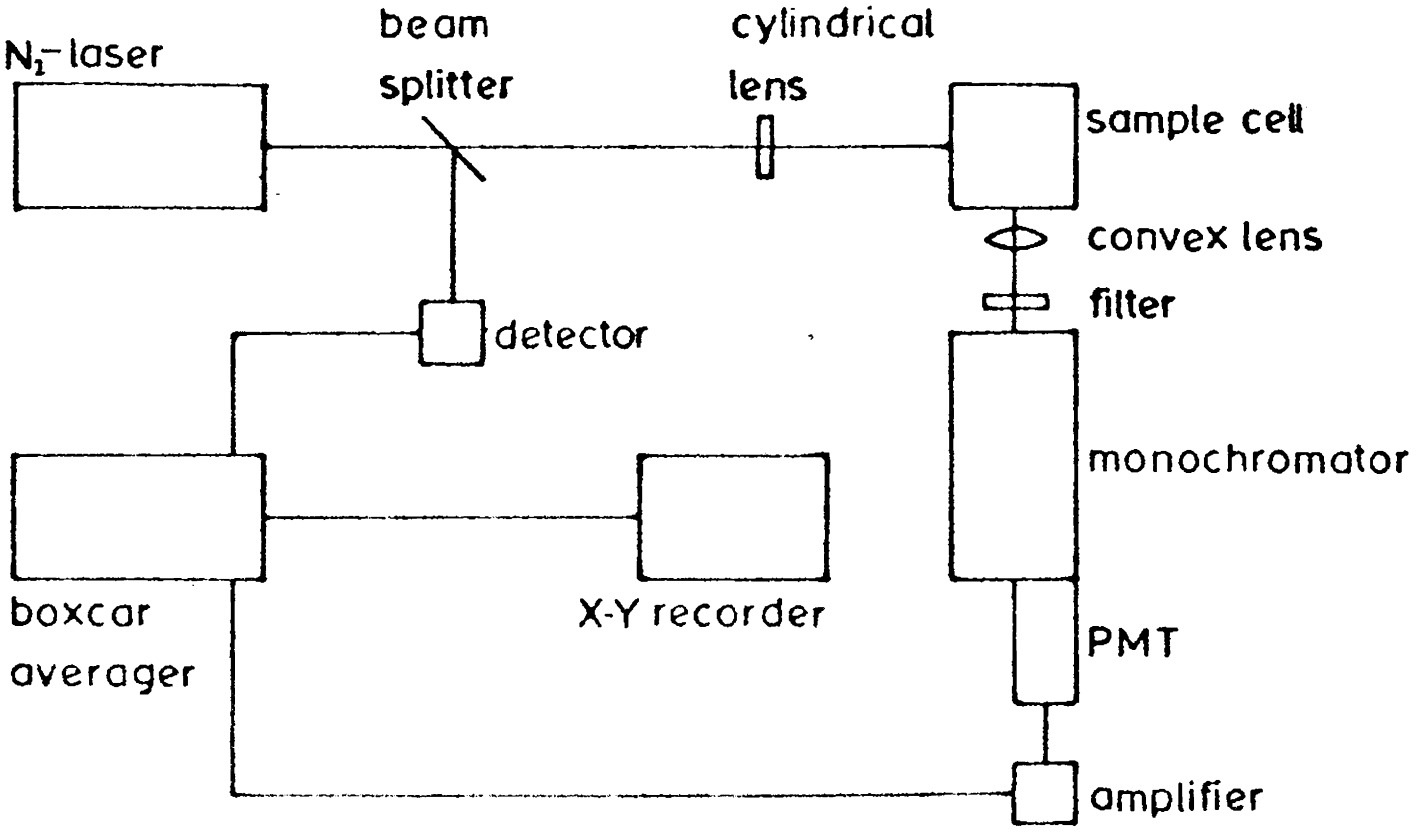

Fig.4.5B Block diagram of the set up for fluorescence lifetime measurement.

already described in the previous chapters. The spark gap of the laser is flushed continuously by N_2 at a pressure of one atmosphere. The spark gap is operated in a free running mode where the repetition rate depends on the applied voltage. The repetition rate used is about 25 pps. The pulse width of the laser is about 8nsec. The laser beam is focused on to the crystal using two cylindrical quartz lenses.

4.42 Monochromator

In this set up a Jarrell-Ash 0.5M spectrometer with a grating blazed at 5000Å is used. An EMI photo-multiplier tube is placed directly in front of the exit slit. An S-20 cathode is used and its dark current at room temperature and at 1.3KV is about $1x10^{-9}$A. The high voltage required for the PMT is obtained from a DC power supply.

4.43 Signal processing electronics

The signal processing electronics consists of a broad band, high gain amplifier and a box car averager to eliminate the noises.

(a) Pre-amplifier

Since the signal current from the PMT is low and also because the event is fast, an amplifier with high gain and wide band width is required. Moreover, this amplifier should have minimum noise current. EG&G model 184 current sensitive preamplifier along with the input amplifier in the Model 124A lock in amplifier mainframe was found to be sufficient for the present work.

The current sensitive preamplifier is basically a low noise inverting operational amplifier, whose summing junction is the input connector itself, followed by a conventional non-inverting gain-of-ten feedback amplifier having a FET input stage. The preamplifier has a unity gain crossover value of 50MHz. Additional amplification is obtained by using the selective amplifier for the main frame of the lock in amplifier. The output was taken through the BNC connector provided on the mainframe.

In the flat mode, this selective amplifier can be used as a pure voltage amplifier with a bandwidth greater than 210KHz[26]. This set up was checked with a pulse of rise time 1 μs. The pulse was found to be amplified without any distortion. The noise current of the preamplifier was

less than 1 pA. The 184 preamplifier sensitivity was set at 10^{-5} A/V and for the weakest signals the main frame amplifier gain was set at 1mV/100mV. These settings gave an overall gain of 10^{-9}A/10mV, sufficient for the next signal processing unit.

(b) Boxcar averager

The actual signal current corresponding to the fluorescent light, in practice, is immersed in various types of noises. The main noises interfering with the signal are (1) external light that may come through the collection optics, (2) scattered laser light from the sample, (3) dark current of the PMT which is a DC level of a few nA, (4) shot noise from the PMT whose periodicity is very low, (5) Johnson noise, (6) amplifier noises and (7) the intense noise produced by the laser discharges.

External stray light can be suppressed by using proper baffles. To eliminate scattered laser light, an edge filter of the wavelength pass type for 337.1nm is used. Even then a small part of the scattered light passes through the filter. Since the pulse width of the laser light is only 8ns, the noise due to this remained only for the first 8ns.

Most of the remaining noises can be eliminated by using a boxcar averager. In the present work, EG&G Model 162 Boxcar Averager with 164 module, is used. The input was given in the AC coupling mode so that all the DC noises are eliminated at the input side itself. The aperture duration selected was 5μs and the gated integrator (164 module) time constant as 10μs. Aperture delay ranges were selected between 50μs to 1000μs. The 162 time constant was selected as 1-3 secs.

The values of the above being fixed, in the scanned operation a minimum scan time should be given. The formula for

$$MST = 5\left[(MFTC)^2 + \left(\frac{GITC}{AD \times rr}\right)^2\right]^{\frac{1}{2}} \times \frac{ADR}{AD}$$

where

MFTC - Main frame time constant,

GITC - Gated integrator time constant,

ADR - Aperture delay range,

AD - Aperture duration, and

rr - Repetition rate.

For a typical case of 500μs ADR the minimum scan time becomes 23 sec. If a scan time greater than this is selected the resulting resolution will be the aperture

duration itself. In the present case it is 5μs. The scan time selected for all the recordings were above 150 secs.

The trigger pulse for the boxcar should have an amplitude of 0.5V and duration of 10ns. This is actually obtained from a photodiode which senses a fraction of the laser beam. Since the photodiode output does not always satisfy the above requirement, to achieve reliable operation, the output of the diode is fed to the trigger input of the Oscilloscope (Tektronix Model 466). The oscilloscope in turn gives an output of 5 volts corresponding to a positive going rectangular pulse coincident with the sweep time. The boxcar can be triggered by the positive slope of this rectangular pulse.

The processed signal is available at a BNC connector on the main frame. Also a 0-10V, scan ramp voltage is available. These two signals can be given to a X-Y recorder and a decay time curve can be obtained.

The electromagnetic interference from the laser discharges is also found to affect the detection system. This comes to the detection system in two ways,

(1) through radiated interference and (2) through conducted interference. The radiated interferences affecting the electronic circuits are minimised by using shielded connecting cables and also by using minimum length of the cables. However, it is not possible to completely eliminate these interferences. The conducted interference is minimised by giving very good earth connections to the power lines. Ground loop currents, produced in the various electronic instruments is avoided by giving the ground connections to the instruments in 'Tree' configuration[27].

The recorder used for the decaytime measurements is Omniscribe Model 2000 recorder. The transient fluorescence is measured for three different concentrations of Ho^{3+} in CaF_2 at both RT and LNT using the above set up. A typical decay curve is shown in Fig.4.6.

4.50 Observations and discussions

4.51 Fluorescence spectra

The fluorescence spectra of CaF_2:Ho^{3+} for 0.2, 0.4 and 1% of Ho^{3+} is shown in Figs.4.3A, 4.3B and 4.3C. In addition to the bands at 370nm and 420nm, which have been observed for pure CaF_2 also (see Fig.3.4), one

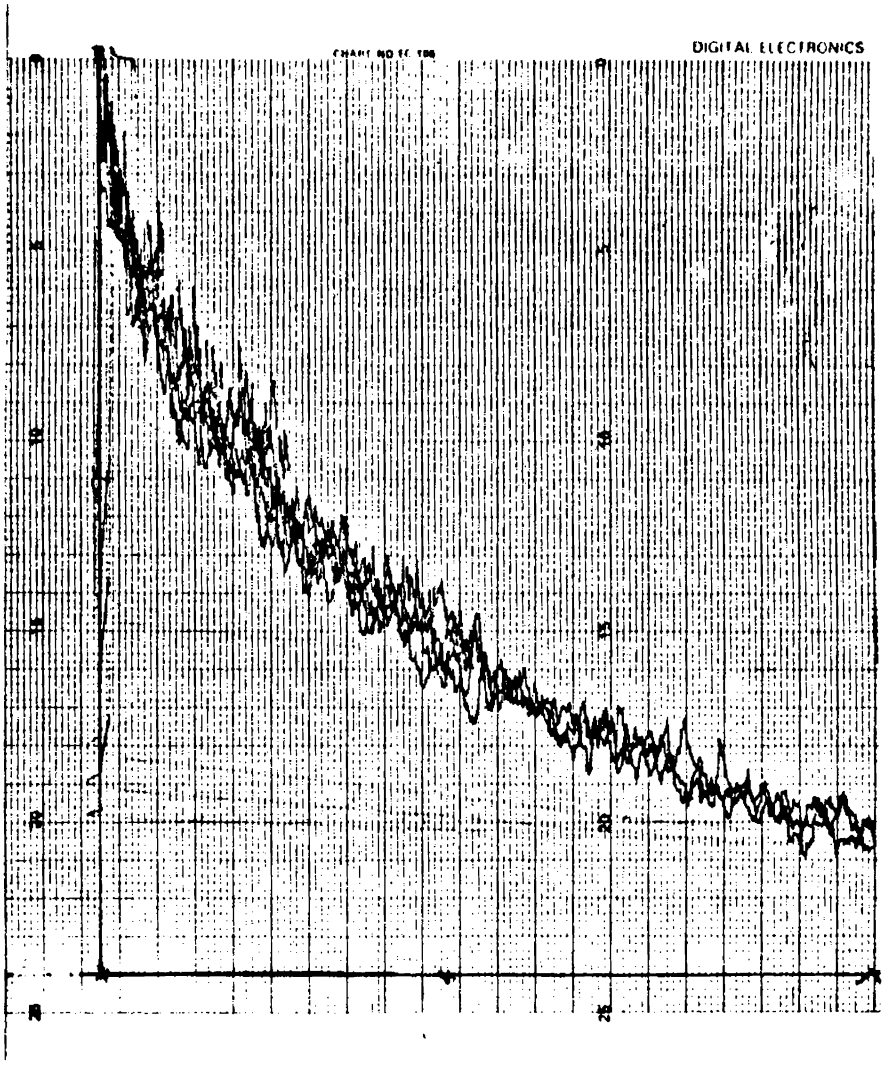

Fig.4.6 A typical decay curve ($CaF_2:Ho^{3+}$)

Time base - 1msec.
Gate width - 5μsec.
Scan time - 150 sec.
164 Time constant - 10μs
162 Time constant - 2 secs
No.of scans - 4

more band system appears at 530nm. The first two bands appear in the emission spectra of pure CaF_2, SrF_2 and BaF_2 also. Spectral characteristics of these bands suggest that these are due to two different centres A and B respectively. These are concluded to be due to some colour centres formed by vacancy complexes.

(a) 370nm band

This band is found in both pure and Ho^{3+} doped CaF_2 with slight intensity variations. Intensity of this band increases with Ho^{3+} concentration as can be seen in the spectra shown in Figs.4.3A, B and C. At 1% concentration the intensity of the band increases considerably and is prominent even at RT.

When Ho^{3+} is doped in CaF_2, it will incorporate in the host lattice through substitution in Ca^{2+} position. Presence of trivalent impurities in Ca^{2+} sites will produce more Ca^{2+} vacancies (V^{-}) and interstitial fluorine ion (F^{-}) which in turn produce more anion vacancies (ionised F centre, F^{+}). When Ho^{3+} concentration increases it will result in the formation of more point defects which may aggregate to form ($V^{-}F^{+}$). Cations Ca^{2+} near F^{+} and anions F^{-} near V^{-} will form a complex $(CaF)^{+}$ in

the vicinity of (V^-F^+). Population of this complex $(CaF)^+$ will increase as concentration of Ho^{3+} increases. The band at 370nm is due to the excitation and emission of $(CaF)^+$ by 337.1nm of N_2 laser. This explains the increase in the intensity of this band as concentration of Ho^{3+} is increased.

At room temperature, diffusion of vacancies resist the formation of (V^-F^+) complex ie, $(CaF)^+$ dissociates which explains the decrease in intensity of 370nm band at RT for pure CaF_2 and low concentration of Ho^{3+} in CaF_2. However, at higher concentration of Ho^{3+} (1%) population of $(CaF)^+$ complex will be so large that even at RT the 370nm band appears with considerable intensity.

(b) 420 nm band

Intensity variation of the broad band at 420nm is just opposite to that of 370nm band. It is observed that the intensity of the 420nm band decreases as concentration of Ho^{3+} increases. This band is due to the excitation and emission of the quasi molecular F_2^{--} complex formed by two fluorine ions in the vicinity of cation vacancy away from anion vacancy. At low concentrations

of Ho^{3+}, existence of $(V^-F)^+$ complex and independent V^- will give rise to both 370nm band and 420nm band. At higher dopant concentration, number of V^- and interstitial F^- increases, so that number of $(CaF)^+$ complex will increase thereby reducing independent V^- position. This will lower the population of F_2^{---} in the lattice and so the intensity of 420nm band is less for 0.4% of Ho^{3+} than for 0.2% of Ho^{3+} and is still less for 1% of Ho^{3+}.

(c) 530nm band

One more band system appears in the green region for CaF_2:Ho^{3+} which is not seen in the emission spectra of pure CaF_2. This shows that this band system in the green region is due to Ho^{3+} and is in agreement with earlier reports. Bansi Lal et al[2] have observed similar bands for 0.01% and 0.1% of Ho^{3+} in CaF_2 under Ar^+ laser excitation and has attributed this fluorescence group to the transition from $^5F_4$ and $^5S_2$ states of E level to $^5I_8$ state of Ho^{3+}. Table 4.2 gives the relative intensities of various emission peaks at RT and LNT.

As seen in the Figs, RT spectra show eight well separated narrow bands at 533.5, 535.9, 540.5, 542.2, 547.6, 549.6, 551.3 and 552.7nm. At RT the band intensity

Table 4.2

Intensities of various emission bands of $CaF_2:Ho^{3+}$ (0.2%)at RT and LNT

Wavelength (nm)	Energy (cm^{-1})	Intensity at RT (I_1) (arb. units)	Intensity at LNT(I_2) (arb. units)	Ratio I_2/I_1
552.7	18092	25.1	19.6	0.78
551.3	18138	18.5	7.1	0.38
549.6	18195	20.3	5.6	0.28
547.6	18261	16.5	4.5	0.28
542.2	18443	17.4	7.8	0.45
540.5	18501	18	6.7	0.37
535.9	18660	12	---	---
533.5	18744	8.9	---	---

decreases as concentration of Ho^{3+} increases. This can be due to concentration quenching, reabsorption processes and aggregate Ho^{3+} formation.

At LNT, one of the interesting features noted is that the band intensity decreases considerably as compared to RT which shows that decrease in intensity is not due to collisional quenching alone. At LNT, collisional effect being less we should expect increase in intensity contrary to the observation. But in the present case the total fluorescence intensity of this green band is reduced at LNT and also two fluorescence lines, specifically at 533.5 and 533.9nm found at RT even vanish at LNT. From the spectr it is also clear that the ratio in which the band intensity decreases is not the same for all the lines. The intensitie of all the lines except 552.7nm and 542.2nm have been reduce to one-third at LNT compared to that at RT while the intensities of these two bands have been reduced only by a lesser amount (see table 4.2). So we can assume that the radiations at 533.5nm and 535.9nm are reabsorbed thereby increasing the intensities of 552.7nm and 542.2nm bands.

The excitation spectra of $CaF_2:Ho^{3+}$ reveal strong absorption at 370nm and 420nm (Fig.4.3A & B). The 530nm emission is due to $^5F_4 \longrightarrow {}^5I_8$ and $^5S_2 \longrightarrow {}^5I_8$ of Ho^{3+}

line structure being due to transitions between various stark levels. These emission lines are produced by energy transfer or by the reabsorption of the emission from A centre (which is responsible for the 370nm emission) and B centre (which is responsible for the 420nm emission). When Ho^{3+} concentration increases, the intensity of 370nm band increases and that of 420nm band decreases showing that the fluorescence at 530nm at higher Ho^{3+} concentration is mainly due to reabsorption of 420nm emission. In the excitation spectra also it is seen that the absorption at 420nm increases at higher Ho^{3+} concentration. As 420nm iemission has the same intensity at RT and LNT, it is clear that only reabsorption and not energy transfer is taking place between B centre and Ho^{3+}. When Ho^{3+} concentration increases, the reabsorption effect also increases which explains the increased intensity of some of the fluorescence lines at higher concentration.

4.52 Lifetime determination

The decaytimes of the 370nm band and 420nm band are found to be less than 10 μs which is the limit of our experimental set up and hence could not be determined accurately.

Decay times of fluorescence at 530nm from $^5F_4$ and $^5S_2$ of E levels of Ho^{3+} in CaF_2 have been measured both at

RT and LNT. The decay times of each of the eight distinct peaks observed in the emission spectra are measured. The variation of lifetime with Ho^{3+} concentration at RT and LNT for each line is shown in the figure (Fig.4.7). In all the cases the lifetime is found to decrease rapidly with concentration. This indicates that there is a large contribution from Concentration Dependent Relaxation Processes (CDRP). A similar dependence of decay time on concentration has been studied by Asawa and Robinson for Nd^{3+} in LaF_3[28]. The CDRP can be due to ion-ion interaction and energy migration which may lead to resonant and non-resonant ion-pair transitions. It is observed in the present study that the contribution of CDRP is different for different emission peaks. It is also noted that for most of the peaks the CDRP is higher at LNT than at RT showing a decrease in lifetime at the lower temperature compared to the higher temperature.

The decay time of the emission at 552.7nm shows both concentration and temperature dependence. The decay time at RT is less than that at LNT for all concentrations. This can be easily understood because at room temperature the contribution from the non-radiative multiphonon transitions will be higher. The decay times of the lines 551.3nm, 549.6nm and 547.6nm emission are found to decrease

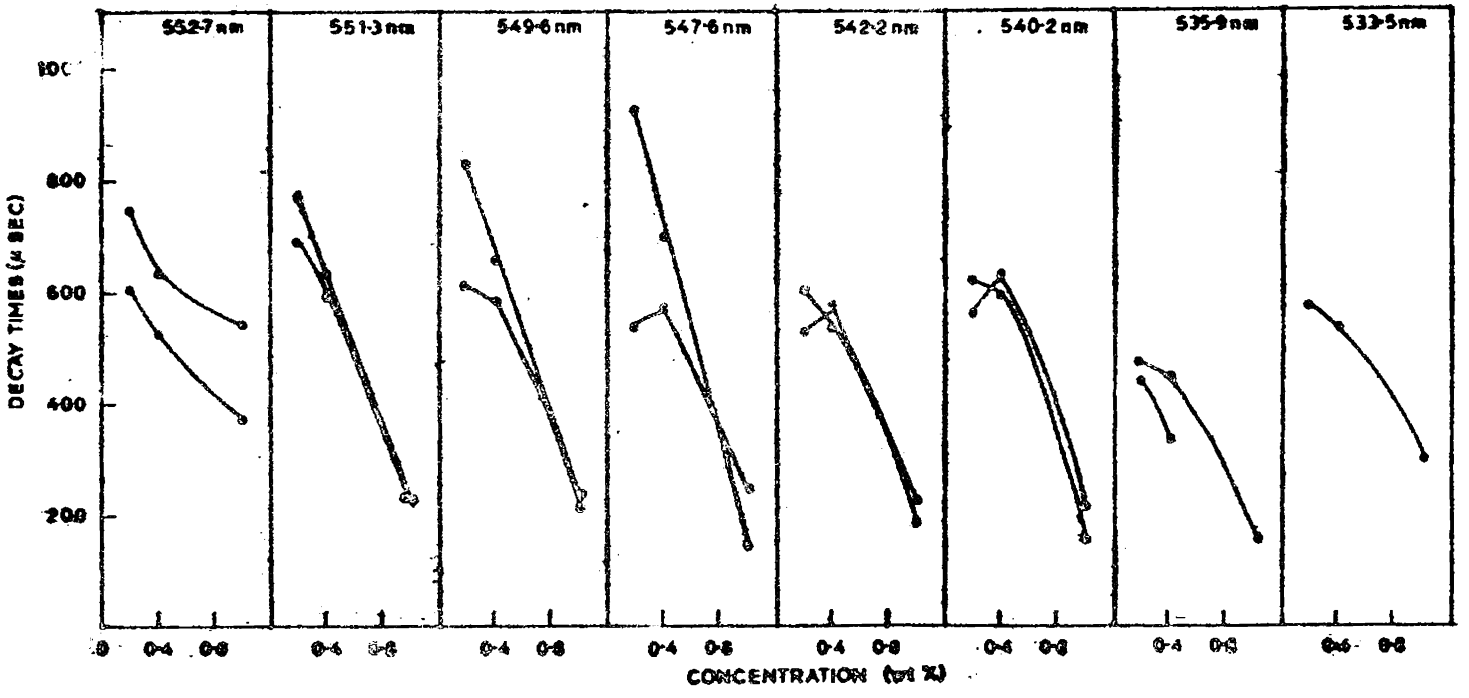

Fig.4.7 Variation of lifetime with Ho^{3+} concentration and temperature. ○ ○ at RT ○—○ at LNT.

very fast with concentration. Moreover, the first two lines have almost the same lifetime at RT and LNT for higher Ho^{3+} concentrations (value of τ is $223\mu s$) This indicates a possibility for the decrease in decay time at RT due to multiphonon transitions for these two lines being compensated by the increase in decay time due to CDRP at RT compared to the observed one at LNT. In other words, the contribution of the CDRP is maximum for these levels, whereas the decrease in lifetime due to non-radiative multiphonon relaxation processes are minimum. The contribution from the CDRP may possibly be less at RT than at LNT for 542.2nm, 540.2nm and 535.9nm lines which have decay times higher at RT than at LNT. Similar observation has been previously noted in the case of $LaF_3:Nd^{3+}$[29]. The lifetime variation of 533.5nm could be done only at RT as this emission does not have considerable intensity for lifetime measurements.

The contrasting behaviour of lifetime quenching observed for some of the lines at low temperature may possibly dbe due to the accidental matching of transitions. From the energy level considerations of Ho^{3+} it can be seen that a cross-relaxation is possible.between $(^5F_4, ^5I_8) \rightarrow (^5I_4, ^5I_7)$ (Fig.4.8). The Ho^{3+} ions at $^5F_4$ level can relax to

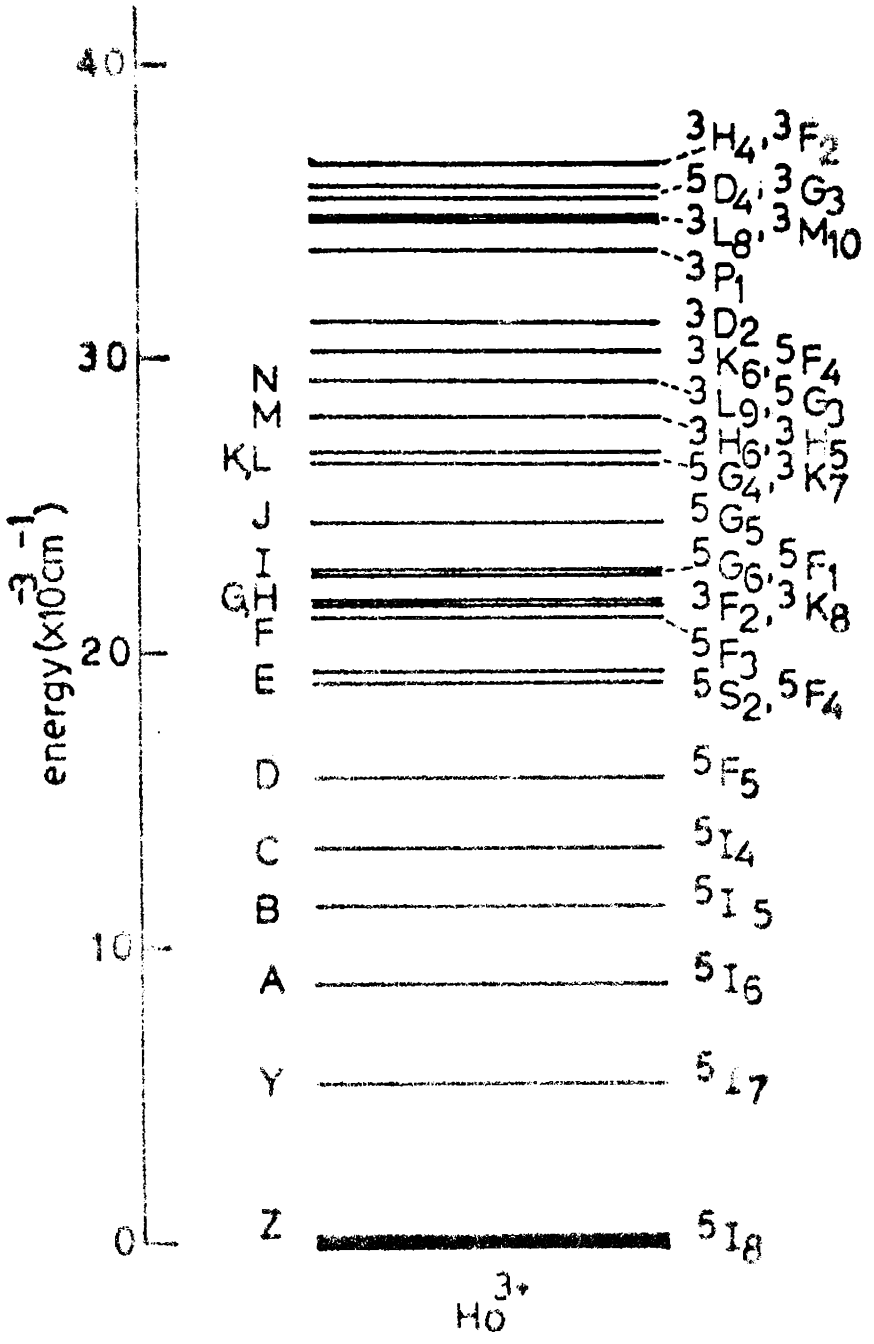

Fig.4.8 Schematic diagram of energy levels of Ho^{3+} in CaF_2.

$^5I_4$ level so that the corresponding energy can be used to excite an Ho^{3+} ion from the ground state $^5I_8$ to the level $^5I_7$. It should be noted that the energy difference between $^5F_4$ and $^5I_4$ is the same as that between $^5I_8$ and $^5I_7 \backsim 5175\ cm^{-1}$. Thus the lifetime quenching observed for the fluoresence lines at 547.6, 542.2 and 540.5nm is due to the ion pair relaxation. For low concentrations of Ho^{3+} in CaF_2 these observations have not been noted.

An increase in lifetime is noted for the intermediate concentrations for the fluorescence emission lines at 547.6nm, 542.2nm and 540.5nm. Extensive experimental as well as theoretical investigations[30,31] have established that, at higher concentrations the decay times are shortened due to interactions between neighbouring ions. The increase in the decay time (Fig.4.7) for intermediate concentrations may be due to reabsorption of the fluorescence radiation. The rate equation of the system in which fluorescence light is reabsorbed is given by

$$\frac{dN}{dt} = -A(1-B)N,$$

where A is total transition probability of the fluorescing level, N its population and B is the fraction of the fluorescence radiation reabsorbed[32]. The value of the

term (1-B) is always less than unity (for B=1 no fluorescence will be observed). The transition probability is therefore, lower than the true transition probability and will lead to longer decay times.

At low concentrations, both reabsorption as well as ion-ion interaction are negligible processes. But with the increase in Ho^{3+} concentration, the reabsorption process may become dominant so that the decay times will increase with increase of concentration. As the concentration is further increased a stage will be reached where the ion-ion interaction is the dominant process, resulting in a decrease in the decay times.

4.6 Calculation of non-radiative efficiency

The fundamental problem of non radiative relaxation process in rare earth doped crystals is of great importance in the wake of its use in solid state lasers. In solid state lasers sensitizers are often used to improve the emission efficiency and in choosing these sensitizers, a measure of the non radiative relaxation processes from the higher levels to the fluorescing level of the acceptor ion is of great use.

Stimulated emission in the green region (551.2nm) has been already observed from $CaF_2:Ho^{3+}$ due to the

transition $^5S_2 \longrightarrow {}^5I_8^{23}$. A relative measurement of the non-radiative relaxation rates from higher excited levels to $^5S_2$ level which is the upper lasing level for green emission of $CaF_2:Ho^{3+}$ is done using only the absorption and excitation spectra in the following manner.

Let a parallel monochromatic light beam of intensity I_o (incident flux) be incident on a crystal of thickness 'l'. The interaction of weak incident radiation with matter is described by the expression

$$I = I_o \exp(-K_{(\lambda)} l) \qquad (1)$$

where I is the transmitted intensity. The absorbed intensity will be therefore,

$$I_o - I = I_o (1 - e^{-K(\lambda)l}) \qquad (2)$$

ie., the number of photons absorbed will be '$\beta_{(\lambda)} I_o$' where $\beta_{(\lambda)}$ is the fraction of photons absorbed

$$\beta_{(\lambda)} I_o = 1 - e^{-K(\lambda)l} \qquad (3)$$

Some of the ions thus excited will relax to the fluorescing

level below. Let $\gamma_{u \to L}$ be the ratio of number of ions in the upper level. Then

$$\text{Number of ions relaxed} = \gamma_{u \to L} \beta_{(\lambda)} I_o \qquad (4)$$

Some of the ions will then return to the ground state by radiative transition and the rest of the ions will relax to ground state by different non-radiative processes. The radiative emission from the fluorescing level depends on η, the quantum efficiency for radiative transition to the ground state. Hence the total number of photons emitted 'I_e' can be expressed as

$$I_e = \eta \gamma_{u \to L} \beta_{(\lambda)} I_o \qquad (5)$$

$$\therefore \gamma_{U \to L} = \frac{I_e}{I_o} \Big/ \eta \beta_{(\lambda)} = \frac{E_{(\lambda)}}{\eta \beta_{(\lambda)}} \qquad (6)$$

'$E_{(\lambda)}$' ie, I_e/I_o can directly be obtained from the excitation spectra.

The radiative quantum efficiency

$$\eta = \frac{\Sigma A_{mn}}{\Sigma A_{mn} + \Sigma C_{mn}} \qquad (7)$$

where ΣA_{nm} is the radiative transition probability and $\Sigma A_{nm} + \Sigma C_{nm}$ is radiative plus non-radiative transition probability.

$$\text{But } \Sigma A_{nm} + \Sigma C_{nm} = \frac{1}{\tau} \tag{8}$$

$$\text{and} \qquad A_{nm} = \frac{0.22}{\lambda^2} f_{nm} \tag{9}$$

where 'τ' is the observed lifetime of the fluorescing level and 'f_{nm}' is the oscillator strength.

Substituting equations (8) and (9) in (7) we get

$$\eta = \frac{0.22}{\lambda^2} f_{nm} \tau \tag{10}$$

Again substituting the value of η from equation (10) in equation (6) we get,

$$\gamma_{u \to L} = \frac{4.5 \lambda^2}{f_{nm} \tau} \frac{E_{(\lambda)}}{\beta_{(\lambda)}} \tag{11}$$

The relative value of $\gamma_{u \to L}$ for the 551.2nm emission of Ho^{3+} in CaF_2 is calculated and tabulated in Table 4.3. The value of $\beta_{(\lambda)}$ is obtained from the

Table 4.3

Relaxation rates to $^5S_2$ level of $CaF_2:Ho^{3+}$(1%) from higher levels

λ - 551.3nm, τ - 374 μs

Level	$\beta_{(\lambda)}$ %	$E_{(\lambda)}$ %	$\frac{\beta_{(\lambda)}\ \%}{E_{(\lambda)}\ \%}$	$\gamma_{u \to L}$ f_{nm}
480nm($^5F_3$)	68.18	0.15	2.2×10^{-3}	0.080
465nm($^5G_6$)	44.01	0.15	3.408×10^{-3}	1.242
445nm($^5F_1$)	71.63	0.226	3.155×10^{-3}	1.151
415nm($^5G_5$)	68.02	0.111	1.632×10^{-3}	0.060
382nm($^5G_4$,$^3K_7$)	46.74	0.042	8.986×10^{-4}	0.033
357nm	66.71	0.087	1.304×10^{-3}	0.048
345nm	50.34	0.039	7.747×10^{-4}	0.028
330nm	53.23	0.03	5.636×10^{-4}	0.021
280nm	68.18	0.15	2.2×10^{-3}	0.080

absorption spectra taken on a Cary-14 spectrophotometer and $E_{(\lambda)}$ is obtained from the excitation spectra taken using Aminco Bowman spectrofluorometer. $\beta_{(\lambda)}$ and $E_{(\lambda)}$ are tabulated in percentage. The values of τ, λ and f_{nm} are the same for each calculations. In the present study 'f_{nm}' could not be found out and hence only a relative value could be obtained. The value of τ(374 μs) determined by N_2 laser excitation, and λ the wavelength of fluorescence emission from $^5S_2$ level (551.2nm) is also substituted to find the value of '$\gamma_{u \to L} \times f_{nm}$'.

From the table it can be seen that more efficient relaxation to the $^5S_2$ level takes place from ($^5G_6$, $^5F_1$) level at 21505 cm^{-1}. It is thus clear that for enhancing the population of the $^5S_2$ level of Ho^{3+} by sensitization, the activator should be so chosen that it should have a level from which efficient energy transfer can take place to the ($^5G_6$, $^5F_1$) level of Ho^{3+}.

REFERENCES

1. A.A.Kaminskii, Laser crystals - their physics and properties, Springer Verlag, New York (1981) 8.

2. Bansi Lal and D.Ramachandra Rao, Chem.Phys.Letts, 53, 251 (1978).

3. H.Goberchet, Ann.Phys. 31, 755 (1938).

4. E.J.Mechan and G.O.Nulting, J.Chem.Phys. 71, 1002 (1939).

5. H.G.Khale, Z.Phys, 145, 357 (1956).

6. S.Singh, Ph.D. Thesis, The Johns Hopkins University, USA (1957).

7. F.H.Spedding and M.T.Rothwell, J.Chem.Phys, 48, 4843 (1968).

8. J.C.Walling and R.L.White, Phys.Rev, 10, 4737 (1974).

9. G.H.Dieke and B.Pandey, J.Chem.Phys, 41, 1952 (1947).

10. K.Rajnak and W.F.Krupke, J.Chem.Phys, 48, 3343 (1968).

11. J.L.Merz and P.S.Parshan, Phys.Rev, 162, 235 (1967).

12. L.F. Johnson, J.F.Dillon and J.P.Ramuka, J.Appl.Phys, C4, 1499 (1969).

13. D.E.Wortman and D.Sanders, J.Chem.Phys, 53, 1247 (1970).

14. P.J.Becker, Phys.Status Solidi, B43, 583 (1971).

15. M.J.Weber and B.Matsinger, J.Chem.Phys, 57, 562 (1972).

16. D.E.Wortman, C.A.Morrison and R.T.Pariar, J.Opt.Soc. Am, 62, 1329 (1973).

17. R.Reisfeld and J.Hormadaly, J.Chem.Phys, 7, 1002 (1939).

18. H.H.Caspers, H.E.Rast and J.L.Fry, J.Chem.Phys, 53, 3208 (1970).

19. A.M.Tkachuk, Bull.Acad.Sci. USSR, Phys.Ser, 31, 2110 (1967).

20. M.Schelsinger and P.W.Whippey, Phys.Rev, 177, 563 (1969).

21. A.A.Kaplyanshii, Opt.& Spect. 39, 437 (1975).

22. M.B.Seelbinder, Phys.Rev.B, 20, 4308 (1979).

23. Yu.K.Voron'ko, A.A.Kaminskii and V.Osiko, Sov.Phys. J.E.T.P 22, 295 (1966).

24. L.F.Johnson, J.Appl.Phys, 34, 897 (1963).

25. S.L.Naberhuis and K.Fong, J.Chem.Phys, 56, 1174 (1972).

26. Instruction Manuals, Lock-in-amplifier and current sensitive preamplifier Model 124A and Model 184, Princeton Applied Research, USA.

27. Electrometer Measurements, Keithley Instruments Inc, USA (1977) 24.

28. C.K.Asawa and M.Robinson, Phys.Rev. 141, 251 (1966).

29. H.Jagannath, S.K.Basu and P.Venkateswaralu, Chem.Phys. Letts, 66, 313 (1979).

30. P.S.Botden, Philips Res.Rept., 6, 415 (1951).

31. L.G.Van Uitert and S.Lida, J.Chem.Phys, 37, 986 (1962).

32. G.E.Barash and G.H.Dieke, J.Chem.Phys. 43, 988 (1965).

CHAPTER V

FLUORESCENCE SPECTRA OF Nd^{3+} IN CaF_2, SrF_2 AND BaF_2

5.10 Introduction

From the beginning of laser technology to the present day, Nd^{3+} in various host lattices has been one of the most powerful and flexible laser active materials[1,2]. At present, there are more than one hundred different crystals doped with Nd^{3+} for which emissions have been stimulated. The most fully investigated crystals containing Nd^{3+} for which the stimulated absorption spectra have been identified with absorption and fluorescence spectra are $CaWO_4$[3-5], $PbMoO_4$[6] and LaF_3[7].

A number of lasers have been operated using the cubic fluoride hosts of CaF_2, SrF_2 and BaF_2. These crystals can be grown with excellent optical quality by the Stockbarger technique[8]. Among them CaF_2 crystals have been the most widely used host. Laser action in the BaF_2 and SrF_2 hosts is more difficult to achieve than in CaF_2. Some of the various hosts in which laser action has been achieved with Nd^{3+} and the corresponding emission wavelengths are listed in Table 5.1.

Table 5.1

Properties of some laser crystals with Nd^{3+} activator

Host crystal	% of Nd^{3+} activator	Emission wavelength (μm)	Temperature (K)	Excitation sp.range (μm)	Luminescence lifetime (ms)	Laser transition	Ref
$LiNbO_3$	0.2-2	1.0846	300	0.4-0.9	0.5	$^4F_{3/2} \rightarrow {}^4I_{11/2}$	31
$CaAl_4O_7$	0.4	1.0786	300	0.5-0.9	0.28	,,	32
KY_2O_3	1	1.073	77	0.4-0.9	0.26	,,	33
$LiYF_4$	2	1.0471	300	0.4-0.9	0.5	,,	34
CaF_2	0.4-0.6	1.0448	77	0.5-0.9	1.1	,,	35
SrF_2	0.1-0.8	1.0370	295	0.5-0.9	1.25	,,	36
BaF_2	---	1.060	77	0.4-0.9	---	,,	37
LaF_3	1-2	1.04065	300	0.5-0.9	0.6	,,	38
$KY(WO_4)_2$	2	0.9137	77	0.5-0.9	0.11	$^4F_{3/2} \rightarrow {}^4I_{9/2}$	39

There have been several investigations of the optical spectra of Nd^{3+} in CaF_2. The infrared fluorescence has been well described by Feofilov[9]. Kiss[10] has attempted to compare the observed absorption spectrum with the theoretical spectrum based on the assumption of a cubic field. In CaF_2:Nd^{3+}, emission at room temperature has been observed at λ = 1046.1nm[11]. Later five more emission lines were observed at temperatures from 90° to 15°K[12]. The crystals in which stimulated emission was investigated contained 0.07 to 1.0% by wt of Nd^{3+}.

Nd^{3+} can be distributed in CaF_2 crystals among differently formed centres characterised by unlike spectra. The formation of any particular optical centre depends, among other factors, on the concentration of the activator in the CaF_2 crystals. The symmetry of the neighbourhoods of different Nd^{3+} optical centres in CaF_2 has been studied by means of electron paramagnetic resonance[13]. Thus it has been reported that Nd^{3+} can be located in a crystal field exhibiting tetragonal symmetry and two kinds of rhombic symmetries. The intensity of the latter was found to increase with the Nd^{3+} concentration. It was reported by Vincow et al[14] that CaF_2: Nd^{3+} crystals have a spectrum corresponding to a cubic crystalline field.

The absorption, fluorescence and stimulated emission spectra and the lifetimes of the excited Nd^{3+} state in CaF_2 have been investigated by Voronko et al[15]. The crystal field splittings in Nd^{3+} in CaF_2 has been computed by Synek et al[16]. Table 5.2 gives the stark levels of Nd^{3+} in CaF_2. The mechanism of interaction of Nd^{3+} ions and the nature of concentration quenching in CaF_2, SrF_2 and BaF_2 crystals have been investigated by Voronko[17]. They have also measured the lifetimes of the excited states of various centres of the Nd^{3+} ions.

Currently Nd^{3+} is one of the most widely used activators in laser condensed media. Nd^{3+} readily exhibits stimulated emission at room temperatures on the principal $^4F_{3/2} \longrightarrow {}^4I_{11/2}$ and the additional $^4F_{3/2} \longrightarrow {}^4I_{13/2}$ transitions. Extensive spectroscopic information accumulated by numerous research groups engaged in studying Neodymium doped laser crystals has permitted elucidation of the most important regularities of their properties, which have proved very useful in the search for new materials.

Various studies on the properties of Nd^{3+} are being carried out by several groups of researchers. The

Table 5.2

Stark levels of Nd^{3+} in CaF_2 at 77K

SL J manifold	Stark level positions in (cm^{-1})	Number of components Th.	Exp.
	Stark levels of L centre		
$^4I_{9/2}$	0, 82, 202, 744	5	4
$^4I_{11/2}$	1977,2084,2094,2103,2462	6	5
$^4F_{3/2}$	11594,11707	2	2
$^4F_{7/2}$+ $^4S_{3/2}$	13541,13594,13638,13761	6	4
$^2P_{1/2}$	23480	1	1
$^4D_{3/2}$	28106,28280	2	2
	Stark levels of M centre		
$^4I_{9/2}$	0,36	5	2
$^4I_{11/2}$	2028,2052,2191	6	3
$^4F_{3/2}$	11582, 11622	2	2
$^4F_{7/2}$+$^4S_{3/2}$	13468,13706,13712,13770	6	4
$^2P_{1/2}$	23416	1	1
$^4D_{3/2}$	28272,28288	2	2

Table 5.2 (contd.)

SL J manifold	Stark level positions in (cm^{-1})	Number of components Th.	Exp.
	Stark levels of N centre		
$^4I_{9/2}$	0, 42	5	2
$^4I_{11/2}$	2031, 2061, 2085	6	3
$^4F_{3/2}$	11602, 11641	2	2
$^4F_{7/2}$+ $^4S_{3/2}$	13486, 13602, 13727, 13732	6	4
$^2P_{1/2}$	23441	1	1
$^4D_{3/2}$	28281, 28320	2	2

temperature shift and broadening of luminescence and absorption lines of Nd^{3+} ion in fluoroapatite crystals are discussed in detail by Minkov et al[18]. The behaviour of the population of the $^4I_{11/2}$ level of Nd^{3+} in glasses interacting with high power coherent radiation is also reported[19]. Singh et al[20] have obtained improved fluorescent lifetime of the $^4F_{3/2}$ state of Nd^{3+}. The concentration quenching and temperature dependence of the fluorescence of Nd^{3+} have also been subjects of considerable interest studied in various hosts[21].

In all the above studies only the infrared fluorescence of Nd^{3+} are investigated and very little studies have been made on the visible fluorescence of Nd^{3+}. The first report of the absorption and fluorescence of Nd^{3+} in the visible and ultraviolet regions was made by Kumar et al[22]. This observation was made on Nd^{3+} doped LaF_3 and the exciting surce was N_2 laser. Fluorescence has been observed from five levels L,K,D,E and R in the optical region. They have also studied the absorption spectra of LaF_3:Nd^{3+} in the optical region and have identified a few lines in the region 253.0nm to 354.0nm in addition to the known absorption spectrum in the visible region. Fluorescence was also observed in the region 352.0nm to 901.3nm from LaF_3:Nd^{3+} under

N_2 laser excitation. Jagannath et al[23] have studied the relaxation rates and concentration quenching of L and K levels of $LaF_3:Nd^{3+}$.

Later some more investigations on the UV and VUV luminescence of Nd^{3+} were reported[24]. For the first time a VUV band of emission at 174.0nm attributed to the 5d 4f transitions of the Nd^{3+} ion and characterised by a high quantum yield was observed by Devyatkova et al[25]. From the above review it appears that the fluorescence emission spectra of Nd^{3+} in CaF_2, SrF_2 and BaF_2 are not fully investigated in the UV and visible regions under a powerful source like N_2 laser.

In the present study, strong blue emission has been observed from $CaF_2:Nd^{3+}$ and $SrF_2:Nd^{3+}$ on N_2 laser excitation. The blue emission band is also seen in $BaF_2:Nd^{3+}$ with much less intensity. The visible fluorescence in the blue region could be obtained due to the high excitation energy available with the N_2 laser.

5.20 Experimental

The fluorescence spectra of CaF_2, SrF_2 and BaF_2 doped with 1% and 2% Nd^{3+} were charted at RT and LNT. The crystals were excited by an N_2-laser (1.5 Mw/cm^2) and

the spectra were recorded with the help of a monochromator, PMT and a chart recorder. While recording the spectra the slit widths of the monochromator were kept at 30μm for SrF_2:Nd^{3+}, 320μm for CaF_2:Nd^{3+} and 740μm for BaF_2:Nd^{3+}. The resolutions achieved are therefore 0.048nm, 0.51nm and 1.18nm respectively.

5.30 Results

5.31 CaF_2:Nd^{3+}

The fluorescence spectra were charted in the region 350nm to 500nm for 1% Nd^{3+} and 2% Nd^{3+} at RT and LNT. The fluorescence spectrum of CaF_2:Nd^{3+} at 1% is shown in Fig.5.1, and is found to have a broad emission band extending from 409nm to 470nm. The band consists of two peaks and could not be further resolved into lines even with very narrow slit width.

The peak positions and the relative intensities of the two peaks for 1% and 2% Nd^{3+} in CaF_2 and also at RT and LNT are given in Table 5.3. For CaF_2 doped with 1% Nd^{3+} the peak positions are at 425nm and 435nm at RT while at LNT, the new positions of the peaks are at 420nm and 425nm. The emission intensity is also found to increase at LNT compared to RT.

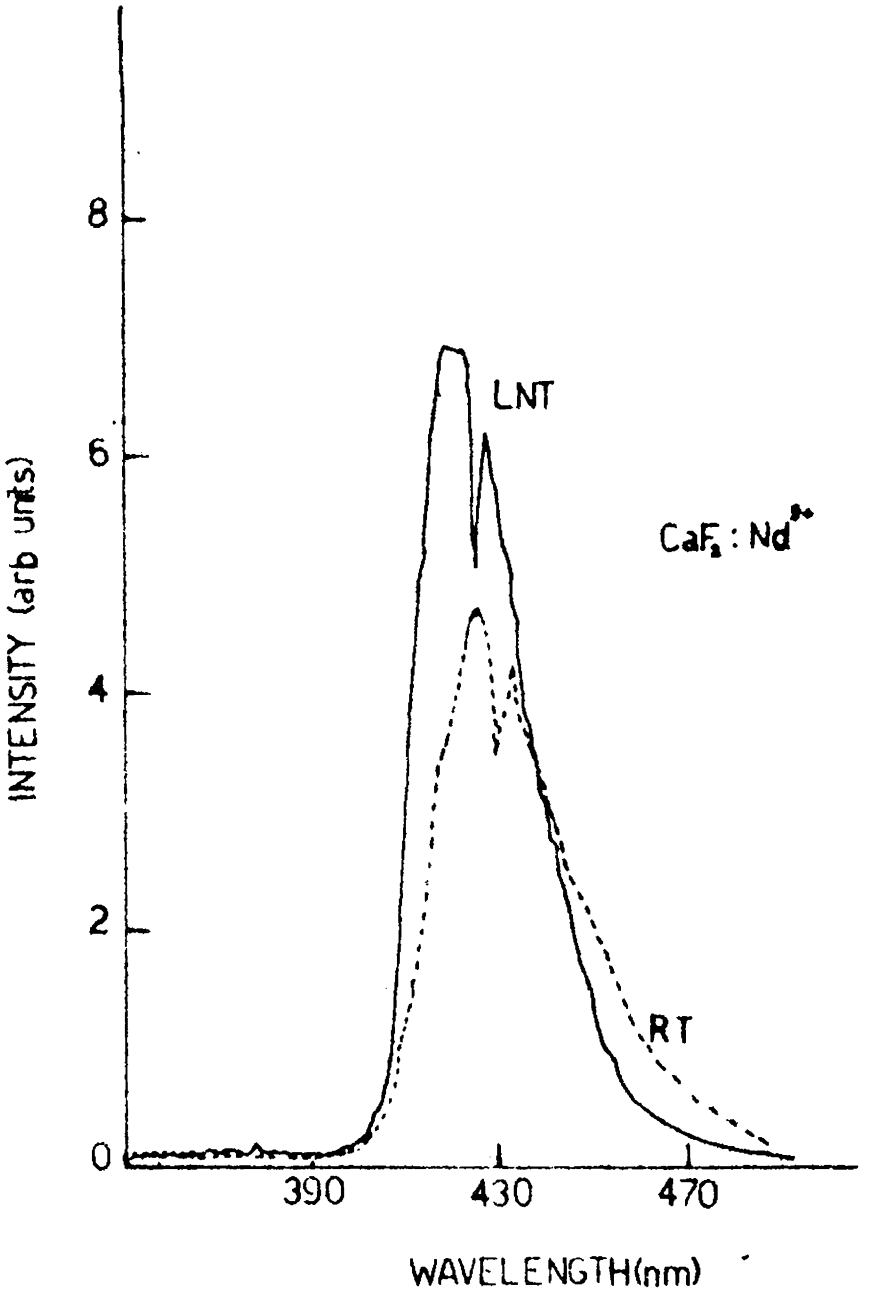

Fig.5.1 N_2 laser excited fluorescence spectra of CaF_2:Nd^{3+}(1%) at 420nm region.

Table 5.3

Relative intensities of emission at 420nm for 1% and 2% Nd^{3+} in CaF_2

CaF_2: Nd^{3+} (1%)				CaF_2:Nd^{3+} (2%)			
Emission wave-length (nm)		Intensity (in arb. units)		Emission wave-length (nm)		Intensity (in arb. units)	
RT	LNT	RT	LNT	RT	LNT	RT	LNT
425	420	12.1	17.2	421	425	7.7	9.6
435	425	10.6	15.2	429	429	6.5	8

For 2% Nd^{3+}, the band intensity is considerably reduced due to concentration quenching. For these crystals also the double band appears. The excitation spectra of $CaF_2:Nd^{3+}$ show two strong absorptions at 337nm and 370nm (Fig.5.2).

In the present study two emission bands at 370nm and 420nm have been observed from pure CaF_2 and have been attributed to colour centres formed by vacancy complexes. (Chapter II). But for $CaF_2:Nd^{3+}$ the 370nm emission band has not been recorded. From the excitation spectra it is clear that the 370nm emission of the pure crystal is absorbed by Nd^{3+} ions to get excited. The 420nm emission overlaps the Nd^{3+} emission in the same region. Hence it can be concluded that the Nd^{3+} ions absorb 337nm radiation of N_2 laser and 370nm emission of pure CaF_2 to give the blue fluorescence.

Nd^{3+} ions in LaF_3, SrF_2 and BaF_2 are reported to have two main fluorescing levels at 28420 cm^{-1} and 11460 cm^{-1} [26]. The strongest fluorescent transitions from these levels are at 412nm (24270 cm^{-1}) and 1085nm (7450 cm^{-1}) respectively. The energy level scheme for these emissions are shown in Fig.5.3. The N_2 laser frequency is about 29,656 cm^{-1}. This excites the Nd^{3+} ion to phonon coupled

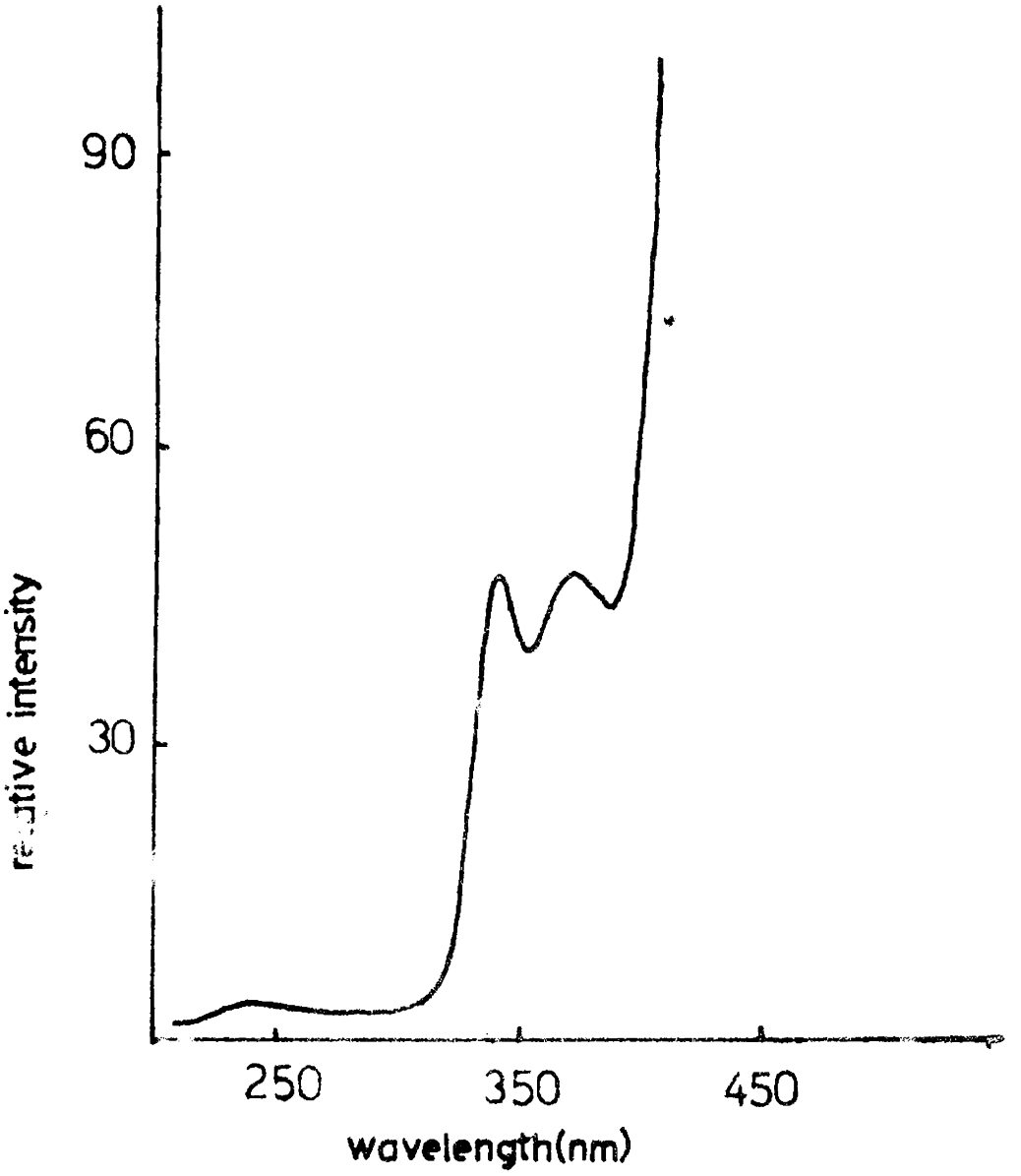

Fig.5.2 Excitation spectra of $CaF_2:Nd^{3+}$ at 420nm region.

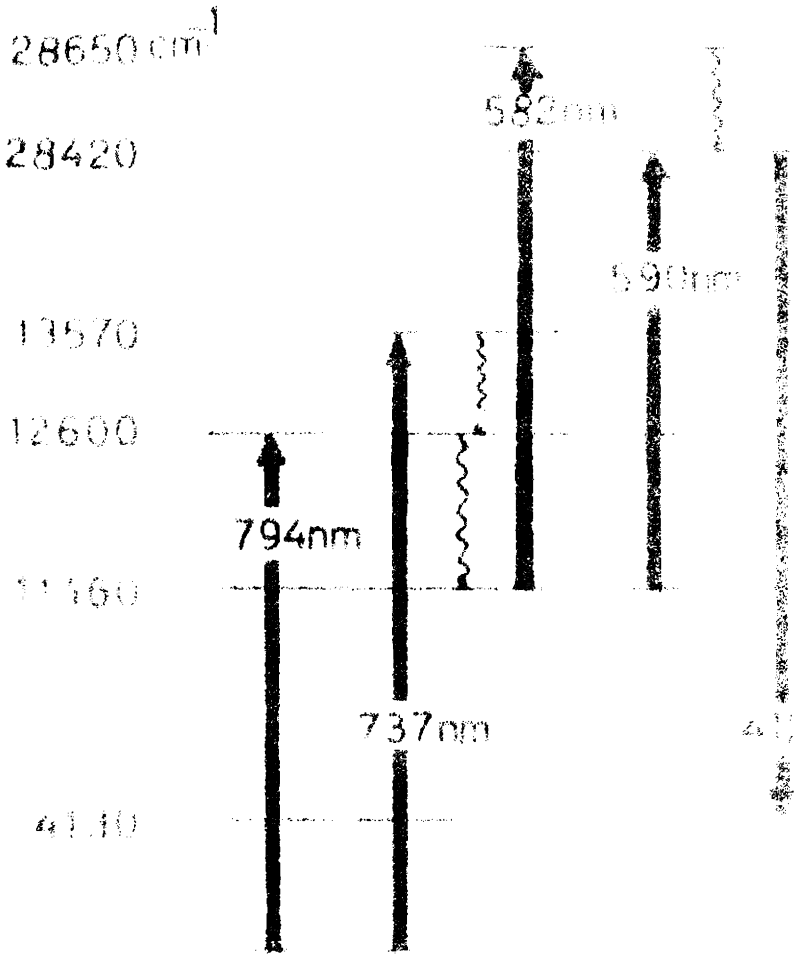
28650 cm⁻¹
28420
582nm
590nm
13570
12600
794nm
11160
737nm
4110

stark levels of the 'L' level of Nd^{3+}. The excited state then relaxes through multistep processes to the 'K' level of Nd^{3+}. The transition from the 'K' level to the lower 'X' level gives the blue fluorescence of Nd^{3+}. Fig.5.6 shows the energy levels of Nd^{3+} and the transition involved in the observed fluorescence of Nd^{3+}.

The appearance of a double band can be either due to the overlapping of the 420nm emission of pure crystals with the emission of Nd^{3+} or due to the presence of some reabsorption processes taking place. The chances for the reabsorption processes cannot be excluded as the Nd^{3+} ions in the crystal have a number of stark levels to which reabsorption can take place. The observed increase in the intensity at LNT compared to RT is due to the decreased probability of non-radiative transitions at lower temperature.

The lifetime of the emission bands are found to be less than 10μs which is the limit of our experimental set up. The crystals do not give any other fluorescence emission in the visible region.

5.32 $SrF_2:Nd^{3+}$

A. Emission spectra

Under N_2 laser excitation $SrF_2:Nd^{3+}$ is also

found to give a strong blue emission, much more intense than $CaF_2:Nd^{3+}$ (Fig.5.4). The fluorescence band observed in this case also is found to consist of two peaks, the peak positions being at 417nm and 425nm at RT and at 415nm and 418nm at LNT. Thus it can be seen that the peaks are slightly shifted to the high energy side in SrF_2 compared to CaF_2. This is possibly due to the fact that the rare earth ions are in a stronger field in SrF_2 than in CaF_2.

In $SrF_2:Nd^{3+}$ also, the band intensity increases by a large amount at LNT and the whole band becomes narrower. Thus it can be seen that the non-radiative process is higher in $SrF_2:Nd^{3+}$ than in $CaF_2:Nd^{3+}$ resulting in a larger temperature dependence of band intensity. The excitation spectra of this crystal also revealed absorptions at 337nm and 370nm and hence the Nd^{3+} ions are first excited by 337nm and from there it relaxes to the level 'K' and transition to 'X' level give the fluorescence at 420nm region.

The fluorescence spectra of $SrF_2:Nd^{3+}$ show one more band system at 720nm region. For $CaF_2:Nd^{3+}$ this band system could not be detected as the intensity is very weak. Even for $SrF_2:Nd^{3+}$ this band system is much weaker compared to the one at 420nm.

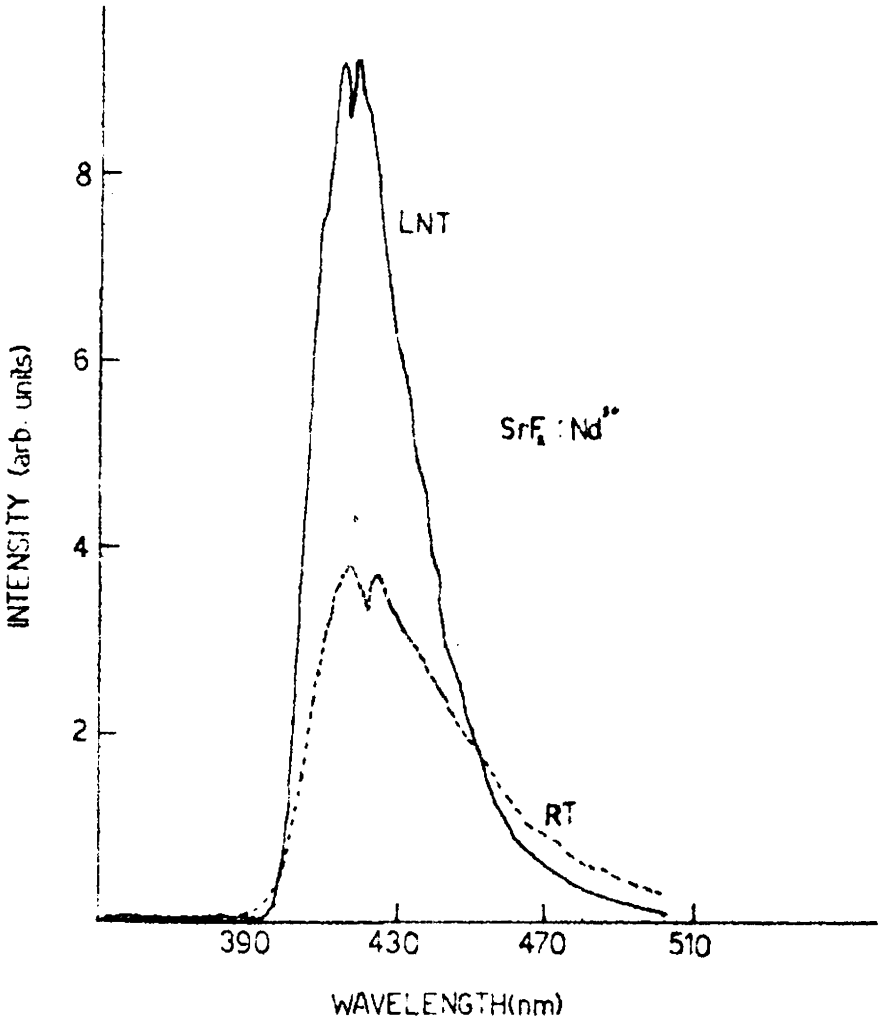

Fig.5.4 N_2 laser excited fluorescence spectra of $SrF_2:Nd^{3+}$(1%) at 420nm region.

The spectra of SrF_2:Nd^{3+} at 720nm region are charted at RT and LNT for 1% and 2% Nd^{3+}. The decay time measurements are also carried out. The emission spectra of both 1% and 2% Nd^{3+} in SrF_2 at both RT and LNT are shown in Fig.5.5. Fluorescence spectra of SrF_2:Nd^{3+} (1%) in the 720nm region consist of four intense (725nm, 729nm, 734nm and 745nm) and two weak bands (749nm and 740nm) at both RT and LNT. But for SrF_2:Nd^{3+} (2%) only 725nm, 729nm and 734nm lines are observed.

The spectra show strong temperature and concentration dependence. It can be seen that when the Nd^{3+} concentration is higher, the fluorescence intensity of all the peaks are reduced considerably. It is also noted that the relative intensity of the 729nm line is more compared to that of the 725nm line at both the temperatures for 1% Nd^{3+} while the intensity ratio is reversed for 2% Nd^{3+} at LNT.

B. Lifetime measurements

Lifetime study of this fluorescence group also reveals a strong concentration and temperature dependence. Lifetimes of the excited states of Nd^{3+} giving fluorescence in the 720nm region is given in Table 5.4. For 1% Nd^{3+}

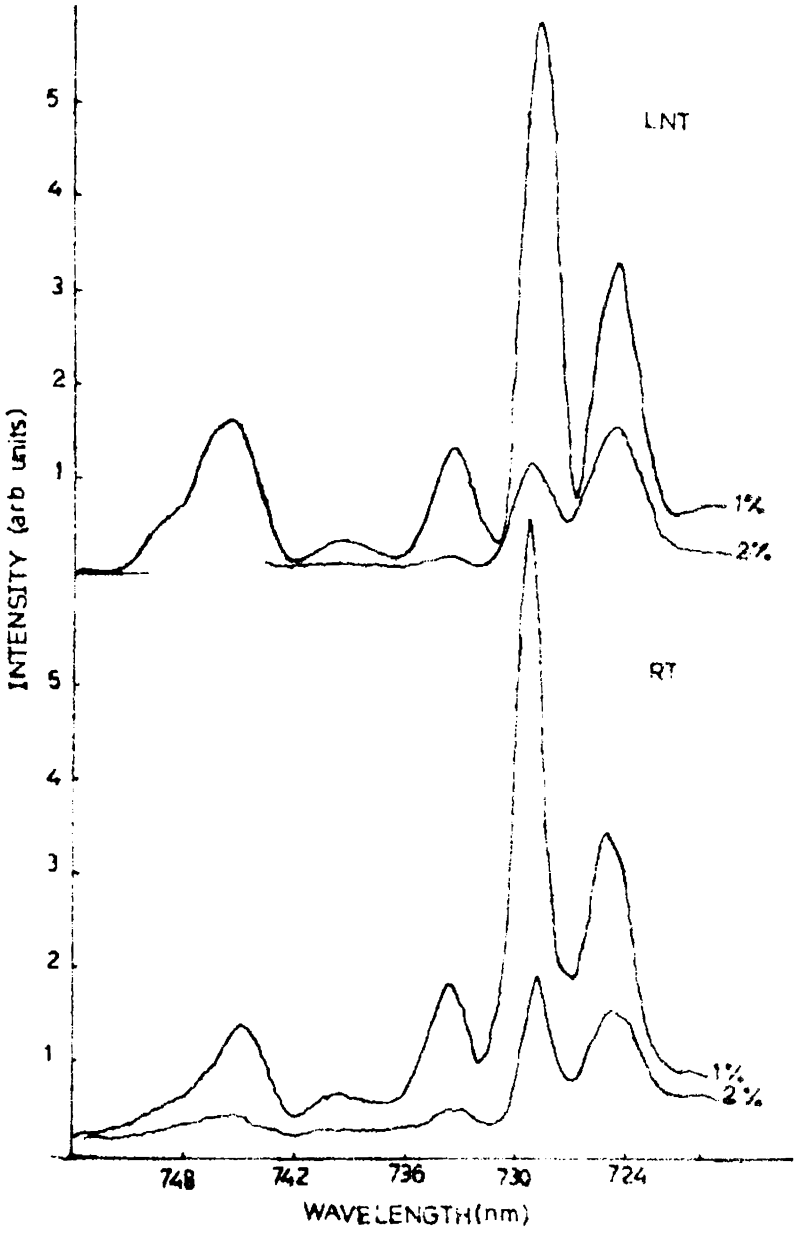

Fig.5.5 N_2 laser excited fluorescence spectra of $SrF_2:Nd^{3+}$ at 720nm region.

Table 5.4

Lifetime of the excited states of Nd^{3+} in SrF_2

Emission wavelength	Lifetime of excited state (μs)			
	$SrF:Nd^{3+}$ (1%)		$SrF:Nd^{3+}$ (2%)	
	RT	LNT	RT	LNT
725nm	134	284	83	15
729nm	132	296	89	121.8
734nm	136	292	81	87
745nm	128	304.5	—	—

in SrF_2, the lifetimes of all the states are found to increase at LNT compared to those at RT showing less contribution of multiphonon relaxation processes at LNT.

But as the Nd^{3+} concentration is increased (ie, for 2% Nd^{3+}) the lifetimes of all the states are decreased from those for 1% Nd^{3+}. This sharp decrease is due to the effect of some Concentration Dependent Relaxation Processes (CDRP). The concentration dependent relaxation processes are due to ion-ion interaction and would lead to resonant and non-resonant ion pair transitions. In the present study, it is also observed that at 2% Nd^{3+} concentration,

$$\tau_{725}\ (\text{LNT}) < \tau_{725}\ (\text{RT})$$

$$\tau_{729}(\text{LNT}) > \tau_{729}(\text{RT})$$

and

$$\tau_{734}(\text{LNT}) \simeq \tau_{734}(\text{RT})$$

This clearly indicates that the contribution of CDRP is different for different excited states. In contrast to the general behaviour, an increase in lifetime at RT is observed for the 725nm line compared to its lifetime at

LNT. This shows that for this specific excited state the contribution of CDRP at RT is much less compared to that at LNT. Similar results have been obtained for L, K and R levels of Nd^{3+} in LaF_3 lattice[21,23]. For the line at 734nm, however, the lifetimes are almost equal at both the temperatures for 2% Nd^{3+} concentration. This indicates a possibility of the increase in transition rate due to the multiphonon transitions being compensated by a decrease in the transition rate due to CDRP at RT from the observed rate at LNT.

The temperature dependence of the contribution from the CDRP suggests the possibility of the higher Stark levels taking part in the ion pair transitions. It is also possible that the phonon assisted ion pair transitions are contributing significantly. The various possible ion pair transitions have already been identified for Nd^{3+} in LaF_3[21,27].

The nature of variation of lifetime of 725nm line shows that it originated from a distinct level which is influenced by various CDR processes resulting in a very high transition rate.

The N_2 laser excitation raises Nd^{3+} ions in SrF_2 to one of the higher Stark levels of L state which

is reported to have 10 Stark components[22]. From this level energy transfer can take place to K level either by phonon assisted non radiative or by ion pair transitions. From the energy level considerations of Nd^{3+}, we can see that there exists a possibility for ion pair transitions (L,Z) → (K,Y) (since L-K=Y-Z). The 725nm line of the observed spectra is therefore due to the transitions between Stark levels of K state and S state while the other lines are due to transitions between lower Stark levels of L state and other lower electronic states of Nd^{3+}. It is to be noted that a blue fluorescence from the L level has also been observed for the same crystal. The energy levels and transitions involved in the process are shown in Fig.5.6.

The decrease in lifetime and the increase in relative intensity of the 725nm line observed at high concentration and low temperature indicates that the magnitude of non-radiative transitions from K level is very much less compared to that from other levels.

Thus it is observed that for $SrF_2:Nd^{3+}$ N_2 laser excitation gives two fluorescence bands, one at 420nm and the other at 720nm of which only the first one has been observed for $CaF_2:Nd^{3+}$.

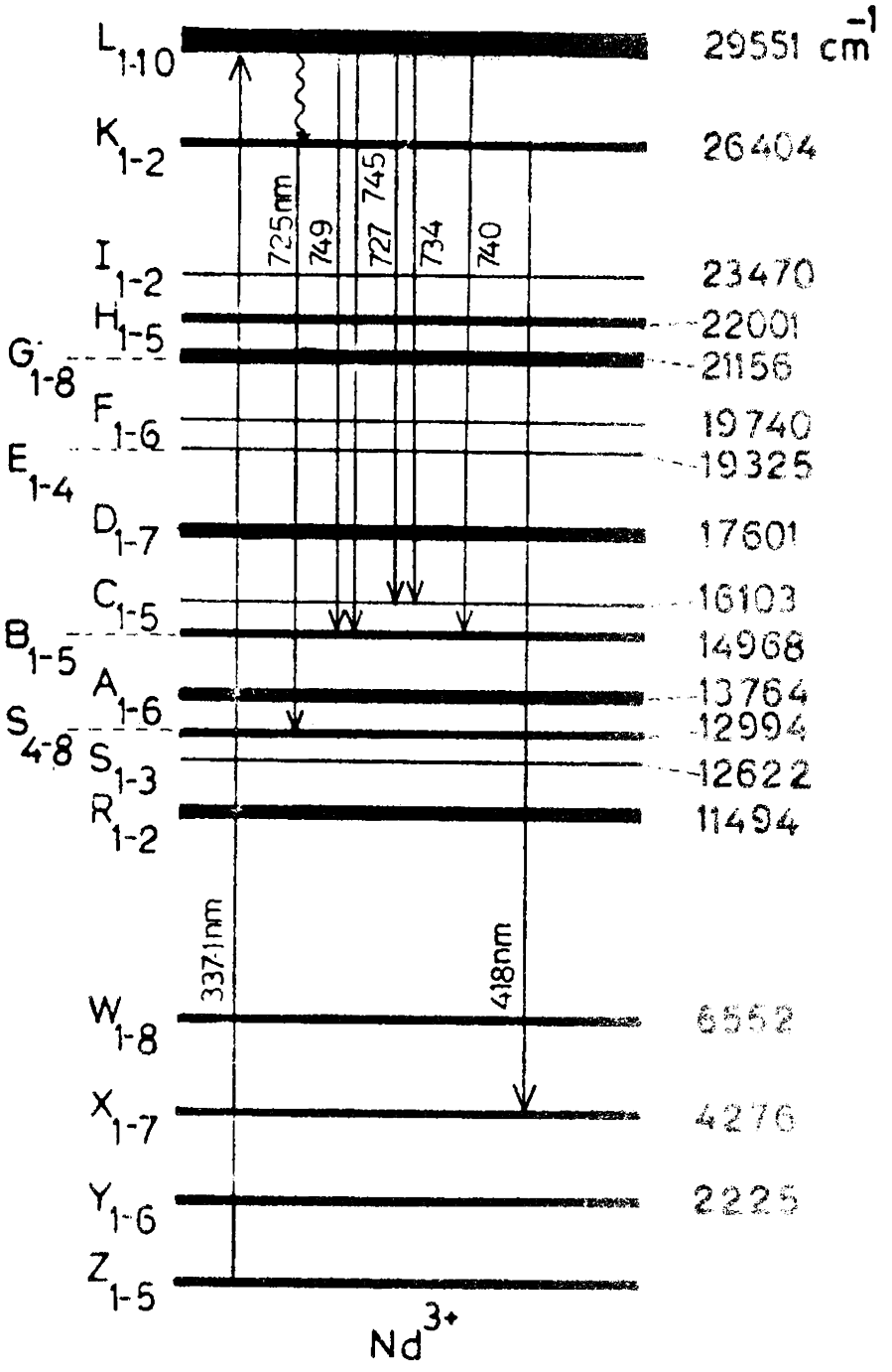

Fig.5.6 The schematic energy level diagram and transitions involved in the visible fluorescence of Nd^{3+}.

5.33 $BaF_2:Nd^{3+}$

The fluorescence emission from Nd^{3+} in BaF_2 was very weak compared to that of CaF_2 and SrF_2. The emission spectra at RT and LNT were charted and the spectra at LNT is shown in Fig.5.7. The emission spectrum has a peculiar nature. Almost all the peaks coincide with the vibrational bands of N_2 which may appear due to the high sensitive detecting system used for charting the spectra. But in the spectrum it is very clear that two emission bands appear with peaks at 388nm and 412nm. Compared to the emissions of Nd^{3+} in CaF_2 and SrF_2 these peaks are found to be much more shifted to shorter wavelength side. This may possibly be due to the fact that in BaF_2 the Nd^{3+} ions are under the influence of a stronger field than in CaF_2 and SrF_2.

5.40 Conclusion

In general, the N_2 laser excitation of Nd^{3+} in CaF_2, SrF_2 and BaF_2 gives fluorescence emission in blue region and is found to consist of two peaks. The emission band is due to the transition between 'K' level and 'X' level of Nd^{3+}. The fluorescence efficiency is found to be greater in SrF_2 than in CaF_2 and BaF_2.

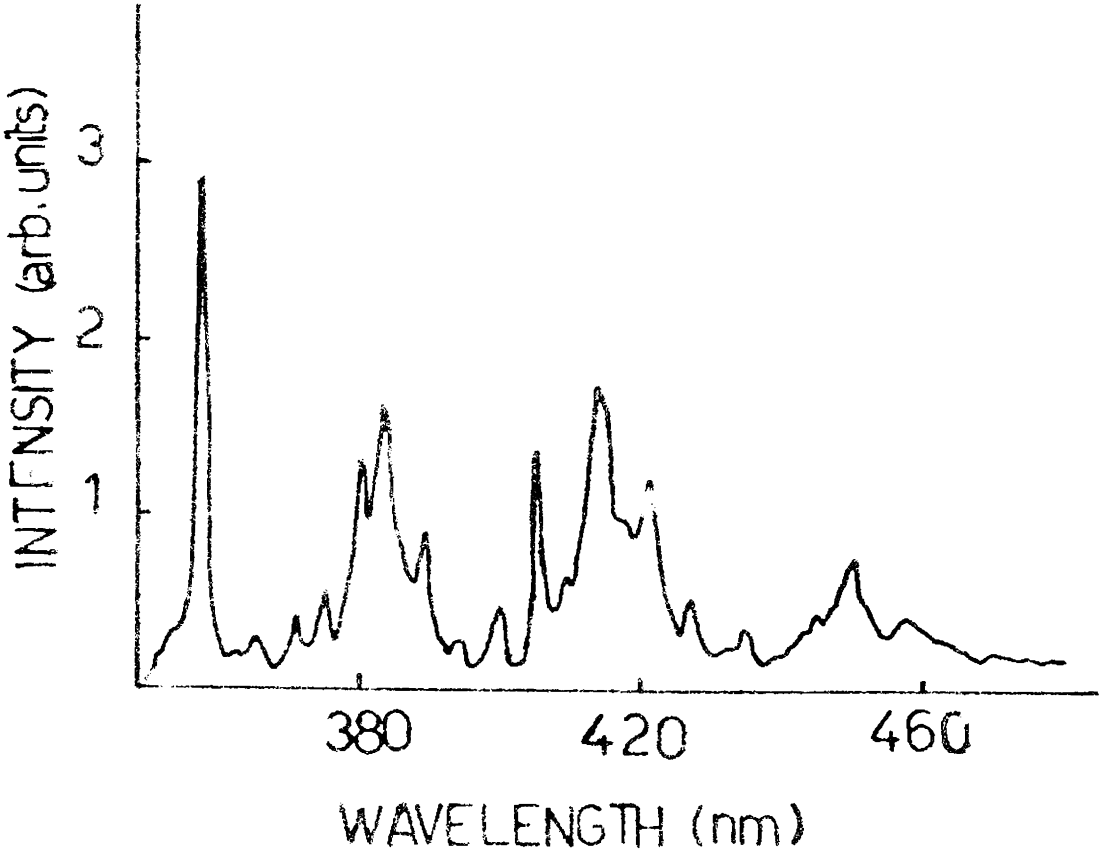

Fig.5.7 N_2 laser excited fluorescence spectra of $BaF_2:Nd^{3+}(1\%)$ at LNT.

In $SrF_2:Nd^{3+}$ one more band system was observed at 720nm region which showed a temperature and concentration dependence. The lifetime study of this band system indicates the presence of CDRP taking place in the system.

REFERENCES

1. M.Garbany, Optical Physics, Academic Press, New York & London (1965).

2. A.Yariv, Quantum Electronics, John Wiley & Sons Inc., New York, London & Sydney (1968).

3. L.F.Johnson and K.Nassau, Proc.IRE, 49, 1704 (1961).

4. Johnson, Boyd, Nassau and Soden, Phys.Rev, 131, 2038 (1963).

5. Kariss, Morozov and Feofilov, Opt.Spectroskopiya, 17, 887 (1964).

6. Ya.E.Kariss and P.P.Feofilov, Opt. Spectroskopiya, 17, 718 (1964).

7. L.F.Johnson, J.Appl.Phys. 34, 897 (1963).

8. H.Guggenheim, J.Appl.Phys. 33, 2482 (1963).

9. P.P.Feofilov, Inv.ANSSSR, Ser fiz. 26, 435 (1962), Columbia Tech.Transl.p.437.

10. Z.J.Kiss, J.Chem.Phys. 38, 1476 (1963).

11. Kaminskii, Kornienko, Makarenko, Prokhorov and Pursikov, JETP 46, 386 (1964). Sov.Phys.JETP, 19, 262 (1964).

12. Kaminskii, Kornienko and Prokhovov, JETP 48, 476 (1965).

13. Kask, Kornienko and Fakir, FTT 6, 549 (1964), Sov. Phys.Solid. State 6, 430 (1964).

14.

14. G.Vincow and W.Low, Phys.Rev. 122, 1390 (1961).

15. Yu.K.Voronko, Zh.Eksper Theor Fiz, 55, No.5, 1598 (1968).

16. M.Synek and J.Schultz, Ind.J.Phys, 52, 557 (1978).

17. Yu.K.Voronko, A.A.Kamenskii and V.V.Osiko, Sov. Phys. JETP, 22, 295 (1966).

18. B.I.Minkov, E.M.Ostrovskaya, S.A.Sazonova and B.S.Skorobogatov, Opt.& Spectros (USA) 40, 407 (1976).

19. Yu.P.Rudnitskii, R.V.Smirnov, V.M.Chernyak, Sov.J. Quantum Electronics, 16, 1107 (1976).

20. A.Singh, W.A.Bonner, W.H.Grodkiewicz, M.Grasso, L.G.Vanciitert, Appl.Phys.Letts. 29, 343 (1976).

21. C.K.Asawa and Robinson, Phys.Rev, 141, 251 (1966).

22. U.Vigneswarakumar, H.Jagannath, D.Ramachandra Rao and Putcha Venkateswaralu, Ind.J.Phys, 50, 90 (1976).

23. H.Jagannath, S.K.Basu and P.Venkateswaralu, Chem. Phys.Letts, 66, 313 (1979).

24. K.H.Yang, J.A.Deluca, Phys.Rev.B, 17, 4246 (1978).

25. L.I.Devyatkova, P.M.Lozovskii, V.V.Mikhailin, T.V.Uvarova, S.P.Chernov, A.V.Shepelev, P.B.Essel'bakh, Zh.Eksp & Theor Fiz, 27, 609 (1978).

26. M.R.Brown and W.A.Shand in Advances in Quantum Electronics ed. by D.W.Goodwin, AcademicPPress, London (1970) 41.

27. U.V.Kumar, D.Ramachandra Rao and P.Venkateswaralu, J.Chem.Phys, 67, 3448 (1977).

CHAPTER VI

FLUORESCENCE SPECTRA OF $CaF_2:Er^{3+}$

6.10 Introduction

Most of the difficulty normally encountered in studying rare earth doped crystals by optical spectroscopy has been overcome through the development of lasers. Using a narrow band dye laser it is possible to selectively excite absorption lines of specific sites in the crystals. All the important fluorescence transitions from the $^4S_{3/2}$ manifolds for $CaF_2:Er^{3+}$ have been investigated by Tallant et al[1]. Luminescence spectra of Er^{3+} ion in CaF_2, SrF_2 and BaF_2 single crystals have been analysed and a scheme of stark levels of the $^4S_{3/2}$ and $^4I_{15/2}$ states have been reported[2]. Miller et al have done a thorough study on Er^{3+} doped SrF_2[3] and BaF_2[4]. They have observed that in the fluorescence spectra of $SrF_2:Er^{3+}$ multiphonon and energy transfer relaxations are found to take place and have measured the rates of all the relaxation processes for representative sites in CaF_2, SrF_2 and BaF_2.

Miller et al have also studied the fluorescence transients of charge compensated sites in $BaF_2:Er^{3+}$ system and have observed that cluster sites make an

important contribution to fluorescence even at the lowest limit of concentration studied[4]. The importance of defect clustering in the analysis of $BaF_2:Er^{3+}$ optical spectra is reviewed by Miller et al[5].

The distribution of defect sites in $CaF_2:Er^{3+}$ has been measured by Moore and Wright[6] by site selection spectroscopy and has obtained evidence for cluster control of the defect equilibria in fluorite structure crystals. The fluorescence from the $^4S_{3/2} \rightarrow {}^4I_{11/2}$ in Er^{3+} doped crystals has also been observed due to two photon excitation from the $^4G_{11/2}$ level[7]. Theoretical and experimental investigations have also been done to understand two photon absorption spectra of Er^{3+} in CaF_2 by Apanasevic et al[8]. They have shown that the spectrum has a peculiar structure which differs considerably from that of the one photon absorption spectrum. A Q-switched $CaF_2:Er^{3+}$ laser has been developed by Gomelauri et al[9] which gave 0.13J, 30ns pulses at room temperature. The output was at 2.8 μm and was due to the $^4I_{11/2} \rightarrow {}^4I_{13/2}$ transitions.

The fluorescence of Er^{3+} has also been studied in various other hosts like $NaMgF_3$[10], LaF_3[11] and ErAlG[12]. In the present study an attempt has been made to record

the fluorescence spectra of $CaF_2:Er^{3+}$(5%) in the visible range using N_2 laser excitation. But the crystals do not give any fluorescence in the visible region. Hence in order to complete the study in $CaF_2:Er^{3+}$ also the fluorescence spectra of the crystal is recorded with the Xe arc excitation.

6.20 Experimental

Fluorescence spectra of $CaF_2:Er^{3+}$ was taken using an Aminco Bowman Spectrofluorometer. This system includes an optical unit, a power supply for the Xe lamp and a photomultiplier microphotometer. The optical unit of the system has two motor driven monochromators - one for excitation and the other for emission. The optical unit also includes a Xenon lamp as a source of light, a constant temperature cell compartment and a photomultiplier tube detector. The Xe lamp generates continuous, high intensity ultraviolet and visible radiation. The power supply generates stable electrical current for the lamp. The photomultiplier microphotometer provides a stable voltage to the PMT and also it maintains a noise free, stable amplification of the weak signal produced by the PMT.

The operation of the system is as follows:- Light from the Xenon lamp is dispersed by the excitation monochromator into monochromatic radiation incident on the sample. A similar emission monochromator disperses the fluorescence light into the PMT. The PMT output is fed to the photometer where it is amplified and the photometer output is indicated on a meter. The photometer output is also available to the chart recorder. The exciting and scanning monochromator gratings are moved by motor driven cams. Potentiometers connected to the gratings supply the wavelength drive for the recorder. A selector switch enables either excitation or fluorescence spectrum to be plotted.

6.30 Results

$CaF_2:Er^{3+}$ does not show any visible fluorescence under N_2 laser excitation. Excitation of $CaF_2:Er^{3+}$ under 365nm and 285nm of Xe arc source exhibits fluorescence at 410nm, 460nm, 510nm and 550nm. The fluorescence spectra of $CaF_2:Er^{3+}$, excited by the 285nm and 365nm are shown in Figs.6.1A and B. The transitions and the intensities are given in Table 6.1. The energy level diagram of Er^{3+} in CaF_2 is shown in Fig.6.2.

With the 285nm and 365nm excitation, fluorescence

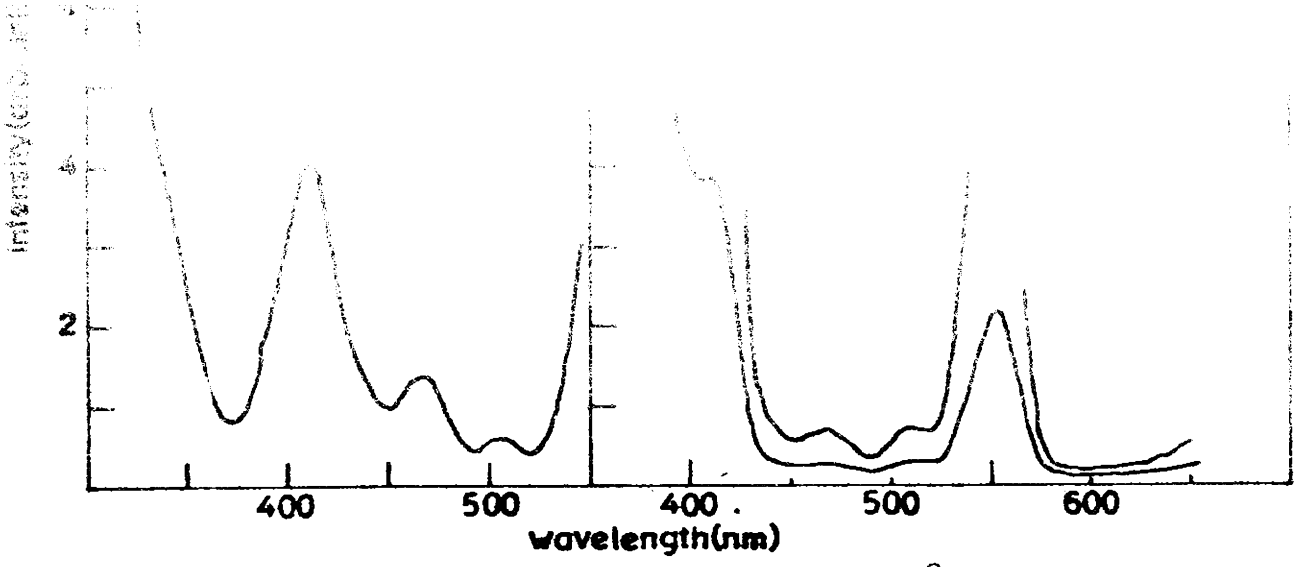

Fig.6.1 Xe arc excited fluorescence of $CaF_2:Er^{3+}$(5%).

(A) - under 285nm excitation

(B) - 1. under 365nm excitation
2. magnified 3 times

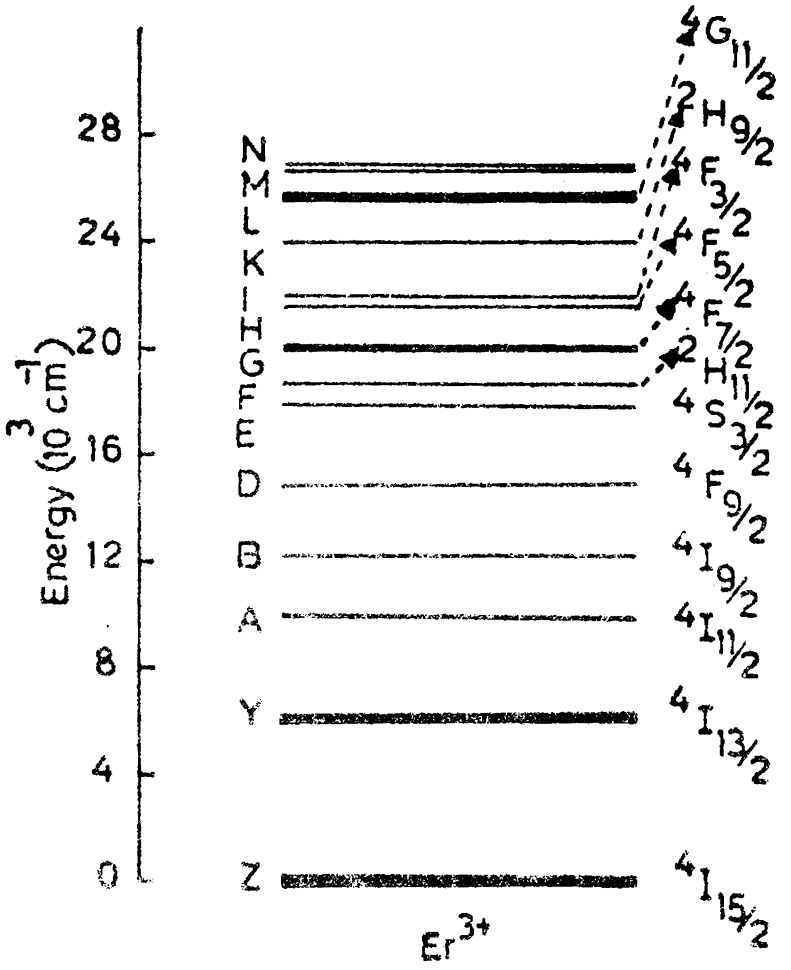

Fig.6.2 Schematic energy level diagram of Er^{3+} in CaF_2.

Table 6.1

Transitions and intensities of the fluorescence of Er^{3+} in CaF_2

Wavelength (nm)	Energy (cm^{-1})	Transition	Rel.intensity under 285nm excitation (arb.units)	Rel.intensity under 365nm excitation (arb.units)
410	24390	$^2H_{9/2} \rightarrow {}^4I_{15/2}$	43	43
460	21739	$^4F_{5/2} \rightarrow {}^4I_{15/2}$	14	3
510	19607	$^2H_{11/2} \rightarrow {}^4I_{15/2}$	6	3
550	18181	$^4S_{3/2} \rightarrow {}^4I_{15/2}$	—	23

transitions occurred from $^4S_{3/2}$, $^2H_{11/2}$, $^4F_{5/2}$ and $^2H_{9/2}$ to the ground state $^4I_{15/2}$ resulting in four fluorescence groups centered around 550nm, 510nm, 460nm and 410nm respectively. Of these 550nm and 410nm lines are intense while the other two are weak. The 410nm fluorescence group is clearly observed under 285nm excitation while the 550nm fluorescence group is observed under 365nm excitation.

When the crystal is excited by the 285nm radiation the Er^{3+} ions are excited to a state higher than the P level of Er^{3+} and from there, by non-radiative processes they relax to the $^2H_{9/2}$, $^4F_{5/2}$ and $^2H_{11/2}$ levels. The transitions from these levels to the ground state ($^4I_{15/2}$) give rise to the three fluorescence groups seen in the spectrum.

Under 365nm excitation, the 410nm emission is masked partly by excitation band. But a new group of fluorescence at 550nm is clearly observed. This band has not been observed in Fig.6.1A as it has been masked by the 2nd order of the 285nm. On comparing the two spectra, a variation in relative intensity between 510nm and 460nm emissions is prominently seen. With 285nm excitation, 510nm fluorescence group is very weak compared to 460nm line. But on exciting with the 365nm radiation

the two bands have almost the same intensity. This indicates that on exciting with 285nm the level $^4F_{5/2}$ gets more populated than $^2H_{11/2}$ giving rise to intense 460nm emission compared to the 510nm emission. 365nm excitation, on the other hand, gives rise to both the emissions in equal intensity and is concluded to be due to an energy transfer between $^4F_{5/2}$ and $^2H_{11/2}$.

REFERENCES

1. D.R.Tallant and J.C.Wright, J.Chem.Phys, 63, 2074 (1975).

2. B.Aizenberg, L'D.Livanova, I.G.Saitkulov, A.L.Stolov, Sov.Phys.Solid State, 10, 2030 (1968).

3. M.P.Miller and J.C.Wright, J.Chem.Phys. 71, 324 (1979).

4. M.P.Miller and J.C.Wright, J.Chem.Phys. 68, 1548 (1978).

5. M.P.Miller and J.C.Wright, Phys.Rev.B, 18, 3753 (1978).

6. D.S.Moore and J.C.Wright, Chem.Phys.Letts, 66, 173 (1979).

7. R.I.Gintoft, A.G.Skripko, Zh.Prikl, Specktrosk, 17, 85 (1972).

8. P.A.Apanasevic, R.I.Gintoft, V.S.Korolkov, A.G.Makhanek, G.A.Skripko, Phys.Stat.Solidi B, 58, 745 (1973).

9. G.V.Gomelauri, L.A.Kulevskii, V.V.Osiko, A.D.Savele'v and V.V.Smirnov, Sov.J.Quantum Electron, 6, 341 (1976).

10. N.Kristianpoller and B.Trieman, J.Luminescence, 24, 285 (1981).

11. H.Wolfrum, K.Lanzinger and K.F.Renk, Optics Letts, 5, 294 (1980).

12. R.C.Naik and N.A.Narasimham, Ind.J.Phys, 30, 222 (1976).

CHAPTER VII

GENERAL CONCLUSIONS

The results and conclusions of the present investigations are summarised in this chapter. The present study is mainly concentrated on the visible fluorescence of Ho^{3+}, Nd^{3+} and Er^{3+} rare earths in alkaline earth fluoride hosts (CaF_2, SrF_2 and BaF_2) using a nitrogen laser excitation.

A nitrogen laser was fabricated and its parametric studies were first carried out. The laser was found to give an output power of 225KW in 8ns. The laser emission spectrum was also analysed using a 0.5m Jarrell Ash monochromator with a grating blazed at 1800Å and was found to consist of a number of vibrational bands in addition to the 337.1nm band. The intensities of the bands were studied by changing the distance between the laser head and the monochromator. It was observed that an amplification had taken place at 331.83nm. This band was observed to have a relative intensity of nearly 29% and was found to be arising from one of the mixed vibrational levels of C and C' states of the molecule.

A serious effort was also made to increase the output power of the N_2 laser. Apart from the various design configurations generally adopted for increasing the power, additives were added to the N_2 gas for increasing the laser power output. The additives tried were vapours of electronegative and low ionisation potential, organic and inorganic solvents having saturated vapour pressures of the order of a few torrs. Of these, an increase in power of about 71% was observed with 1-2, Dichloroethane, 46% with carbon tetrachloride and 41% with Thionyl Chloride. 1,2-Dichloroethane was more effective in increasing the output power at higher N_2 pressures while the power increase with carbon tetrachloride and Thionylchloride was found to be uniform in the pressure range 50-150 torr. It was concluded that the power enhancement with 1,2-Dichloroethane was due to the increase in thermal conductivity of N_2 molecules whereas the power increase with carbon tetrachloride and Thionyl Chloride was due to the fast deactivation processes made possible from the $B^3\Pi_g$ state by vibrational quenching. Some other additives were also tried. In these experiments, though power enhancement could be achieved, the pulse width was found to increase with the additives.

A fluorescence emission spectrometer and a lifetime spectrometer were set up to carry out the fluorescence experiments. The main components of these experimental set up were the laser source, monochromator, sample holder (cryostat), PMT, amplifier, signal processing electronics and recorder. The source, the sample holder, amplifier and some of the electronics for noise rejection were fabricated.

The fluorescence spectra of pure CaF_2, SrF_2 and BaF_2 were investigated with the N_2 laser excitation. Though these alkaline earth fluorides are wide band gap materials, two new emission bands with peaks at 370 and 420nm were observed for the first time. The excitation spectra showed absorption peaks at 305 and 350nm corresponding to the two emission bands. The emission bands at 370 and 420nm were observed in the emission spectra of CaF_2:Ho^{3+} also, the 370nm band with enhanced intensity while the 420nm band showing a decrease in intensity. These emission bands were found to influence the characteristic emission of Ho^{3+} ion in CaF_2. A possible mechanism for the origin of these bands was suggested to be due to colour centres formed by quasi molecular complexes - $(RF)^+$ and (F_2^{--}) - near anion and cation vacancies present in the crystal.

The fluorescence spectra of $CaF_2:Ho^{3+}$ in the 530nm region were studied for different Ho^{3+} concentrations and also at both RT and LNT. This fluorescence group consisted of eight well separated narrow bands at 533.5, 535.9, 540.5, 542.2, 547.6, 549.6, 551.3 and 552.7nm and were due to the transition from $^5F_4$ and $^5S_2$ levels of Ho^{3+} to $^5I_8$ ground state. Strong concentration quenching was observed for this fluorescence group. The lifetime study of this fluorescence group also showed strong concentration and temperature dependence. The decay times of all the emission bands were found to decrease very rapidly at higher Ho^{3+} concentration and was concluded to be due to the presence of some concentration dependent relaxation processes. In the present study lifetime quenching at low temperature was also observed for most of the lines. From the energy level considerations of Ho^{3+}, it is seen that ion-pair relaxation is possible between ($^5F_4$, $^5I_8$) and ($^5I_4$, $^5I_7$). The accidental matching of transitions and the strong quenching observed with concentration imply that ion-pair relaxation may be the dominant relaxation mechanism responsible for the CDR processes in the system. A great deal of research on the concentration and temperature quenching of RE^{3+} luminescence was undertaken by several researchers. But

most of the work was concentrated on Nd^{3+} in LaF_3. Such observations in Ho^{3+} are reported here for the first time.

Nitrogen laser excitation of Nd^{3+} in CaF_2, SrF_2 and BaF_2 gave strong blue emission and is found to have greater intensity in SrF_2. One more band system was observed at 720nm region for SrF_2:Nd^{3+} which consisted of six narrow emission bands. The variation of the fluorescence and lifetime of this fluorescence group with concentration and temperature showed that the influence of CDRP is different for the different emission peaks. From the energy level considerations and excitation spectra it is concluded that the N_2 laser frequency 29,656 cm^{-1} excites the Nd^{3+} ion to phonon coupled stark 'L' levels of Nd^{3+}. The excited state then relaxes to 'K' state and transition from 'K' state to lower 'X' state gives the blue fluorescence of Nd^{3+} at 420nm region. All the other transitions are also identified.

Nitrogen laser excitation of CaF_2:Er^{3+}(5%) did not give any visible fluorescence. Due to the high concentration of the dopant, it is likely that the excited ions may undergo a number of non-radiative processes. The

fluorescence of the crystal was therefore studied using the 285nm and 365nm excitation of the Xe arc. The spectra obtained with both the excitation were compared and a variation in relative intensity was noted for the 460nm band. It is inferred that energy transfer is possible between $^4F_{5/2}$ and $^2H_{11/2}$ levels of Er^{3+} which may give rise to intensity variation.

To increase the efficiency of laser crystals it is necessary to study the spectroscopic features of these crystals and hence the concentration and temperature quenching observed for Ho^{3+} and Nd^{3+} are of importance. Moreover, the absorption and emission observed in the present study in the pure alkaline earth fluorides are also of special interest, since these crystals find applications as laser windows and optical components.